SCUOLA DI DOTTORATO
UNIVERSITÀ DEGLI STUDI DI MILANO-BICOCCA

Dipartimento di Biotecnologie e Bioscienze

Dottorato di Ricerca in Biologia e Biotecnologie Ciclo XXX

Curriculum in Biotecnologie

Regulation of DNA-end resection at DNA double strand breaks and stalled replication forks

Cognome VILLA Nome MATTEO

Matricola 732155

Tutore: Prof. Maria Pia Longhese

Coordinatore: Prof. Marco Vanoni

ANNO ACCADEMICO 2016-2017

Università degli Studi di Milano-Bicocca

Dipartimento di Biotecnologie e Bioscienze

Dottorato di Ricerca in Biologia e Biotecnologie - XXX Ciclo

Regulation of DNA-end resection at DNA double strand breaks and stalled replication forks

Matteo Villa

732155

Coordinatore: Prof. Marco Vanoni

Tutor: Prof. Maria Pia Longhese

Anno Accademico 2016-2017

Index

Abstract

Genome instability is an hallmark of cancer cells and can be due to DNA damage or replication stress. DNA double strand breaks (DSBs) are the most dangerous type of damage that cells have to manage. In response to DSBs, cells activate an highly conserved mechanism known as DNA damage checkpoint (DDC), whose primary effect is to halt the cell cycle until the damage is repaired. DDC is activated by the apical kinases Tel1/ATM and Mec1/ATR, which phosphorylate and activate the effector kinases Rad53/CHK2 and Chk1/CHK1. The Homologous Recombination (HR)-mediated repair of a DSB starts with the nucleolytic degradation (resection) of the 5' ends to create long ssDNA tails. In *Saccharomyces cerevisiae*, resection starts with an endonucleolytic cleavage catalyzed by the MRX complex together with Sae2. More extensive resection relies on two parallel pathways that involve the nucleases Exo1 and Dna2, together with the helicase Sgs1. Resection must be tightly controlled to avoid excessive ssDNA creation. The Ku complex and the checkpoint protein Rad9 negatively regulate resection. While Ku inhibits Exo1, Rad9 restrains nucleolytic degradation by an unknown mechanism.

The absence of Sae2 impairs DSB resection and causes prolonged MRX binding at DSB that leads to persistent Tel1 and Rad53-dependent DNA damage checkpoint. *SAE2* deleted strains are sensitive to DSBs inducing agents, like camptothecin (CPT). This sensitivity has been associated to the resection defect of *sae2*Δ cells, but what causes this resection defect and if the enhanced checkpoint

signaling contributes to the DNA damage sensitivity of *sae2*Δ cells is unknown.

For these reasons, we tried to identify other possible mechanisms regulating MRX/Sae2 requirement in DSB resection by searching extragenic mutations that suppressed the sensitivity to DNA damaging agents of ***sae2Δ*** cells. We identified three mutant alleles (*SGS1-G1298R, rad53-Y88H* and *tel1-N2021D*) that suppress both the DNA damage hypersensitivity and the resection defect of *sae2*Δ cells.

We show that Sgs1-G1298R-mediated suppression depends on Dna2 but not on Exo1. Furthermore, not only Sgs1-G1298R suppresses the resection defect of *sae2*Δ cells but also increases resection efficiency even in a wild type context by escaping Rad9-mediated inhibition. In fact, Rad9 negatively regulates the binding/persistence of Sgs1 at the DSB ends. When inhibition by Rad9 is abolished by the Sgs1-G1298R mutant variant, the requirement for MRX/Sae2 in DSBs resection is reduced.

Rad53-Y88H and Tel1-N2021 are loss of function mutant variants that suppress *sae2*Δ cells sensitivity in a Sgs1-Dna2 dependent manner. Furthermore, abolishing Rad53 and Tel1 kinase activity results in a similar suppression phenotype which does not involve the escape from the checkpoint mediated cell cycle arrest. Rather, defective Rad53 or Tel1 signaling bypasses Sae2 function in DSBs resection by decreasing the amount of Rad9 bound at DSBs. This increases the Sgs1-Dna2 activity that, in turn, can compensate for the lack of Sae2. We propose that persistent Tel1 and Rad53 checkpoint signaling in

*sae2*Δ cells causes DNA damage hypersensitivity and defective DSB resection by increasing the amount of Rad9 that, in turn, inhibits Sgs1-Dna2.

Replication stress can induce fork stalling and a controlled resection can be a relevant mechanism to allow repair/restart of stalled replication forks. We show that loss of the inhibition that Rad9 exerts on resection exacerbates the sensitivity to replication stress of Mec1 defective yeast cells by exposing stalled replication forks to Dna2-dependent degradation. This Rad9 protective function is independent of checkpoint activation and relies mainly on Rad9-Dpb11 interaction. We propose that Rad9 not only regulates the action of Sgs1-Dna2 at DSBs but also at stalled replication forks, supporting cell viability when the S-phase checkpoint is not fully functional.

Introduction

1 Genome instability and cancer onset: a tight connection

Cancer is a disease characterized by an abnormal cellular growth. So far, more than 100 types of different cancers have been described, indicating its huge complexity. The World Health Organization (WHO) has estimated that, in 2012, cancer was responsible for 8.8 million death worldwide with respect to 14 million new cases, approximately. Moreover, WHO predicts that these numbers are destined to augment in the next two decades. In addition, it has been estimated that in 2010, the economic cost for cancer treatment was around 1.16 trillion dollars [1]. From these data, it comes to light that cancer is both an economical and medical problem whose resolution is far from being found.

In the last twenty years, cancer has become a central issue for biological, medical and clinical research. In this contest, at biological level, great efforts were done to understand and analyze the features of cancer cells. In 2000, Hanahan and Weinberg, based on the fact that cancer cells have defects in regulatory circuits that govern normal cell proliferation and homeostasis, defined that tumor cells share at least six common traits that were called “hallmarks of cancer cells” [2]. This way to rationalize such a complex disease, creates new chances for a combined therapeutic approach that has the objective to interfere with one or more of these features. In 2011, the same authors added four new characteristics to cancer cells [3] (**Figure 1**). Among them, genomic instability was defined as an enabling characteristic. In fact,

while all the hallmarks are acquired during a multi-step transformation process, genome instability is the engine of tumor progression.

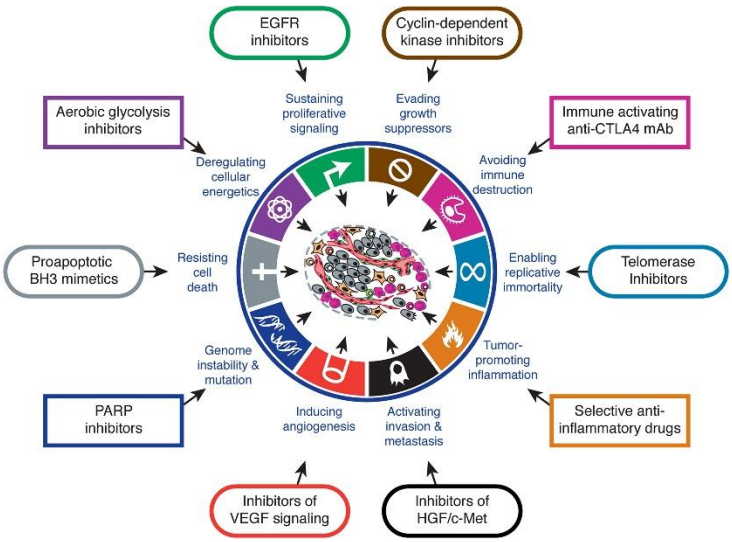

Figure 1 Representation of the hallmarks of cancer and drugs that interfere with each of the acquired capability. Adapted from [3]

Genome instability is the result of mutational events at different levels from point mutations to chromosome rearrangements. Cancer cells show three main levels of genetic instability [4–6]. In the first, there are single base-pair mutations, like point mutations, deletions, insertions and microsatellite contractions or expansions (MIN); in the second level there are alterations in chromosome numbers and in the last, other types of genome alterations, like gross chromosomal rearrangements (GCRs), copy number variants (CNVs), hyper recombination events and loss of heterozygosity (LOH). In most cases,

these alterations arise as the consequence of damaged DNA, left unrepaired or repaired in the wrong way. DNA could be damaged by a variety of agents, chemicals and/or physicals deriving from both cellular or extracellular environment [7]. Different agents are able to cause different types of DNA damage that span from alterations of single bases to the complete disruption of the entire DNA molecule. Eukaryotic cells face DNA damages by activating a complex and conserved response named DNA damage response (DDR) [8]. Different proteins are involved in the DDR, with some of them implicated in the recognition and signaling of the damage, while others responsible for the repair [4,5,8].

The genome of cancer cells is highly unstable and genome instability appears early during the tumor transformation process. In fact, precancerous lesions from different tissues show activation of the DDR [9,10]. Furthermore, loss of function mutations in genes involved in the repair of damaged DNA are thought to be responsible for hereditary tumors like breast cancer or colon-rectal cancer [4]. In addition, rare monogenic syndrome due to mutations in DDR genes, like Bloom syndrome, Werner syndrome or Ataxia telangectasia, are characterized by an increased incidence of cancer [4,11]. These observations are consistent with the “mutator hypothesis”, which states that mutations in genes of the DDR (caretaker genes) drive tumor development by increasing the spontaneous mutational rate. According to this hypothesis, genomic instability seen in precancerous lesions could be attributed to mutations in caretaker genes, especially

those implicated directly in the repair of damaged DNA. In this context, endogenous or exogenous sources of DNA damage, like normal cell metabolism products, UV-light, cigarette smoke or an incorrect diet can increase the number of DNA damages that cells have to fight [1,7]. If repair pathways are not fully functional, the likelihood of incorrect repair events increases together with the mutational rate.

However, high-throughput sequencing studies have failed in identifying recurrent mutations in caretaker genes in sporadic cancer. Thus, in these types of cancer, the molecular basis of genome instability must be different [4]. Indeed, the most frequently mutated genes in sporadic tumors are genes that control cell growth positively and/or negatively, like *RAS* and *PTEN*. This, together with the observation that oncogenic activation is able to induce genetic instability [12,13], led to the formulation of the "oncogene induced DNA replication stress" model [14]. The term DNA replication stress includes all that situations in which the DNA replication process is hindered by different causes. Several evidences link oncogene activation with replication stress [10,14,15]. Anyway, if the mechanisms that lead to genome modification in hereditary cancers are logical and well defined, how oncogene activation induces DNA replication stress is not so clear.

One possibility is that oncogenes can alter the activity of the Cyclin-Dependent Kinase (CDK) complexes which are responsible for the control of the cell cycle.

In this context, oncogene activity can deregulate DNA replication at different levels. For example, an high activity of CDK in the G1 phase

of the cell cycle can interfere with the origin licensing process, that precedes DNA replication. If the origin licensing process is partially blocked, the number of available replication origin decreases. In this context, a reduced number of replication forks has to cover longer distances and this increases the chance of fork stalling. Indeed, stalled forks cannot be rescued by incoming forks and this prolonged stall can degenerate in fork collapse and/or DNA breaks.

Replication stress can be induced even by an unscheduled replication that occurs when the timing of replication is altered and/or the number of active replication origin is increased. For example, MYC overexpression leads to an increase in origin firing either directly, by associating with DNA, or indirectly, by its transcriptional regulator role. This increase in origin firing may exhaust substrates required for replication, like deoxyribonucleoside triphosphates (dNTPs) or other replicative proteins. This, in turn, causes fork stalling and a reduction in replication rate.

Moreover, the collision between the transcription machinery and the replication fork has been listed as cause of oncogene-induced replication stress. In fact, these events can induce DNA double strand breaks (DSBs). Indeed, altering transcription in human cells with repression of cyclin E results in a partially suppression of genome instability [6]. This supports the hypothesis of a feedback control of transcription and replication that could be altered in cancer cells.

The understanding of the molecular basis of the maintenance of genome integrity is of high importance in term of cancer therapies. In

fact, it has been estimated that the threshold of tolerable genome instability is around 75% of the genome. That is, a genome recombinant for its 75% can be tolerated by a cancer cell [16]. This underlines how genome instability could be the Achille's heel of cancer cells. Nowadays, the best approach against cancer remains chemotherapy and radiotherapy, that have the objective to increase genomic instability in dividing cells. Anyway, side effects are the main negative features of these treatments.

Recently, the concept of synthetic lethality has been exploited to increase cancer therapies efficacy [17]. Genetically, a synthetic lethal interaction between two genes occurs when the perturbation of either gene alone has no phenotypic effect while the alteration of both genes simultaneously results in loss of viability. In the context of tumor, the synthetic lethality is based on the concept of "oncogene addiction", by which tumors cells rely their viability on a specific pathway. Exploiting this route, different genes have been used as target for synthetic lethal therapies [18]. One of the best result of these studies are the PARP inhibitors that are used to inactivate a specific DNA repair pathway (Base Excision Repair, BER) in cells that have altered the homologous recombination (HR) repair pathway due to mutations in BRCA1 and/or BRCA2 genes [17,18]. Loss-of function mutations in these genes are associated with breast and ovarian cancer and PARP inhibitors are already used in clinics and 16 new inhibitors are currently under clinical trials [19]. Alternatively, synthetic lethal approaches can be used also to increase the cytotoxicity of existing therapeutic agents [17].

Considering that genome instability is compatible with cellular life to a defined extent, increasing genome instability by targeting DNA repair pathways upon genotoxic treatment may be a fertile ground to search for new compounds to use in combination with already-used genotoxic treatment [19].

The difficulty of synthetic lethal approaches lies in the hundreds of tumor query genes and thousands of potential synthetic lethal partner genes that need to be considered. For this reason, genetic interaction studies are conducted firstly on model organisms like the budding yeast, *Saccharomyces cerevisiae* [17]. All recent genes and pathways used for synthetic lethal approaches find a comparison in model organism, in particular in yeast.

The use of budding yeast and other model organisms is justified by the elevated grade of conservation of important pathways, like the ones that maintain genome integrity [20]. For example, using budding yeast, Weinert and Hartwell provided evidences that eukaryotic cells possess mechanisms to defend their genome that have been confirmed, later, also in mammalian cells [21]. With time, the versatility of *S. cerevisiae* has given the opportunity to develop specific genetic systems that allow the identification of different crucial and conserved proteins implicated in the DDR.

This experimental work takes advantage of the use of *S. cerevisiae* to provide data about the regulation and the interplay between the homologous recombination pathway and the checkpoint response after DNA breaks and replication stress. These data help to elucidate the

molecular mechanisms that regulate and link the repair process with the control of the cell cycle, upon genomic insults. Considering that both DNA repair process and the control of the cell cycle are impaired during tumorigenesis [4,5,15], our findings, if confirmed in mammalian cells, could be of general interest in term of increasing knowledge in the DDR and in term of synthetic lethal approaches.

2 Cellular response to DNA double strand breaks

DNA is subjected to endogenous and exogenous insults that can modify its structure or its composition. It has been estimated that DNA is prone to 10^5 lesions per cell per day [22]. Among these lesions, DNA double strand breaks (DSBs), which occur when the phosphate backbone of two complementary strands is broken simultaneously, are the most dangerous one. In fact, failure in repairing them can lead to loss of genetic information, chromosome rearrangements and, as a consequence, to genome instability.

DSB can arise as a consequence of both endogenous and exogenous insults [6,23,24]. Different studies have pointed out that the frequency of spontaneous DSBs is around 1 per 10^8 bp, in both yeast and mammalian cells [24]. The replication process can induce the formation of DSBs *per se* and, in particular, in presence of replication stress. In principle, each situation that causes the block of the replication fork could give rise to DSBs following the collapse of the replisome [6]. For example, topoisomerase inhibitors, like camptothecin (CPT) or etoposide, that are commonly used as chemotherapeutic drugs, can irreversibly bind the topoisomerase enzyme on DNA. This causes the block of the replication forks and the creation of replication intermediates whose resolution can induce DSBs [24]. Furthermore, inhibition of the topoisomerase action by CPT can leave nicks inside the DNA molecule that can be converted in DSBs by the passage of

the replication complex [5]. In addition, other exogenous agents like hydroxyurea (HU) or aphidicolin can impair fork progression by depleting nucleotide pools or inhibiting DNA polymerase, respectively [24]. Indeed, inter-strand crosslink, due to the action of agents like mitomycin C and cisplatin, can stall replication fork, increasing the likelihood of fork collapse [23]. Even physiological processes, like transcription, can be responsible for the creation of DSBs during normal DNA replication [6]. In fact, the interference between transcription and replication machineries represents a major source of endogenous replication stress and collision between the RNA polymerase and the DNA polymerase have been demonstrated to induce ectopic recombination via DSB intermediates [6]. In addition, the presence of R-loops, hybrids between DNA and RNA, can cause the block of replication fork [6].

Outside the replication process, some chemical agents like reactive oxygen species (ROS) and other byproducts of cellular metabolism can interact with DNA and create DSBs directly, by oxidation of the basis of opposite strand, or indirectly, by the activation of other repair pathways that can generate DSB intermediates [22,23]. Furthermore, the exposition to other exogenous chemicals, like ionizing radiation or radiomimetic drugs (i.e. bleomycin and/or phleomycin) can induce DNA breaks directly or indirectly by the formation of clustered nicks, oxidized bases and abasic sites [23].

Interestingly, even if DNA DSBs pose a serious threat to genomic stability, there are physiologically processes that need the formation of

programmed site-specific DNA DSB [24]. This is the case of VDJ recombination and class switch in lymphocytes [23,24].

Moreover, during the meiotic process, self-inducted DSBs made by the highly conserved topoisomerase-like protein Spo11, guarantee meiotic recombination [24]. Indeed, in budding and fission yeast, the first step of mating type switching is dependent on a self-induced DSB [25].

DNA DSBs, especially if self-inflicted, must be under an accurate control in order to avoid dangerous repair events that can lead to ectopic recombination and-or loss of entire tract of DNA. For this reason, cells activate a complex and highly conserved cellular response named DNA damage response (DDR) [8,26]. In the presence of DNA damage or replication stress, the DDR is activated by sensor proteins that recognize the lesion and activate a phosphorylation cascade named DNA damage or DNA replication checkpoint to halt the cell cycle, to promote DNA repair and to activate specific transcriptional responses [8].

3 Sensing DNA double strand breaks: the DNA damage checkpoint

The ability to deal with spontaneous or environmentally induced DSBs is based on the capability to recognize the presence of an even single DSB inside a million bases length genome. Cells have a sophisticated surveillance mechanism that is named DNA damage checkpoint (DDC) [27] whose activation results in cell-cycle arrest, activation of specific transcriptional programs, support and control of the repair processes and, if the damage persists, activation of specific cellular responses that end with the activation of apoptotic or senescence programs [8,27]. In both yeast and mammals, the DDC activation is dependent on the activity of specific proteins that can be divided in three main classes: sensor, mediators and effectors (**Table 1**)

Saccharomyces cerevisiae	*Schizosaccharomyces pombe*	*Homo sapiens*	Function
Mec1	Rad3	ATR	Checkpoint signaling kinase
Ddc2	Rad26	ATRIP	Mec1/ATR binding partner
Tel1	Tel1	ATM	Checkpoint signaling kinase
Mre11-Rad50-Xrs2	Rad32-Rad50-Nbs1	MRE11-RAD50-NBS1	MRX/MRN complex DSB repair Tel1/ATM activator
Rad53	Cds1	CHK2	Checkpoint effector kinase
Chk1	Chk1	CHK1	Checkpoint effector kinase
Ddc1-Rad17-Mec3	Rad9-Rad1-Hus1	RAD9-RAD1-HUS1	9-1-1 complex Mec1/ATR activator
RFC-Rad24	RFC-Rad17	RFC-RAD17	9-1-1 clamp loader
RFC-Ctf18- Dcc1-Ctf8	RFC-Ctf18- Dcc1-Ctf8	RFC-CTF18-DCC1-CTF8	RFC-Ctf18 complex checkpoint mediator
Dpb11	Rad4	TOPBP1	Replication initiation Mec1/ATR activator
Dna2	Dna2	DNA2	Okazaki fragment processing DSB repair Mec1/ATR activator
Rad9	Crb2	53BP1, BRCA1	Checkpoint mediator Rad53/Dun1 activator
Mrc1	Mrc1	CLASPIN	Checkpoint mediator Rad53 activator
Sgs1	Rqh1	BLM, WRN	Rad53 activator

Table 1 Checkpoint factors from yeast to human. Adapted from [28]

3.1 The MRX/MRN complex and the Tel1/ATM kinase as principal sensors of DNA double strand breaks

The recognition of damaged DNA is of extreme importance to mount the correct cellular response. Sensor proteins have the role to identify and signal potentially harmful DSBs by activating mediators protein that, in turn, complete the activation of the DDC by recruiting and triggering effectors proteins [8,26].

One of the first protein complex recruited to a DNA break is the highly conserved MRX/MRN complex (Mre11-Rad50-Xrs2, in yeast, MRE11-RAD50-NBS1, in mammals) (**Figure 2**) [29].

The MRX complex has been firstly identified and purified in yeast and, then, found in mammalian cells and other organisms [30–33]. The Mre11 subunit shows, in its N-terminal region, five phosphodiesterase motifs, that are essential for its nuclease activities (see par. 4.3.1) and the Xrs2/NBS1 binding site. In the C-terminal domain, there are two DNA binding sites and the interaction region with Rad50 [34]. Mre11 binds DNA and the crystal structure of Mre11-DNA complex form *P. furiosus* has revealed important molecular details [35]. In a single MRX complex molecule, Mre11 exists as an U-shape homodimer. This conformation is essential for the DNA binding that is mediated by six DNA recognition loops in which 17 residues interact with the backbone sugar-phosphate of the minor groove of DNA [33–35]. Mre11 binds preferentially some DNA structures like dsDNA with 3'overhangs, hairpins and Y shaped DNA structures containing both ssDNA and

dsDNA [34]. Recently, it has been proposed that both Rad50 and Xrs2/NBS1 assist Mre11 DNA binding [33,34].

Rad50 is an ATPase belonging to the ABC ATPase superfamily. Indeed, its domains organization is similar to the one of the structural maintenance of chromosomes (SMC) family of proteins [36]. N-termini and C-termini contain walker A and walker B motifs that can associate together through the folding of two central coiled-coil domains [36]. In this way, by intra-molecular interactions, walker A and B domains can interact each other and constitute the ATPase domain of Rad50 [34]. The two coiled-coil domains are separated by a “hinge region” that contains a zinc-hook composed by a CXXC motif. Crystal structures of *P. furiosus*, *S. cerevisiae* and human RAD50 show that one Zn^{2+} atom can be coordinated with the cysteine of two different CXXC motifs. This interaction allows the dimerization between two Rad50 molecules in the same MRX complex molecule or between two Rad50 belonging to different complexes [37]. Mutations in the zinc-hook not only abrogate the interaction between Rad50 molecules but also afflict the interaction between Mre11 and Rad50 [37]. The dimerization of Rad50 by its hook motifs covers a critical role in MRX functionality. In fact, yeast strains carrying *rad50* allele deleted for the hook motifs show similar phenotypes of those deleted for *MRE11* or *RAD50* [38]. Within a single MRX complex molecule, each Mre11 subunit of the homodimer interacts with one Rad50 molecule with different alpha helices. The first region of interaction lies in the C-terminal domain of Mre11, where an <HLH (helix loop helix) motif interacts with the root of the coiled-coil

domain of Rad50. The second interaction site is between the capping domain of Mre11 and the ATPase head of Rad50. Mutations in this interfaces, can-not completely rescue genotoxic sensitivities of *MRE11* deleted yeast strain, indicating that the functionality of the complex depends on the correct interaction between Mre11 and Rad50 [39].

In both yeast and mammals, Xrs2/NBS1 exerts a regulatory function for the MRX/MRN complex [34]. It physically interacts with Mre11 and is responsible for the correct localization of the complex in the nucleus [40,41]. In budding yeast, deletion of *XRS2* confers sensitivity to genotoxic agents that can be rescued by fusing a nuclear localization sequence (NLS) to Mre11 [40]. In addition, Xrs2/NBS1 stimulates the activity of both Mre11 and Rad50 by promoting the DNA binding activity of the complex and supporting the nuclease activity of Mre11 [42,43]. Xrs2 and NBS1 share domains organization [34]. In particular, in the N-terminus there are FHA and BRCT domains, implicated in protein-protein interaction. At the C-terminus, there are the NLS sequence, the binding site of Mre11 and the interaction site with Tel1/ATM.

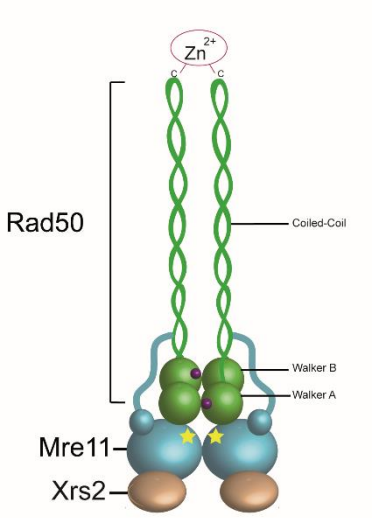

Figure 2 Structural organization of the MRX complex.
The Mre11 nuclease sites are indicated by yellow stars. Purple dots indicate the ATP binding site of Rad50.

This is particularly important in term of checkpoint activation. In fact, the MRX/MRN complex is required for the complete activation of the apical checkpoint kinase Tel1/ATM [44].

In yeast, Tel1 is a member of the phosphoinositide 3-kinase-related protein kinase (PIKK) family and its mammalian ortholog is called ATM (Ataxia Telangectasia Mutated) [45]. The PIKK enzymes are large proteins (270-450 kDa) with a characteristic domains organization that presents N-terminal HEAT repeats followed by a C-terminal kinase domain [46]. The kinase domain is preceded by the FRAP-ATM-TRRAP (FAT) domain, followed by the PIKK-regulatory domain (PRD) and by the FAT-C-terminal (FATC) domain. All these domains participate together in the regulation of the kinase activity by mediating

protein-protein interactions and/or by structural changes [46,47]. Even if deletion of *TEL1* in yeast cells does not result in any obvious sensitivity to genotoxic stress, loss of function mutations in ATM are related to a rare recessive disease named Ataxia Telangiectasia (AT). Symptoms of the AT are ataxia, impaired body movements and telangiectasia. In addition, AT patients show recurrent pulmonary infections, high risk of developing tumors, like lymphomas and leukemia, and premature aging [48,49].

Tel1/ATM is primarily activated by DSBs and the full activation of ATM depends on phosphorylation events [26,50,51]. ATM is predominantly nuclear and exists as a noncovalent homodimer. A recent structural study conducted on *S. pombe* Tel1 has revealed that, in this conformation, HEAT N-terminal repeats fold in an helical solenoid that packs against the FAT and kinase domains inhibiting, by steric hindrance, the binding of substrates and regulators [52]. Following DNA damage, autophosphorylation of ATM on serine 1981 causes the monomerization and the activation of the kinase [53]. In addition, this autophosphorylation requires the acetylation of ATM on the FATC domain by the action of TIP60 [51]. Anyway, some concerns about the biological value of this phosphorylation have been raised by studies in mouse and in *Xenopus* eggs extract [53].

Even though the signals that activate ATM are not fully understood, studies in both yeast and mammals have clarified the mechanism of Tel1/ATM recruitment and some aspects of its activation.

A central role in Tel1/ATM activation is played by the MRX/MRN complex. One of the strongest evidence comes from the finding that hypomorfic mutations in *MRE11* gene give rise to a very rare syndrome, clinically indistinguishable from AT, called AT-like disorder (ATLD). ATLD cells show a reduced level of ATM activation following DNA DSBs, indicating a relationship between ATM activation and the MRN complex [53]. In the regulation of Tel1/ATM, the MRX/MRN complex plays different roles. First, it is responsible for the correct recruitment of the kinase at the site of damage. This happens through the interaction between Tel1 and the C-terminal region of Xrs2/Nbs1 [44,54]. In fact, yeast *xrs2-11* mutants, lacking Xrs2 C-terminus, show impaired Tel1 recruitment to DSB [44]. In addition, as ATM exists as an inactive dimer, it has been proposed that the MRN complex stimulates the shift between inactive dimers to active monomers [54]. In this context, the MRN complex is important to tether DNA ends together and to increase local concentration of DNA. This increase in DNA concentration plays an important role for ATM activation. Furthermore, NBS1 recruits ATM and may act as a specific cofactor for its activation [55]. In this context, it has been demonstrated that the FHA domain of Xrs2 is able to activate Tel1, independently of its C-terminal domain [56]. Studies in yeast have demonstrated that the MRX binding to specific DNA structures formed after genotoxic treatments, like DNA-protein adducts that arise following CPT action, has a stimulatory effect on Tel1 [50]. In addition, *in vitro* studies showed that, in the presence of the MRN complex, ATM can be activated by

long DNA tracts [53]. The role of MRN in this activation is not well understood but additional interactions between RAD50 and ATM could be in part responsible for ATM stimulation [53]. In both yeast and mammals there are evidences that the stimulation of Tel1/ATM activity is independent of the nuclease activity of MRX/MRN [44,50,53].

In summary, once a DSB occurred, the MRX/MRN complex binds to the damaged extremity of the broken DNA, thanks to the DNA binding activity of Mre11 and Rad50. Here, MRX/MRN is able to recruit and activate Tel1/ATM either directly, by Xrs2/NBS1 interaction with Tel1/ATM, and indirectly, by tethering together the DSB ends. Once activated, Tel1/ATM phosphorylates different substrates in order to support the propagation of the checkpoint signal.

3.2 Mec1/ATR, a secondary player in checkpoint activation in response to DNA double strand breaks

Mec1/ATR belongs to the PIKKs kinase family, together with Tel1. Indeed, structural studies demonstrated that Mec1 and Tel1 assume a similar structural architecture with a head region comprising the FAT, kinase, and FATC domains, as well as the curved arm region consisting of large stretches of the N-terminal HEAT repeats [57]. Although Mec1/ATR is mainly activated by replication stress, its activation can be promoted also by DNA DSBs. In fact, yeast Mec1 can be recruited to an HO-induced DSB, whereas ATR foci can form after IR treatment [58,59]. In both yeast and mammals, recruitment of Mec1/ATR at the DSB sites requires the presence of ssDNA, coated by a highly conserved protein complex named Replication Protein A (RPA). This ssDNA-RPA is usually generated by repair processes, like DNA end resection [60] (see par. 4.3). Mec1/ATR recognition of RPA-ssDNA depends on another protein, Ddc2/ATRIP [60]. Ddc2 was first discovered in yeast as a checkpoint protein able to interact with Mec1 and then identified in mammalian cells [61,62]. Biochemical studies have then clarified the interaction between Mec1/ATR, Ddc2/ATRIP and RPA [63]. In particular, a highly conserved domain in the N-terminus of Ddc2 and ATRIP, named checkpoint protein recruitment domain (CRD), is able to interact directly with RPA and to recruit to the site of damage Mec1 and ATR.

The importance of this partnership is underlined by the fact that, in both yeast and mammals, loss of Ddc2 or ATRIP, results in the same phenotype as the loss of Mec1/ATR, suggesting that Mec1-Ddc2 and ATR-ATRIP interaction should be considered mandatory for all the known function of the kinase [61,62]. Although RPA-ssDNA might be sufficient for Mec1/ATR localization to the site of damage, studies in *Xenopus* egg extracts demonstrated that it is not sufficient for ATR activation [64]. In fact, studies in budding yeast have demonstrated that two other proteins contribute to Mec1 activation: Dpb11 and Ddc1 [65]. Ddc1 forms an heterotrimeric complex, together with Mec3 and Rad17, that shows a similar structure to the one of the proliferating cell nuclear antigen (PCNA). This complex is conserved in vertebrate cells and is named 9-1-1. In fact, the mammalian orthologs of the yeast proteins are RAD9, HUS1 and RAD1 [65]. Loading of the complex onto DNA requires the clamp loader formed by the proteins Rfc2-5 and Rad24. Once a DNA lesion has occurred, the Rad24-RFC complex is able to load the 9-1-1 complex at the edge of ss/ds-DNA junctions. Biochemical studies conducted in *S. cerevisiae* showed that the loading of the 9-1-1 complex on the DNA is both required and sufficient for Mec1 activation. Indeed, the Ddc1 subunit of the clamp physically interacts with Mec1 and is responsible for its activation [66]. Moreover, RPA enhances Mec1 activation by the 9-1-1 clamp, likely by bringing Mec1 into close proximity with Ddc1 through RPA-Ddc2 interaction [65]. On the contrary, there are no evidences of conservation in the interaction between the mammalian 9-1-1 complex and ATR. Anyway,

biochemical studies, using *Xenopus* egg extracts, demonstrated that ATR activation is driven by primed ssDNA and not by ssDNA, suggesting a possible direct involvement of the 9-1-1 complex in ATR activation [64]. In this context, studies have shown that HUS1$^{-/-}$ mouse embryo fibroblasts (MEF) and RAD9$^{-/-}$ embryonic stem (ES) cells have checkpoint activation defects and are sensitive to genotoxic agents [67].

In mammalian cells, a key player in ATR activation is the topoisomerase binding protein 1, TopBP1. *In vitro* experiments have demonstrated that purified TopBP1, incubated with ATR, can induce its activation without the requirement of RPA or DNA, indicating that TopBP1 is a direct ATR activator [68]. TopBP1 displays different BRCT domains (breast cancer 1 C-terminal domain) that can mediate protein-protein interaction and two of these BRCT domains, BRCT6 and BRCT7, contain the ATR activating domain (AAD) [68]. Protein mapping and mutational studies showed that the activation of ATR by TopBP1 is mediated by interactions with both ATR and ATRIP [65]. TopBP1 recruitment to the site of damage is mediated by the 9-1-1 clamp. In particular, an N-terminal region of TopBP1 containing BRCT domains I and II binds to the phosphorylated C-terminal domain of RAD9 [69]. The importance of this interaction for checkpoint activation is highlighted by the fact that checkpoint defects of avian RAD9$^{-/-}$ cells can be suppressed by the fusion of the AAD domain of TopBP1 with histone H2A, indicating that inducing TopBP1-ATR interaction is sufficient for ATR activation [65].

TopBP1-mediated activation of ATR is conserved also in *S. cerevisiae* where the Ddc1 subunit of the 9-1-1 complex recruits the TopBP1 ortholog Dpb11 at the site of the lesion [70]. Indeed, biochemical studies not only demonstrated a physical interaction with Dpb11 and Mec1, but also pointed out that Dpb11 is sufficient for the kinase activation even if RPA coated DNA is not present [70]. Anyway, differently from its mammalian counterpart, a minimal activation domain has not been identified yet for Dpb11. A Dpb11 mutant protein that lacks the C-terminal part, fails to activate Mec1, indicating that this region may contain a sort of activation domain [65]. Recruitment of Dpb11 at the site of damage requires the interaction with Ddc1. This interaction needs the phosphorylation of Ddc1 by Mec1, suggesting a partial activation of Mec1 even in the absence of Dpb11 [71]. Indeed, despite the physical interaction, mutations in both Ddc1 and Dpb11 show a positive genetic interaction with regards to genotoxic sensitivities [72]. Therefore, these evidences suggest that, at least in yeast, following a DNA damage, the ssDNA generated by the repair pathways can recruit Mec1-Ddc2 by physical interaction with RPA. The region between ss-DNA and ds-DNA recruits the 9-1-1 clamp that sustains Mec1 activation through Ddc1. At the same time, phosphorylated Ddc1 recruits Dpb11 that, in turn, can support Mec1 activation.

On the contrary, in mammalian cells, evidences for a direct role of the 9-1-1 complex in the activation of ATR are lacking. Anyway, 9-1-1 is

important for TopBP1 recruitment, which in turn is the master activator of the ATR kinase.

3.3 Chromatin modifications and recruitment of the Rad9/MDC1 mediator after Tel1/ATM and Mec1/ATR activation

In yeast, once Tel1/ATM and Mec1/ATR have been activated, they phosphorylate a plethora of substrates. Among them, one of the first phosphorylation event is the one of the H2A histone on serine 129 (ɣ-H2A) [8]. Moreover, using a specific yeast strain in which a single inducible DSB can be created at the *MAT* locus, it has been demonstrated that phosphorylation of H2A depends on both Tel1 and Mec1 and spreads over a region of 50 kb of chromatin surrounding the break [73]. Substitution of the serine 129 with the non-phosphorylable alanine results in an increased sensitivity to genotoxic agent [74]. Phosphorylation of histone H2A is conserved also in mammalian cells where the serine 139 becomes phosphorylated upon DNA damage in an ATM and ATR dependent manner [75]. Similarly to what happens in yeast, mammalian cells that are deficient for the H2AX variant of the H2A histone, are radiosensitive and display high levels of genomic instability. Moreover, $H2AX^{-/-}$ mice are radiation sensitive, growth retarded, immune deficient and mutant males are infertile [8,16,76]. All these data clearly support a role in genome stability maintenance for this chromatin modification. Studies, conducted in different systems, have pointed out that the importance of H2A phosphorylation lies in its ability to be recognized by different proteins. In this way, it can support both repair and checkpoint activation [75].

In terms of checkpoint activation, ɣ-H2A recruits the mediator protein Rad9, in *S. cerevisiae*, and MDC1 in mammalian cells. Mediators are a class of checkpoint proteins that have the role to propagate the checkpoint signal from apical to effector kinases.

S. cerevisiae RAD9 was one of the first checkpoint genes identified. In particular, *rad9* mutant cells are unable to stop the cell cycle in response to IR-irradiation [77]. Later studies have demonstrated that Rad9 is able to physically interact with the effector kinase Rad53, acting as a scaffold that allows Rad53 activation by Tel1 and Mec1 [78]. Nowadays, different works in budding yeast have elucidated the molecular details of Rad9 recruitment to damaged chromatin and its role in the DNA damage checkpoint. Rad9 is a protein of 148 KDa that displays in its C terminus, a tudor domain and a BRCT domain that can mediate protein-protein interactions. Following DNA damage, two parallel pathways act to recruit Rad9 to chromatin; one is dependent on histones modifications and the other is dependent on the interaction with Dpb11[8].

The histone dependent recruitment of Rad9 relies on two histone post-translational modifications: the constitutive methylation of the lysine 79 of histone H3 and the formation of ɣ-H2A upon DNA damage.

In contrast to histone H2A, which is phosphorylated in a DNA-damage dependent manner, methylation of histone H3K79 is constitutive and is mediated by the conserved histone methyltransferase Dot1 [8]. Rad9 binds to H3K79me through its tudor domain and mutations that abrogate this binding show the same phenotype as the deletion of

DOT1. Indeed *dot1* and *rad9* mutant cells show the same impairment of the activation of the G1-DNA damage checkpoint, with *rad9* mutation being epistatic to *dot1* mutation [79,80].

In addition, Rad9 is able to bind phosphorylated H2A-S129 through its BRCT domain. Similar to the interaction with H3K79me, both mutations in the BRCT domain or the presence of a non-phosphorylable H2A allele show the same phenotype, that is a defective G1/S DNA damage checkpoint [81,82]. Moreover, combination of the *rad9-Y798A* allele, defective in H3K79me interaction, with the *rad9-K1088M* allele, defective in ɣ-H2A interaction, results in the same phenotype of each single domain-mutant, indicating that the two modifications work in the same pathway for checkpoint activation [81]. How the two domains work together for checkpoint activation remains to be determined and, to date, different interpretations for the contribution of each single domain are available [81,82]. Anyway, mutations in both BRCT and tudor domain of Rad9 do not result in complete checkpoint impairment. This is because Rad9 could be recruited to DSB by an histone independent pathway based on the interaction between Rad9 and Dpb11. This interaction relies on the Mec1 dependent phosphorylation of the C terminus domain of Dpb11. This event creates a docking site for the BRCT domains of Rad9 [71]. Anyway, some concerns were raised by the fact that in *mec1 tel1 sml1* cells the interaction between Rad9 and Dpb11 is not compromised at all [8]. In this context, Rad9 can be phosphorylated by CDK in a cell-cycle dependent manner. Recently, these CDK phosphorylation sites have been implicated in

supporting Rad9-Dpb11 interaction after genotoxic treatment. Cells harboring the *rad9-aa* allele, that cannot be phosphorylated by CDK, and those with the deletion of *DOT1,* fail to activate DNA damage checkpoint after genotoxic treatment [83]. This indicates that CDK phosphorylation of Rad9 supports Rad9 binding to Dpb11 and contributes to activate the DNA damage checkpoint in a pathway independent of histone modifications. Furthermore, it was recently shown that the interaction between Rad9 and Dpb11 can be also induced by phosphorylation events on Rad9 that are independent of CDK and Mec1 or Tel1, indicating that the regulation of this interaction is complex and not fully understood yet [84].

Once recruited to damaged DNA by the described pathways, Rad9 becomes phosphorylated by Mec1 and Tel1 in the S/TQ cluster domain (SCD). This Rad9 phosphorylation sites are selectively required for activation of the Rad53 effector kinase [85].

Furthermore, phosphorylated Rad9 can be bound by Rad53 that, in this way, moves close to Tel1 and Mec1 increasing the likelihood to be phosphorylated and thus activated [78]. Indeed, Rad9 acts as a mediator that can propagate the Mec1 and Tel1 signal to the effector kinase Rad53.

To date, the most important mediator protein in mammalian cells is MDC1 [86]. Mediator of DNA damage checkpoint (MDC1) is 2089 aa protein that appears to be the most important ɣ-H2A binding factor in mammalian cells. Similar to *S cerevisiae* Rad9, the BRCT domains located in MDC1 C-terminus are responsible for the interaction with

modified histone. Moreover, point mutations in a specific region of the BRCT domains abrogate MDC1 γ-H2A interaction [87]. Interestingly, the inhibition of this interaction compromises the association of several DDR factors like ATM, MRN and other mediator proteins like 53BP1 and BRCA1. Moreover, ATM phosphorylates MDC1 in response to DNA damage and depletion of MDC1 results in checkpoints defects [86,88,89]. These and other evidences [90] suggest that MDC1 is implicated in DNA damage checkpoint activation.

How MDC1 supports DNA damage checkpoint activation?

Even if different, and sometimes opposite, works exist in literature, it seems that the answer relies on the ability of MDC1 to localize and maintain in close proximity different checkpoint proteins. For example, MDC1 is able to physically interact with NBS1 upon phosphorylation [91]. Moreover, abrogation of this interaction results in a compromised MRN complex recruitment and checkpoint defects [90]. However, it is not clear how the MDC1-MRN complex can support checkpoint activation. It is possible that the MRN dependent recruitment of ATM can be the more reasonable explanation. In this context, MDC1 was reported to interact with ATM through its N-terminal FHA domain [88]. In addition, like scRad9, MDC1 can support checkpoint activation by recruiting in ATM in proximity to the effector kinase CHK2 [89]. Moreover, phosphorylated MDC1 is recognized by the ubiquitin ligase RNF8. RNF8, in turns, through ubiquitilation events can recruit RNF168 that, thanks to its stronger ubiquitilating activity, is responsible

for an indirect recruitment of both 53BP1 and BRCA2, two other mediator proteins [90,92].

Even if the exact mechanism of MDC1-mediated checkpoint activation needs much more details to be fully clarified, the importance of this factor in the DDR is highlighted by the fact that MDC1 knock out mice suffer from an increased tumor frequency. Furthermore, loss of function mutations in MDC1 are found in a significant portion of carcinomas [90].

Even mammalian 53BP1 and BRCA1 have been listed as scRad9 orthologs. Loss of function mutations of both 53BP1 and BRCA1 result in DNA damage checkpoint defects but how they can support checkpoint activation remains to be elucidated [69,93,94].

The picture of mediators in mammalian cells seems more complicated than in budding yeast and further studies are needed to shed light on the molecular details that sustain checkpoint activation. In fact, even if protein sequence and domains organization define as Rad9 orthologs, 53BP1, BRCA1 and MDC1, it seems that, during evolution, the role of these proteins has diverged with 53BP1 and BRCA1 being more implicated in the repair of damaged DNA than in signaling.

3.4 Activation of the effector kinases Rad53/CHK2 and Chk1

The DNA damage checkpoint cascade ends with the activation of the two effector serine threonine kinases Rad53/CHK2 and Chk1/CHK1.
In yeast, the principal effector kinase is Rad53 [8,95]. Rad53 was the first checkpoint kinase isolated and, currently, orthologs have been identified in almost all eukaryotes [96]. Rad53 belongs to the Chk2 family of ser/thr kinases, whose components share function and structure. Structurally, at the amino terminus Chk2-like kinases show an SQ/TQ cluster domain (SCD) which is composed by a series of serine or threonine residues followed by glutamine that create a consensus sequence for Tel1/ATM and Mec1/ATR kinases. Following the SCD domain, the forkhead-associated domain (FHA) is responsible for protein-protein interactions by binding phospho-threonine residues. Interestingly, Rad53 is the only Chk2-like kinase that owns a second FHA domain at the C-terminus. The kinase domain occupies a large part of the carboxy terminal domain. It is highly conserved in all eukaryotes and different specific mutants with a compromised kinase activity have been isolated in both yeast and human [95,96]. At the moment, the model of Rad53 activation is based on its interaction with the mediator protein Rad9. In particular, once Mec1 and Tel1 become activated by DNA damage, they phosphorylate Rad9 in its SCD [85]. This event creates a docking site for the FHA domains of Rad53 recruiting the kinase in close proximity to Mec1 and Tel1. The Rad9-

mediated recruitment has two important effects on Rad53 activation. First, it allows Mec1 and Tel1 to phosphorylate Rad53 in its SCD domain, activating the kinase. Second, it recruits other Rad53 molecules by either Rad9 interaction or Rad53 interaction. This increase in Rad53 local concentration promotes Rad53 autophosphorylation *in trans*. Furthermore, Rad53 turns out to be phosphorylated at more than twenty residues with the most being auto-phosphorylation sites [78]. Once hyper phosphorylated, Rad53 is fully active and is released from Rad9 in an ATP dependent manner [97].

In mammals, CHK2 is phosphorylated by ATM after DNA damage on the priming site T68 and on other residues in the SCD domain. These phosphorylation events induce CHK2 dimerization through the binding of phosphorylated SCD domain of one monomer with the FHA domain of another [98]. Similarly to what happens in yeast, this dimerization promotes autophosphorylation at different residues that determines the complete activation of CHK2.

It is worth noting that Rad53 is activated by both Tel1 and Mec1 while CHK2 is activated only by ATM. This implies that, in yeast, Rad53 is activated in response to different genotoxic stresses while mammalian CHK2 is activated mainly in response to DNA DSBs [96,98]. Consequently, Rad53 is the principal effector kinase of the DNA damage checkpoint [8]. On the contrary, in mammalian cells the activation of ATR leads to a CHK1 dependent checkpoint response.

At the sequence level, CHK1 is highly conserved from yeast to human and shows an N-terminal kinase domain, a linker region, a regulatory

SQ/TQ domain and a C-terminal domain with a putative regulatory function [99]. CHK1 is activated upon phosphorylation on Ser-317 and Ser-345 by ATR but the exact mechanism of activation remains elusive. It seems that this phosphorylation promotes a conformational change that relieves the inhibition of the N-terminal kinase domain by the C-terminal regulatory domain [99,100]. In addition, other regulatory events have been described. For example, the protein Claspin can act as a direct activator of CHK1 or the splice variant CHK1-S can inhibit, by protein-protein interactions, the effector kinase [99]. Since ATR is activated by ss-DNA coated by RPA, CHK1 is activated mainly in the presence of replication stress (see par. 5) and in the presence of DNA damage in the G2 phase of the cell cycle.

Once activated, both CHK1 and Rad53/CHK2 can phosphorylate different substrates inducing different cellular responses. One of the most important event following checkpoint activation is the block of the cell cycle. This avoids that cells divide with damaged DNA or in the presence of unreplicated DNA. In this context, cell cycle can be blocked at G1-S transition or at G2-M transition.

Briefly, in both yeast and mammals, if DNA is damaged in the G1 phase of the cell cycle, there is the activation of Tel1/ATM and in turn of Rad53 and CHK2. In budding yeast, Rad53 phosphorylates the Swi6 regulatory subunit of SBF transcription factor, inhibiting it. Thus, G1/S phase cyclins are not transcribed and the B-type cyclin inhibitor Sic1 is not degraded [8]. In mammalian cells, activated CHK2 phosphorylates CDC25A phosphatase targeting it for proteasomal degradation. In this

way, the inhibitory phosphorylation of CDK2 persists and the cell cycle is blocked. Moreover, CHK2 can phosphorylate and stabilize p53 which, in turns, up-regulates the cell cycle inhibitor p21 [98].

When damage occurs in G2 phase of the cell cycle, then the creation of ssDNA is favored and the checkpoint response relies mainly on ATR. ATR activation promotes a CHK1 dependent checkpoint response. Activated CHK1 phosphorylates and activates the WEE1 kinase, leading to the inhibitory phosphorylation of CDK1. In addition, CHK1 phosphorylates the phosphatase CDC25C. This phosphorylation, inhibits the positive action of CDC25C on CDK1, thus strengthening its inhibition [100]. Moreover, activation of ATM can be induced even in G2 phase of the cell cycle and CHK2 can contribute to the G2/M checkpoint by a similar inhibition of CDC25C [98].

On the contrary, in yeast, the G2-M checkpoint halts the cell cycle by inhibiting the metaphase to anaphase transition [8]. In this context, both Rad53 and Chk1, interfere with the degradation of the securin Pds1 by blocking the separation of sister chromatids [8].

Even if the main effect of checkpoint activation is to block the cell cycle, Chk1 and Rad53/CHK2 can promote other important cellular responses like the activation of specific repair pathways, the induction of apoptosis or senescence and the stimulation of specific transcriptional responses [8,96,98–100].

DNA damaging agents are the most commonly used drugs for cancer therapies. Normal cells activate the DNA damage checkpoint in response to these agents. On the contrary, more than 50% of cancer

cells have an impaired G1 checkpoint and their survival relies on the G2-M checkpoint. For this reason, CHK1 and CHK2 inhibitors are currently under investigation alone or in combination with DNA-damaging agents, but, so far, none of them has given positive results due to high side effects [98,99]. Maybe, this is reflecting other physiological roles of the two kinases. In this context, different efforts should be needed to increase the specificity of CHK1 and CHK2 inhibitors in cancer treatment.

4 Repair of DNA double strand breaks

DNA DSBs are the most cytotoxic lesion that living cells have to face. Defects or failures in repairing this type of lesions result in detrimental chromosome rearrangements that can increase genome instability. Eukaryotic cells repair DNA DBSs mainly by two highly conserved mechanisms: Non Homologous End Joining (NHEJ) and Homologous Recombination (HR).

These two pathways are mutual exclusive. In fact, when a DNA DSB is channeled towards the HR then NHEJ is completely inhibited. The interplay between HR and NHEJ is influenced by the cell cycle stage at which the damage has occurred and more and more molecular details are emerging about this regulation [101,102].

4.1 Non Homologous End Joining

The repair of DNA DSBs by the NHEJ consists in the rejoining of the two broken DNA ends. Mechanistically, the process can be divided in three key steps: binding of specific factors to DNA ends, processing of broken strands and relegation.

In both yeast and mammals, the main DNA binding factor is the highly conserved Ku complex, an heterodimer composed by Ku70 and Ku80 proteins [103–105]. The Ku complex has an high affinity for DNA ends and its crystal structure has revealed that the heterodimer has a toroidal shape with a central hole that accommodates duplex DNA

[105]. The central DNA binding site is rich in positively charged amino acids and allows the binding in a sequence independent manner. Moreover, this feature supports the ability of Ku to slide away from DNA ends allowing the recruitment, in mammals, of the DNA-PK kinase [106]. Yeast cells deleted for Ku70 or Ku80 are completely defective in NHEJ even if they do not show any obvious sensitivity to genotoxic agents. On the contrary, *ku70* or *ku80* mutants cannot grow at high temperature, indicating a role for the Ku complex in other physiological processes [103].

In order to rejoin two DNA ends, the extremities of the break have to be held in close proximity. In mammalian cells, this is accomplished by the DNA PKcs-kinase [103]. It belongs to the PI3KK kinase family and it interacts with the KU complex with its C-terminal domain. DNA-PKcs is also able to bind DNA and autophosphorylation events have been linked to its regulation [106]. Anyway, the interaction between DNA-PKs molecules on the opposite DNA ends is necessary to tether DNA ends together. This activity is extremely important in the context of NHEJ, since the Ku complex cannot compensate for the absence of DNA-PKs in end tethering [103].

Yeast cells lack DNA-PKs and the end tethering activity is carried out by the MRX complex [103,104,107]. Plasmid repair assay showed that deletion of any components of the MRX complex causes a dramatic drop in NHEJ efficiency [104]. The tethering activity is carried out by two Rad50 molecules. As described in par. 3.1, Rad50 is an ATPase able to hydrolyze ATP in ADP. In the ATP bound state, the MRX

complex is in a closed conformation. This allows Rad50 molecules placed at opposite DNA ends to interact each through their zinc hook domain [108]. This interaction is responsible for maintaining the two DSB end tethered.

Most of DSBs have incompatible DNA ends that preclude direct ligation. DSB ends could be incompatible owing to chemical modifications, like DNA-protein adducts, or mismatching overhangs. In these cases, the two DNA ends cannot be simply rejoined together but need to be processed and to be made compatible. In both yeast and mammals, different proteins take part in this process.

For example, the mammalian nuclease ARTEMIS is recruited and activated by DNA-PKcs. It has both exonuclease and endonuclease activity with the latter being favored by the interaction with DNA-PKcs [105]. Other proteins, like the MRN complex, CtIP, the helicase WRN, the endonuclease FEN1 and the exonuclease EXO1 have been implicated in DNA processing. Enzymes like aprataxin, polynucleotide kinase and tyrosyl DNA phosphodiesterase 1 are able to modify the DNA ends at the base level [105]. In yeast, the most characterized NHEJ endonuclease is Rad27, ortholog of FEN1. Anyway, the activity of Mre11 endonuclease cannot be excluded [104]. Importantly, the activities of these proteins at DNA termini have an important consequence: the loss of tract of genetic information. This is a key concept in NHEJ mediated repair. In fact, since no homology directed repair steps is envisaged, this processing of DNA ends results in different modifications of the initial sequence. This makes NHEJ a

mutagenic repair process. In addition, nuclease digestion of little tracts of DNA is not often enough to give back compatible DNA ends. In this situation, a specific group of polymerase are recruited by direct interaction with the Ku complex. In mammalian cells, DNA polymerase μ (POLμ) and λ (POLλ) can fill the gaps left by the processing factor listed above [105]. These polymerases can incorporate both nucleotides or ribonucleotides in a template-independent manner. In yeast Pol4, that belongs to the same class of the mammalian POLμ and POLλ, acts in NHEJ [104].

Once the DNA ends have been processed, the ligation is carried out by the DNA ligase IV. In mammalian cells, the DNA ligase IV exists in a complex with the scaffold proteins XRCC4, XLF and PAAX. DNA ligase IV complex is recruited by KU to the DNA ends and is able to rejoin together blunt ends. Importantly, the presence of XLF and PAAX promotes the ligation of mismatched and non-cohesive overhangs [105,106]. In yeast, the relegation process is carried out by the Lig4-Lif1 complex. Differently from mammalian cells, this complex is recruited at DSBs mainly by a direct interaction between the Xrs2 subunit of the MRX complex and Lif1. Anyway, it has been shown that also the presence of Ku70 is required for Lig4-Lif1 recruitment to DNA [103].The current model of the NHEJ (**Figure 3**) provides that, once the break occurred, the Ku complex, thanks to its high DNA biding affinity, is recruited to the DNA ends. Here, it protects the extremity of the break from the uncontrolled attack of nucleases. Then, it acts as a scaffold for the recruitment of other key NHEJ factors. Among them,

the bridging factor DNA PKcs, in mammalian cells, is important to tether together the broken DNA ends. On the contrary, in yeast this is carried out by the MRX complex, which binds DNA independently of yKu. If the DNA ends are compatible, the Ligase IV complex is recruited. Otherwise, processing factors like nucleases and polymerases are recruited by protein-protein interactions with the Ku complex. Once their action has created joinable ends, DNA ligase can complete the repair process.

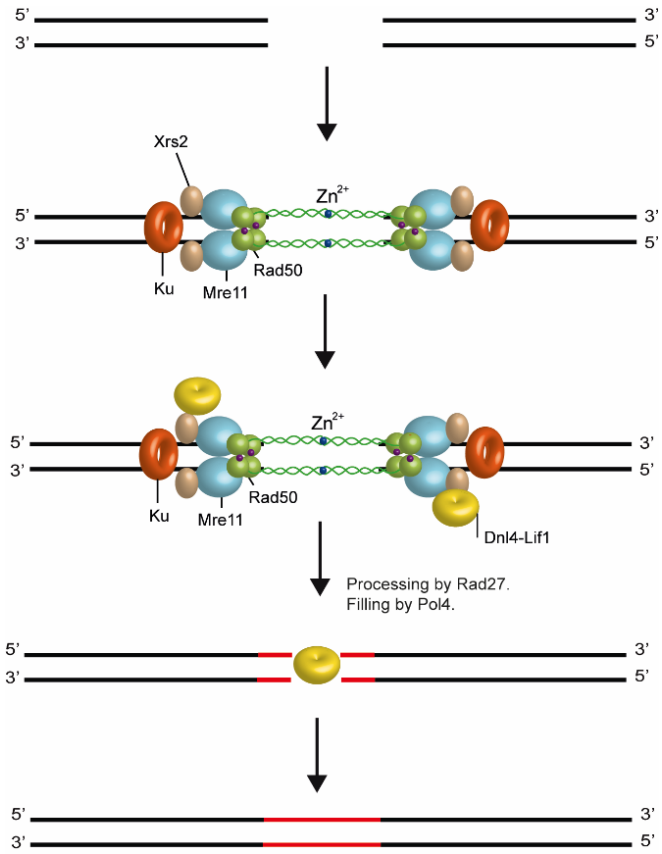

Figure 3 Non homologous end joining in *S. cerevisiae*.
After DNA double strand break formation, both the Ku complex and the MRX complex are recruited to the DSB ends. Ku protects the DNA ends from nucleases while the Rad50 subunit of the MRX complex tethers together the two broken ends. If the DNA ends are compatible, they are relegated by the action of the Dnl4-Lif1 complex, recruited by Xrs2. If the DNA ends are not re-joinable, they are processed by Rad27 and the gap filled by the low-fidelity DNA Pol4 (red lines). Subsequently, Dnl4 completes the repair process.

4.2 Homologous Recombination

The Homologous Recombination (HR) process could be defined as the repair of a DNA DSB using homologous sequences. Depending on which kind of homologous sequence is used as repair template, the HR process can lead to different genetic consequences. For example, if sister chromatids are used for repair, this results in sister chromatid exchange that is the more precise way to repair DSBs. Anyway, it could happen that repair occurs between misaligned repetitive sequences giving rise to unequal sister chromatid exchange, which can create deletions or duplications events. Furthermore, the use of homologous chromosome for HR may result in the loss of heterozygosity (LHO) that, for example, is associated with cancer development (see par. 1). In addition, if the recombination occurs between ectopic positions, which are sites with very low homology dispersed in the genome, this results in deletions, duplications, inversion and translocations. All these events are associated with genetic diseases and cancer. For these reasons, HR can be seen as a two side coin: on the one hand, it is an error free process for the repair of DSBs because it exploits the information on an homologous donor. On the other, if not controlled, it can generate genetic alterations that are associated with genetic instability.

Most of our knowledge about the molecular mechanisms of HR comes from studies of the mating type switching in *S. cerevisiae* [109]. Currently, different models of HR have been described: the double strand break repair model (DSBR), the synthesis-dependent strand

annealing (SDSA) and the break induce replication (BIR) (**Figure 4**) [110].

These three models differ each other for the repair outcomes but share some key steps:

- Nucleolytic processing of the extremity of the DSB to obtain ssDNA (DNA end resection)
- Formation of a recombinase ssDNA filament.
- Strand invasion and Holliday junction(s) creation.
- DNA synthesis.
- Resolution of the Holliday junction(s) and completion of the repair process.

Once a DNA DSB is created, in order to be channeled toward the HR repair pathway, the DNA ends are subjected to a complex processing that has the goal to create ssDNA. This processing is known as DNA end resection and the molecular details will be described in paragraph 4.3. This process involves large number of proteins with nuclease and helicase activities and it is tightly controlled. In fact, the ssDNA created by this process can be highly unstable and subjected to degradation. For this reason, in both yeast and mammals, the ssDNA created during resection is rapidly coated by the RPA complex [110,111].

Nevertheless, the so formed RPA-ssDNA is not able to invade the intact donor DNA. In fact, the strand-invasion reaction is catalyzed by the Rad51 recombinase. The structure of Rad51 is highly conserved among eukaryotes and resembles the one of RecA bacterial protein

with particular conservation of those residues that bind DNA and function in ATP hydrolysis [110].

The importance of this protein in DNA repair is highlighted by the high sensitivity of *rad51* yeast mutant cells to genotoxic agents. Moreover, *RAD51* is an essential gene in mammalian cells [111]. Similar to bacterial RecA, Rad51 assembles onto ssDNA or dsDNA to form a right-handed helical polymer that can span thousands of base pairs. Anyway, Rad51 is not able to displace RPA from ss-DNA because of the higher affinity for ssDNA and the higher concentration of the RPA complex respect to the one of Rad51 [112] . For this reason, in both yeast and mammals, the exchange between RPA and Rad51 requires other proteins known as mediators. The most important mediator in yeast is Rad52 [110,113]. Yeast cells deleted for *RAD52* are extremely sensitive to genotoxic agents. Different genetic and biochemical assays have demonstrated that Rad52 is able to interact with both RPA and Rad51 [110]. Mechanistically, it has been proposed that Rad52 forms a complex with Rad51 delivering it to the RPA-ssDNA complex. Moreover, since Rad52 works in multimers of 11 subunits it is able to put in close proximity at least eleven molecules of Rad51, increasing the likelihood of the exchange with RPA [110]. Other mediators like Rad55 and Rad57, have been identified in yeast and are able to mitigate the inhibition of Rpa1 on Rad51. In addition, the Shu complex, conserved only in *S. pombe*, has been implicated in the positive regulation of the Rad51 filament formation [113]. In mammals, the most important mediator is BRCA2 and loss of function mutations are

associated with ovarian and breast cancer [114]. BRCA2 binds RAD51 by two distinct domains: the BRC repeats and a carboxy-terminal domain, named CTRB. Moreover, BRCA2 is able to bind DNA with three OB fold domain and to interact with RPA with an N terminal region [110]. All these features resemble the ones of yeast Rad52 protein. Biochemical studies have defined that the BRC3/4 repeats possess recombination mediator activity. In this context, the two Rad51 biding domains cooperate to displace RPA from ssDNA in order to create the presynaptic filament [110]. Moreover, DSS1 and PALB2 work together with BRCA2 and support its mediator function. [113].

Once the pre-synaptic Rad51 filament has been assembled, there is the invasion of the intact DNA molecule. From studies conducted in *E. coli*, it is plausible that the homology search process occurs by random collisions between the Rad51 filament and the donor DNA. Once the interaction is stable, there is the formation of the synaptic complex. The Rad51-filament invasion induces the displacement of the same-polarity strand. This event creates a particular structure, known as D-loop that is extremely important for DNA synthesis. In yeast, all the steps of pairing, homology searching and D-loop formations are positively regulated by Rad54 [112] which is a member of the Swi2/Snf2 superfamily of proteins and has dsDNA-ATPase, DNA translocase and chromatin remodeling activities. In particular, it promotes the D-loop formation on chromatinized substrates and, *in vitro*, promotes the association between ssDNA and a double strand plasmidic DNA. Furthermore, Rad54 induces strand separation, thus facilitating the

pairing between Rad51 filament and the donor DNA. Rad54 is also able to negative regulate the binding of Rad51 on dsDNA, avoiding an incorrect use of Rad51 by the cell. Interestingly, once the synaptic complex is formed, Rad54 removes some Rad51 molecules at the 3'-OH filament in order to allow the binding of the DNA polymerase complex [112]. In this regard, genetic assay in yeast has allowed the study of the proteins required for DNA synthesis during HR. In particular, in the context of the D-loop the synthesis seems to be carried out by Polδ, even if with a lower processivity than the one showed during S-phase. In addition, there is also the requirement for the replicative proteins PCNA and Dpb11 [112]. At this point, different ways to conclude the HR repair exist (**Figure 4**). The first model proposed was the double strand break repair model (DSBR), in which the D-loop anneals with the other 3'-OH strand on the damaged molecule that was not engaged by the strand invasion process. This primes a second round of DNA replication and results in the formation of four way intermediates DNA molecules known as Holliday junctions (HJs). In order to complete the repair process, different nucleases and helicases have been implicated in the HJs resolution. HJs can be resolved by the action of two protein complexes: the yeast Mus81-Mms4 and Slx1-Slx4 complexes, orthologs of the human SLX1-SLX4-MUS81-EME1 complex, and the STR complex composed by Sgs1, TopIII and Rmi1 and their human orthologs BLM, TOP3α and RMI1/2 [115,116]. In the first case, HJ are resolved by an endonucleolytic cleavage. This way of resolution induces the formation of both cross-

over (CO) and non-cross-over products (NCO). In the second case, the concerted work of the Sgs1/BLM helicase and topoisomerase activity of TOP3 generates only non-cross-over products.

The Synthesis Dependent Strand Annealing (SDSA) model of HR was generated in order to justify the higher number of NCOs then the one of COs events. The SDSA model proposes that the 3'-OH strand invades the homologous donor forming the D-loop that, after limited DNA synthesis is displaced. If DNA synthesis has elongated enough the invading strand to allow the re-annealing with the damaged molecule, then the repair process is concluded by fill-in synthesis and ligation. Consequently, only NCO products are generated.

The last model of Homologous Recombination repair is the break induced replication (BIR). BIR is a recombination dependent replication process that results in nonreciprocal transfer of DNA from the donor to the recipient chromosome. During BIR only a single strand of one DSB end invades the homologous duplex and starts replication. This induces the migration of the D-loop. As far as the replication continues, using donor as template, the invading strands serves as template for the lagging-strand replication process. BIR can occur by several rounds of strand invasion, DNA synthesis, dissociation and it can lead to chromosome rearrangements when dissociation and reinvasion occur within repetitive inter-dispersed sequences [112].

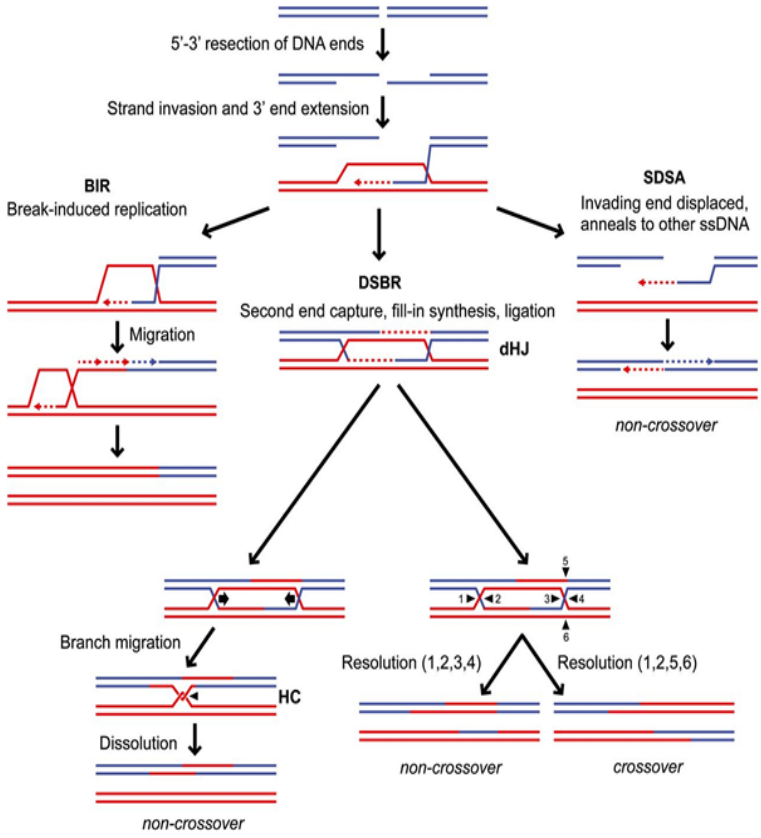

Figure 4 Models for homology-dependent DSB repair**.**
Homologous recombination repair of a DSB is initiated by 5' to 3' resection of DNA ends. The resulting 3' strand invades the homologous donor template (red). The strand invasion induces the displacement of the same polarity strand of the donor. This generates the displacement loop (D-loop) and the leading strand DNA synthesis starts. The classical double strand break repair (DSBR) model predicts that the displaced strand from the donor anneals with the complementary strand on the damaged DNA molecule. This allows a second round of DNA synthesis and generate a double Holiday junction intermediate (dHJ). Different ways of resolution of dHJ (numbers) give rise to Cross Over (CO) and Non Cross Over (NCO) products. If the D-loop is displaced after limited DNA synthesis, the invading strand reanneals with its original partner and the repair is concluded with gap filling (Synthesis Dependent Strand Annealing, SDSA). SDSA gives rise to only NCO products. In the break induced replication (BIR) model, a migrating D-loop is established together with a conservative DNA replication. Adapted from [112].

4.3 DNA-end resection: a crucial step in the HR dependent repair of DSBs

The HR mediated repair of a DNA double strand break starts with the nucleolytic degradation of both the 5' ends of the break in order to create long stretches of ssDNA. This process, named resection, involves the action of different proteins with different enzymatic activities that are well conserved throughout evolution.

According to the current model, DSB resection is a bidirectional two-step process. In the first step, named "short-range" resection, the MRX/MRN complex is recruited at DSB ends where, together with Sae2/CtIP, catalyzes an endonucleolytic cleavage of 50-300 nucleotides away from the DSB ends. Then, the Mre11 exonuclease degrades in the 3'-5' direction. In this way, the MRX/MRN complex provides an entry site for the nucleases Dna2/DNA2 and Exo1/EXO1. Furthermore, it has also a structural role in allowing their recruitment to the DSB. Once recruited, Exo1/EXO1 and Dna2/DNA2, with the help of the helicase Sgs1/BLM, degrade DNA in the 5'-3' direction creating long stretches of ssDNA. This second phase is known as "long range resection". The "short range" resection is of fundamental importance in the presence of complex DNA ends, like in the presence of protein-DNA adducts. On the contrary, at enzyme-induced DSB, the nucleases implicated in long range resection can process DNA without the presence of the MRX/N-Sae2/CtIP complex [26,112,117].

Once a DSB is subjected to nucleolytic degradation its fate is sealed. In fact, DNA end resection commits DSB repair to HR preventing NHEJ [111]. Therefore, the resection process must be strictly controlled. In fact, if resection takes place in G1 phase of the cell cycle, when only the homologous chromosome is available, then the chances of an incorrect repair will increase because the recombination will happen between two non-homologous sequences. Furthermore, resection must be controlled also in the S/G2 phase of the cell cycle as an excessive generation of ssDNA could be detrimental for genome stability. In fact, recent studies have demonstrated that in some tumor types there are evidences of clustered mutations (kataegis) that are associated with the action of deaminase APOBEC3A/B on ssDNA [118]. Moreover, the control of the resection process acquires an extremely high importance when DNA damage occurs during DNA replication (see par. 5). In fact, an excessive resection can induce the destabilization of the DNA polymerase and the inability to complete DNA replication (119).

4.3.1 End resection by MRX/MRN, Sae2/CtIP, Exo1 and Sgs1/BLM - Dna2

One of the first protein complex that binds DSB is the MRX/MRN complex [29]. As described in par. 3.1, it is formed by the Mre11, Rad50 and Xrs2/NBS1 proteins. Mre11 exhibits, *in vitro,* manganese-dependent endonuclease activity on double-stranded DNA. Moreover, Mre11 has a exonuclease activity with 3’ to 5’ polarity [117,120]. This

opposite polarity with respect to the one required for resection has created debate about the role of the Mre11 enzymatic activity, *in vivo*. The use, in budding yeast, of different Mre11 mutants with reduced or abolished endonuclease activity has revealed that the endonucleolytic activity is dispensable in the presence of DSBs with “clean ends”, like the one generated by endonucleases [111]. On the contrary, when the DSB termini are blocked by proteins such as the Ku complex or topoisomerases, the endonucleolytic activity of Mre11 becomes essential for a correct HR-mediated repair. In fact, *mre11* mutants defective in the endonuclease activity are sensitive to camptothecin, that extends the half-life of DNA topoisomerase cleavage complex, as well as to ionizing radiations that can generate single and double strand breaks or DNA-protein crosslink [112,121]. Furthermore, biochemical experiments with purified Mre11 from *Pyrococcus furiosus* have demonstrated that the endonucleolytic cleavage of 5’ strand by Mre11 is stimulated by protein blocks [120]. Since the nick is important for the access to blocked DNA ends of the downstream nucleases, the current resection model is based on a bidirectional processing of the DSB: on the one hand the processing by Mre11 in the 3’ to 5’ direction; on the other the processing of nucleases in the 5’ to 3’ direction. The same model was then confirmed in mammalian cells using different compounds able to inhibit the endonuclease or the exonuclease activity of MRE11 [122].

The enzymatic activity of Mre11 is influenced by Rad50 ATPase. As described in par.3.1, Rad50 associates with two α-helices of Mre11

located near the nuclease domain [108,111]. ATP binding and hydrolysis of Rad50 induces conformational changes in both Mre11 and Rad50. In fact, in the presence of ATP, Mre11 and Rad50 adopt a closed conformation, in which Rad50 head domains dimerize and occlude the nuclease active site of Mre11[120]. ATP hydrolysis drives a conformational change that induces the disengagement of Rad50 dimer and DNA melting, so that the Mre11 active sites can access DNA to initiate DSB resection [108,112,120]. In other words, ATP hydrolysis can switch from a “closed” MRX/N complex, where the nuclease action of Mre11 is inhibited, thus favoring the functions of the complex in checkpoint activation and in NHEJ repair (see par. 3.1 and 4.1), to an “open” MRX/N complex that promotes HR repair by initiating DSB resection. Since the ATP hydrolysis rate of Rad50 is quite low [120], it is plausible that, in the cellular environment, the complex is mostly in its closed conformation. Anyway, in budding yeast, it has been recently found that the telomeric Rif2 protein is able to increase ATP hydrolysis rate of Rad50, shifting the balance towards the “open” conformation [107]. The Xrs2/NBS1 subunit of the MR complex is the less conserved. Both Xrs2 and NBS1 are responsible for nuclear localization of Mre11 and for the interaction with Tel1/ATM. Moreover, both proteins contain BRCT and FHA domains that are separated from the ones that bind Mre11 and Tel1/ATM, indicating that it can modulate protein-protein interaction. In fact, both Xrs2 and NBS1 can bind the regulatory protein Sae2/CtIP [111]. A recent study conducted in yeast, has analyzed the effect of deleting *XRS2* on resection, checkpoint

activation and NHEJ. The results clearly demonstrate that Xrs2 is dispensable for resection but necessary for nuclear localization, Tel1 activation and NHEJ function of the MRX complex [123].

In both yeast and mammals, Sae2/CtIP has been implicated in the support of MRX/MRN complex function in DSB resection [124–126]. Structurally, both Sae2 and CtIP are predicted to be, for most of their sequence, intrinsically disordered proteins. They are able to oligomerize and to bind DNA and the MRX/MRN complex [126]. Moreover, different CDKs phosphorylation sites have been mapped on Sae2 and CtIP, suggesting a regulatory feedback on their protein activity. In this context, Sae2 Ser-267 must undergo phosphorylation to allow resection both *in vivo* and *in vitro* [121,127]. Yeast cells deleted for *SAE2* are sensitive to DNA damaging agents and show a delay in DSB resection initiation [128]. How Sae2 participates in DSB resection is still a matter of debate. A biochemical study by Cannavo and Cejka, demonstrated that Sae2 activates the endonuclease activity of Mre11 within the contest of the MRX complex. This function is dependent on the ATPase activity of Rad50 [129]. On the contrary, Paull and colleagues have biochemically demonstrated an endonuclease activity of Sae2. Furthermore, they have isolated specific *sae2* mutants with an impaired endonuclease activity [130,131]. Since no other laboratories, out of Paull's lab, have detected this enzymatic activity of Sae2, the biochemical role of Sae2 remains an open question. On the contrary, it is clear that deletion of *SAE2* results in a stronger phenotype then the one of *mre11-nd* mutants. The explanation for this

observation comes from different studies in which additional roles of Sae2 have been identified in end tethering, in yKU and MRX removal after DSB formation and in checkpoint activation [128,132–134].

As for Sae2, the role of CtIP in DSB resection is not completely understood. Cells depleted for CtIP are sensitive to DSB inducing agents and show defects in HR mediated repair [135]. CtIP is phosphorylated by CDKs and this phosphorylation is required only for its role as co-factor and not for its putative enzymatic activity. Upon CDK phosphorylation, CtIP interacts with the tumor suppressor BRCA1, an ubiquitin ligase whose role in DSB resection lacks molecular details. Moreover, it has been recently demonstrated that CtIP can positively influence the activity of long range resection nucleases [136]. To sum up, both Sae2 and CtIP promotes the initial step of DSB resection by influencing the activity of the MRX/MRN complex. Further studies are needed to investigate whether they have a more direct role in the processing of DSB ends through a putative endonucleolytic activity.

The MRX/MRN complex, together with Sae2/CtIP, is responsible for a limited nucleolytic degradation.

The more extensive resection is catalyzed by two nucleases Exo1 and Dna2 that act in two parallel pathways [137].

Exo1 is a member of the XPG family of nucleases. It shows 5'-3' dsDNA exonuclease activity and is able to degrade from a dsDNA end or an internal nick, releasing mononucleotide products. Two different studies conducted on reconstituted protein complexes *in vitro*

demonstrated that Exo1 is stimulated by both RPA and MRX complex [124,138]. RPA is able to stimulate Exo1 by avoiding non-productive Exo1-ssDNA bindings. On the contrary, the MRX complex promotes Exo1 DNA binding [138,139]. Exo1 has an affinity for 5' recessed DNA ends, that are created by Mre11 processing. In addition, MRX can create also branched structured by a putative helicase activity that are recognized by Exo1 [124]. Anyway, Exo1 activity is stimulated by the presence of both RPA and MRX complex, even in the absence of the nuclease activity of Mre11 [124].

In this context, recent data implicate the 9-1-1 checkpoint clamp complex in stimulating the activity of Exo1 [140,141].

Since yeast Exo1 exerts its nuclease activity starting from dsDNA, no helicase activity has been required for DNA unwinding. On the contrary, it has been demonstrated that the processivity of human EXO1 is increased by the action of the BLM helicase [142]. Moreover, human EXO1 is regulated by CDK dependent phosphorylations that restrict its action only in S/G2 phase of the cell cycle, and by DNA damage induced degradation [143,144]. Similarly, in yeast, Exo1 levels are controlled upon DNA damage by the RNA processing factor Npl3 [145].

Deletion of Exo1 in yeast does not result in any obvious DNA damage sensitivities. Moreover, the analysis of the resection process in *exo1*Δ cells show a residual nucleolytic degradation indicating that a parallel pathway of DNA processing exists. In this context, deletion of the Sgs1 helicase completely abolishes the long range resection process [125].

Sgs1 is an helicase that belongs to the RecQ helicases family that are able to unwind dsDNA by an ATP dependent 3'-5' translocation on the 3' terminated strand [146]. RecQ enzymes have three conserved domains that are commonly found in most helicases of this family: the core helicase domain, the RecQ-C-terminal (RQC) domain and the helicase-and-RNaseD-like-C-terminal (HRDC) domain. While the RQC domain has been implicated in protein stabilization and in DNA binding, the role of HRDC domain is not so clear and different biochemical studies have hypothesized that it mediates interaction with both DNA and other proteins [146,147]. Consistent with the fact that extensive resection is carried out by two parallel pathways, *sgs1* mutants are not extremely sensitive to genotoxic treatments. Anyway, combining *SGS1* deletion with the one of *SAE2* results in a synthetic lethality. Even if this has been attributed to defect in telomere replication [148], the current interpretation of this data is that cell death of the double mutant is caused by a strong defect in repairing endogenous DNA damage. In fact, the partially loss of function allele *sgs1-D664Δ,* which is defective in DSB resection, shows a strong negative genetic interaction with the deletion of *SAE2.* Moreover, this phenotype can be imputable to the resection defect of *sgs1-D664Δ* since overexpression of Exo1 suppresses the slow growth phenotype of *sae2Δ sgs1-D664Δ* double mutant [149]. Sgs1 interacts with Rmi1 and Top3 which are both required for DNA end resection activity *in vivo,* independently of the topoisomerase activity of Top3 [121,147]. In this context, it has been observed that the heterodimer formed by Rmi1 and Top3 strongly

stimulates Sgs1 helicase activity. Moreover, the MRX complex physically interacts with Sgs1 and can be involved in its recruitment at the DSB. In addition, it is also able to increase the helicase activity of Sgs1 supporting its function in end resection [150]. Furthermore, as for Exo1, biochemical and genetic data involves the 9-1-1 complex in supporting the resection function of Sgs1 [141]

The mammalian ortholog of Sgs1 is BLM. Mutations in this helicase are responsible for a recessive disease known as Bloom syndrome [147]. BLM inactivation in human cells treated with camptothecin results in a defect in RPA foci formation, indicating an involvement of BLM in the resection process [151]. Similarly to what happens in yeast, TOPOIIIα and RMI1, which form a complex with BLM, enhance the helicase activity of BLM whose recruitment to the DSB depends on the MRN complex [152,153]. Recently, also the WRN helicase has been implicated in DSB resection, in alternative to BLM [154].

In both yeast and mammals, the helicase activity of Sgs1/BLM is necessary for creating the right substrate for the nuclease Dna2/DNA2. Dna2 is a bifunctional helicase-nuclease responsible for removing DNA flaps arising during lagging strand synthesis. Moreover, Dna2 translocates in the 5'-3' direction and its acts as an endonuclease preferentially at free ssDNA 5' ends [155].

Its first involvement in the resection process was provided by Zhu and colleagues which demonstrated that Dna2 interacts with Sgs1 and is responsible for end resection [156]. Furthermore, using specific yeast mutants that abrogate the helicase activity, *dna2-R1253Q*, or the

nuclease activity, *dna2-E675A*, the same authors provided evidences that only the nuclease activity is required for DNA end resection. In contrast to this data, recently, two independent groups have provided biochemical and genetic evidences that the helicase activity of Dna2 supports its function in DNA end resection [157,158]. Biochemically, the Dna2 helicase activity helps the protein to be in proximity of the ssDNA-dsDNA junctions by fueling its translocation in the 5'-3' direction. This results in the formation of 5-100 nucleotides long degradation products. By contrast, abolishing the helicase activity results in the formation of products of 5-12 nucleotides [158]. Moreover, *dna2-hd* (helicase dead) mutants show a defective resection process in an *exo1*Δ background [157,158].

Dna2 has the ability to process both 5' and 3' DNA ends. In the context of the resection process, degradation of the 3' end would be against the polarity required by the resection. In any case, Dna2 correct polarity is maintained by the RPA complex whose binding to 3'-tailed DNA, promoted by Sgs1 unwinding, protects against Dna2 endonucleolytic activity on the 3' end [159]. These data lead to a model for Sgs1-Dna2 resection, where Sgs1 unwinds DNA moving in a 3'-5' direction. The 3' terminated ssDNA is rapidly coated by RPA that shields it from Dna2-endonuclease activity. On the contrary, Dna2 translocates with a 5'-3' polarity on the second strand unwound by Sgs1, that is in the same general direction of Sgs1 movement onto DNA. This translocating activity is supported by Dna2 helicase activity and allows the protein to

be next to ssDNA-dsDNA junction. In this way, the processivity of resection increases and the polarity is kept in the right direction.

Dna2 is highly conserved in mammalian cells where it is implicated in DNA end resection by interacting with BLM [152]. In addition to all the biochemical features already described from yeast Dna2, recent biochemical studies have demonstrated that mammalian DNA2 is able to increase the helicase activity of BLM [117,160]. Moreover, the activity of BLM-DNA2 complex is enhanced by both RPA and CtIP [136,152,153]. Interestingly, and differently from yeast, it was recently shown that DNA2 promotes long resection also by interacting with WRN [154,160] .

In conclusion, different proteins mediate DNA end resection in order to reach, at least in yeast, 2 to 4 kb of ssDNA at a rate of 4.4 kb per hour [111]. The biological meaning of obtaining such long strands of ssDNA could rely in the activation of DNA damage checkpoint and/or in increasing the likelihood to find the right annealing in the strand invasion step of the HR. This could be extremely important in that organisms whose genome is full of repetitive sequences.

4.3.2 Regulation of DNA end resection

The action of the nucleases involved in the resection process must be controlled in order to avoid the process to take place in G1 phase of the cell cycle and/or to produce excessive ssDNA.

The first level of regulation relies in the activity of the CDK-cyclin complexes. Evidences in yeast have shown that resection process is

controlled by the activity of CDK1 [137,161,162]. In this context, Sae2 and Dna2 show S-phase specific phosphorylations and are targets of Cdc28 mediated regulation of end resection [127,163]. In particular, Sae2 is phosphorylated on Ser267. Substitution of this serine with a non-phosphorylable alanine residue results in a phenocopy of *SAE2* deletion [127]. Which is the biological effect of this phosphorylation on Sae2 remains to be determined.

Similarly, substitution of Thr847 of CtIP with alanine impairs resection in human cells [164]. Differently from Sae2, CtIP presents 12 CDK consensus sites. In this context, S327 phosphorylation is required for subsequent damage-induced phosphorylation by ATM and/or ATR ensuring activation of CtIP at the correct cell-cycle stage. Moreover it is required for CtIP-BRCA1 interaction [165].

In yeast, CDK activity targets the endonuclease Dna2 at T4, S17, and S237 stimulating its recruitment to DSBs and, consequently, DNA-end resection [163]. Mutant cells harboring *dna2-T4A/S17A/S237A* allele are able to resect DSBs only in the presence of a functional Exo1. Interestingly, T4 and S17 lie within a bipartite nuclear localization signal, suggesting a timely regulated nuclear import of Dna2, upon phosphorylation, during G1/S transition [166]. Other resection factors have been found to be phosphorylated by CDK, like the MRN complex, RPA and EXO1. Anyway, only phosphorylation of mammalian EXO1 seems to have a proved regulatory role [166].

Even if only Sae2/CtIP, EXO1 and DNA2 activities have been shown to be influenced by CDK activity, the fact that the resection process is

strongly reduced in G1 phase of the cell cycle, even in the absence of NHEJ factors, like yKU, supports the hypothesis that the cell cycle stage controls the efficiency of the DSB resection.

Another level of resection control relies on the KU complex. The first evidence for KU involvement in resection control, came from the fact that deletion of *yKU70* is able to suppress the sensitivity to genotoxic agent of cells harboring a non-functional MRX complex, or cells deleted for *SAE2* [167]. This suppression requires mainly the action of Exo1. More details about this suppression originated from the isolation of different *yku70* mutants able to suppress the sensitivity to genotoxic agents of the *mre11-3* nuclease defective allele. Furthermore, they have been isolated as NHEJ proficient, demonstrating that the function in Exo1 inhibition and in the NHEJ repair are genetically separable [168]. Biochemical analysis of two of the mutants revealed that suppression of the sensitivities of the *mre11-3* nuclease defective allele depends on a reduced affinity for DSB ends and a propensity to diffuse inward on linear DNA. In these ways, the DSB ends are free and able to recruit Exo1[168]. These data lead to a model where Ku binding to DNA ends hides them from Exo1. In order to resection to take place, the activity of Sae2-MRX induces the displacement of the Ku complex from the DNA allowing Exo1 to initiate resection.

The inhibition of the Ku complex on Exo1 was also observed in human cells [169]. Furthermore, as in yeast, removal of KU by MRN is important for resection initiation in the presence of “dirty DNA ends” [139].

In yeast, DSB resection is inhibited also by the checkpoint protein Rad9 [170]. As described in par.3.3, Rad9 is recruited to damaged DNA in two different ways. One dependent on chromatin modifications and the other dependent on the interaction with Dpb11. Rad9 is able to interact with a methylated lysine on histone H3 (H3-K79), and with the phosphorylated serine 129 on histone H2A [82,170]. While the first modification is constitutive, the S129 phosphorylation is dependent on the Tel1 and Mec1 checkpoint kinases [8]. Inhibition of DSB resection by Rad9 requires its chromatin association as the lack of H3-K79 methyltransferase Dot1 or the presence of the non-phosphorylable variant *h2a-S129A* increases the resection efficiency [58,170]. On the contrary, deleting the chromatin remodeler Fun30 results in an increase binding of Rad9 and a defect in DNA resection [171–174]. Interestingly, a Cdk1 control on Fun30 was recently identified, linking the Rad9 regulation of resection with the Cdk1 control of resection [174]. Furthermore, Fun30 is recruited to DSB by physical interaction with Dpb11, which is also implicated in Rad9 recruitment [171]. Whether this can be another way of controlling Rad9 binding, remains to be determined. Studies on the human ortholog of Fun30, SMARCAD1, demonstrated that it has a positive effect on the resection process mediated by EXO1 [173]. Alteration of chromatin status is able to influence Rad9 binding. In fact, deletion of *RIF1* causes a decrease in DSB processing dependent on Rad9 [175]

In addition to Fun30, it has been demonstrated that the scaffold protein complex Slx4-Rtt107 is able to reduce Rad9 binding in the chromatin

surrounding DSB by competing for the binding to γ-H2A [176]. Consequently, deletion of *SLX4* and/or *RTT107* decreases the efficiency of resection [177].

Several lines of evidence indicate that Rad9 acts as a barrier toward end processing enzymes by restricting the access of Sgs1-Dna2.

First, the lack of Rad9 increases the resection efficiency also in a wild type context in a Sgs1-dependent manner [170,178]. Moreover, cells depleted for *SAE2* show a defect in resection initiation [132]. Furthermore, this defect causes an increase of Rad9 bound close to the DSB [178]. Deletion of Rad9 suppresses both the resection defect and the sensitivity to genotoxic agents of *sae2*Δ cells. Anyway, this suppression requires the activity of Sgs1, since its depletion makes *sae2*Δ *rad9*Δ cells sensitive again to genotoxic agents. Moreover, the identification and characterization of an Sgs1 mutant protein from our research group, strengthens the hypothesis that Rad9 inhibits the Sgs1-Dna2 pathway of resection (details are reported in the result section).

The human structural and functional ortholog of Rad9 in DSB resection is 53BP1. As Rad9, 53BP1 was reported to inhibit DNA end resection in the G1-phase of the cell cycle [179]. In particular, 53BP1 inhibits BRCA1-CtIP mediated resection by recruiting RIF1 at DSB sites [180,181]. Depletion of 53BP1 or RIF1 restores resection in BRCA1 depleted cells indicating that 53BP1 and RIF1 inhibit DNA end resection [181]. Anyway, phosphorylation and consequent activation of the BRCA1-CtIP complex in S-phase, displace 53BP1-RIF1 from DNA

ends, promoting resection. This evidence leads to a model in which 53BP1-RIF1 protects DSB ends from resection in G1 phase of the cell cycle, favoring NHEJ mediated repair. On the contrary, the activation of CtIP and BRCA1 induce the displacement of 53BP1-RIF1 facilitating the action of the MRX complex. More recently, other two 53BP1 interacting partners have been isolated and implicated in resection inhibition: PTIP and REV7/MAD2L2 [165,182].

In mammalian cells, another negative regulator of the resection process has been identified. In fact, the HELB protein is recruited to ssDNA by RPA and is able to inhibit both EXO1 and BLM-DNA2 mediated resection [183].

Another level of resection control, lies in the DNA damage checkpoint cascade (**Figure 5**). In fact, in both yeast and mammals, Mec1/ATR and Tel1/ATM, regulate the formation of ssDNA upon DSB creation. In yeast, deletion of *MEC1* accelerates DSB resection, whereas the presence of the hypermorphic allele *mec1-ad* impairs the process [58,184]. Mec1 can influence DSB resection at least in three ways: (a) by inducing Rad53 phosphorylation and activation, that, in turn, inhibits Exo1 [185]; (b) by promoting the binding of Rad9 through H2A-S129 phosphorylation, thus inhibiting resection; (c) by phosphorylation of different targets like Sae2, favoring the process [167]. Resection in *mec1*Δ cells is not as efficient as in *rad9*Δ cells, suggesting that Mec1 can also positively regulate DNA resection. On the contrary, the lack of Tel1 only slightly reduces the efficiency of resection [186]. This can be

ascribed to a recently identified role of Tel1 in structurally supporting MRX functions at DNA DSB, independently of its kinase activity [107]. Furthermore, the effect of the checkpoint on DSB resection becomes clear when the resection process is not completely efficient. In this context, *sae2*Δ cells, which suffer from a resection defect, show an increase in Rad9 binding close to the DSB and a persistent MRX association, which in turn induces an unscheduled Tel1 activation [133,134]. In this thesis, I provided evidences that hypomorphic mutations in *RAD53* and *TEL1* promote DSB resection acting on Rad9 recruitment at DSB ends . Moreover, Mec1 phosphorylation regulates also the recruitment of Slx4-Rtt107 complex favoring its persistence at DSBs instead of the one of Rad9 [187]. A similar mechanism has been individuated also in mammalian cells [187]. Furthermore, ATM and ATR regulate resection by phosphorylating CtIP, EXO1 and DNA2 [165]. Moreover, a resection mechanism regulated by ATR has been identified at telomeres [188]. In addition, in yeast, it was recently demonstrated that RNA processing proteins can influence the resection process acting on checkpoint activation [189].

In conclusion, checkpoint activation and DSB resection are two interconnected processes. In yeast, when a DSB occurs, the MRX complex recruits Tel1 and activates the DNA damage checkpoint by H2A phosphorylation and Rad9 accumulation at the DSB. Tel1, in turn, sustains the activity of the MRX complex by structural stabilization. The ssDNA created by Exo1 and Sgs1-Dna2 is covered by RPA and recruits Mec1. Therefore, as resection proceeds there is a shift from

Tel1 to Mec1 signaling. Mec1, in turn, phosphorylates histone H2A, recruits Rad9 and inhibits Exo1. This has two consequences: fueling of checkpoint activation and limiting of the accumulation of ssDNA. Limiting ssDNA means also checkpoint dampening. Therefore, checkpoint can both favor and limit ssDNA generation (**Figure 5**).

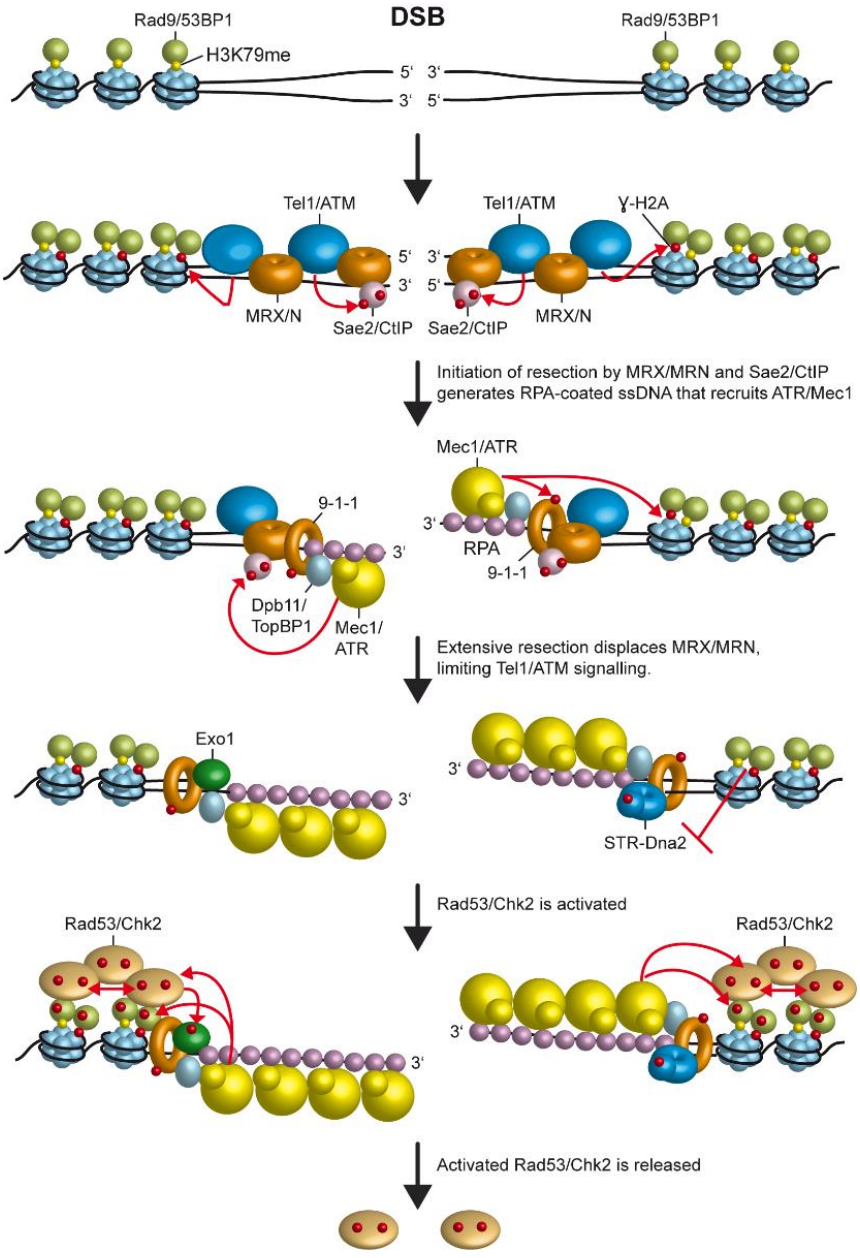
DSB
Rad9/53BP1
H3K79me
Rad9/53BP1
5'
3'
3'
5'
Tel1/ATM
Tel1/ATM
γ-H2A
MRX/N
Sae2/CtIP
Sae2/CtIP
MRX/N
Initiation of resection by MRX/MRN and Sae2/CtIP generates RPA-coated ssDNA that recruits ATR/Mec1
Mec1/ATR
9-1-1
RPA
9-1-1
Dpb11/ TopBP1
Mec1/ ATR
Extensive resection displaces MRX/MRN, limiting Tel1/ATM signalling.
Exo1
STR-Dna2
Rad53/Chk2 is activated
Rad53/Chk2
Rad53/Chk2
Activated Rad53/Chk2 is released

Figure 5 Interplays between checkpoint and DSB resection
Recognition of the DSB by MRX/MRN (MRX/N) leads to recruitment of Tel1/ATM, which phosphorylates histone H2A (γH2A). MRX/MRN and Sae2/CtIP start the resection process. Long range resection is carried out by Exo1, Sgs1-Top3-Rmi (STR) and Dna2. The ssDNA tails obtained are coated by the RPA complex. RPA-ssDNA recruits the Mec1-Ddc2/ATR-ATRIP complex. Tel1/ATM, acting on the MRX/MRN complex, promotes DSB resection, which activates Mec1/ATR and concomitantly inhibits Tel1/ATM signaling. Mec1/ATR activation requires Dpb11/TopBP1 and the 9-1-1 complex. The 9-1-1 complex is also implicated in recruiting Exo1 and STR-Dna2, promoting end resection. Once recruited to the DSB, Mec1/ATR regulates the generation of 3′-ended ssDNA by phosphorylating Sae2/CtIP and histone H2A.
γH2A induces the recruitment of Rad9 that inhibits STR-Dna2 dependent resection. Furthermore, Mec1 activates the downstream checkpoint kinase Rad53/Chk2 by phosphorylating Rad9 and Rad53/Chk2 itself. Moreover, phosphorylated Rad9/53BP1 promotes activation of Rad53/Chk2 by allowing its in-trans autophosphorylation. Activated Rad53 is then released from DNA and can regulate both DSB processing by phosphorylating and inhibiting Exo1 and its specific targets in the checkpoint cascade. Adapted from [26].

5 Maintenance of replication fork stability upon replication stress

DNA replication stress can be defined as the transient slowing or stalling of replication forks in response to a variety of situations like hard to replicate genomic regions, DNA lesions or in the presence of DNA replication inhibitors [190,191].

Replication fork arrest can be artificially induced by a variety of genotoxic agents such as hydroxyurea (HU), ultraviolet radiations, methyl methane sulfonate (MMS), camptothecin (CPT) and inter strand crosslinking agents such as mitomycin C. These agents induce fork arrest or collapse at much higher rate than endogenous agents and, for this reason, have been used in basic research to characterize the cellular response to replication stress. Recently, HU and CPT have been used as chemotherapeutics in order to reduce replication rate in cancer cells [191].

5.1 DNA replication checkpoint

To cope with replication stresses, cells activate an highly conserved transduction cascade named DNA replication checkpoint, whose main player is the Mec1/ATR kinase [28,191,192].

As depicted in par. 3.2, Mec1/ATR is activated by ssDNA. If at DNA DSB ssDNA is provided by the resection process, how ssDNA is formed at stalled replication forks?

Following HU treatment, yeast cells accumulate short tracts of ssDNA at the replication forks [193]. This ssDNA regions have been associated with the uncoupling of the leading and lagging strands polymerases [191,193]. Alternatively, biochemical studies using *Xenopus* eggs extract have provided evidences that these ssDNA regions are the result of the uncoupling between replicative helicases and polymerases [194]. In this context, electron microscopy (EM) analysis, in both yeast and *Xenopus* eggs extract, revealed that the average length of these ssDNA tracts reached 300 nt [195]. Anyway, fully activation of Mec1/ATR requires Dpb11/TopBP1 and the action of the 9-1-1 complex. Since it requires ssDNA/dsDNA junction to be recruited onto DNA, the uncoupling of replicative helicases and polymerases cannot fully justify checkpoint activation. The observation that DNA replication continues at a stalled fork through the synthesis and elongation of new primers, solved the problem [196]. In fact, using *Xenopus* eggs extract, it has been demonstrated that Polα primase can be hyper-loaded on both leading and lagging strand at stalled replication fork. New primers are then extended by replicative polymerase creating ssDNA/dsDNA junction that supports checkpoint activation by 9-1-1 and TopBP1 [196]. This model fits perfectly with agents that stall replication fork. Anyway other genotoxic treatments, like inter-strand cross-link, could block DNA replication without a significant uncoupling between helicases and polymerases because of the stalling of the helicases and not of the replisome. In these cases, active fork remodeling and DNA processing, such as resection and/or

fork reversal are capable of activating ATR. Fork reversal is a mechanism by which stalled replication forks reverse their direction by the annealing of nascent DNA strands [190,192]. This results in a four-way structure with the formation of a dsDNA ends that resembles the one of a DSB. In this context, if the lagging strand is shorter than the leading strand, a 5' ended ssDNA-dsDNA junction, responsible for ATR activation, would be formed. Furthermore, restart of reversed forks needs the activity of helicases, like RECQ1, translocases, like SMARCAL1, and the concerted activity of WRN helicase and DNA2 nuclease [190,192]. In particular, DNA2 is able to process reversed replication forks with a 5′-to-3′ polarity [197]. This ssDNA could activate ATR.

Thus, S-phase checkpoint activation can be sustained by uncoupling between leading and lagging strand polymerases, uncoupling between helicases and polymerases and by fork reversal. Moreover, other situations in which double strand breaks or single strand breaks occur in the proximity of DNA replication origin can create ssDNA by activating homologous recombination-mediated repair.

In addition to the already cited proteins that collaborate in ATR checkpoint activation and propagation, other proteins have been implicated, during S-phase, in the checkpoint cascade. For example, in budding yeast, Dna2 and Sgs1 were associated with checkpoint activation [198–200]. Moreover, Rad9 is substituted with Mrc1/Claspin for Rad53 activation [191].

In particular, a biochemical screen for Mec1 activators has identified Dna2 as a S-phase specific activator of the kinase [201]. This stimulatory activity is independent of both its nuclease and helicase activity and relies on two aromatic residues in its N-terminal domain, Trp128 and Tyr130 [201].

In both yeast and mammals, the mediator of the S-phase checkpoint is Mrc1/Claspin [8,191]. In yeast, Mrc1 is a replicative protein which is associated with the replisome even in unperturbed conditions. Following HU treatment, Mrc1 becomes hyperphosphorylated in a Mec1-dependent manner and interacts with Rad53 [191]. Mrc1 importance in Rad53 activation is highlighted by the isolation of an *mrc1-AQ* allele that cannot be phosphorylated by Mec1. Mutants harboring this allele are unable to induce Rad53 phosphorylation. In mammals, Claspin is recruited to stalled replication forks by Timeless and Tipin proteins. In particular, Tipin interacts with the RPA complex and recruits Timeless that, in turn, may recruit Claspin and CHK1 [8]. This increases the local concentration of CHK1, facilitating its phosphorylation by ATR.

In addition, works from Gasser lab demonstrated both genetically and biochemically that Sgs1 participates in the S-phase checkpoint activation in a parallel pathway to that of Mrc1, and supports checkpoint activation by interacting with both RPA and Rad53 in a Mec1 dependent manner [199,200]. Moreover, evidences have been provided for an implication of the replisome components in checkpoint activation. In fact, both the DNA polymerase ε and the helicases Mcm2-

7 contribute to a full activation of Rad53 upon replication stress [202,203].

Once replication checkpoint is activated, it exerts four main functions to promote survival to replication stress.

First, it induces cell cycle arrest. In yeast, this is achieved by the stabilization of the securin Pds1, required for sister chromatids cohesion. In mammals, cell cycle arrest is obtained by CHK1 dependent inactivation of CDC25 phosphatases (par.3.4) [28,203]. Anyway, delaying mitosis in *mec1* or *rad53* mutants does not suppress their strong sensitivity to HU, indicating that this checkpoint function is not essential for cell viability after replication stress [28].

Second, activation of the replication checkpoint induces an increase in dNTPs synthesis in both yeast and mammals. Deletion of budding yeast *SML1* suppresses lethality of *MEC1* deletion. Sml1 is an inhibitor of the RNR (ribonucleotide reductase) and is degraded in a Rad53 dependent manner. Moreover, Rad53 activation leads to the transcriptional activation of genes encoding for RNR subunits [191]. Similarly, in mammals, CHK1 activation induces the nuclear accumulation of RRM2 subunit of ribonucleotide reductase. Mouse models with increased RRM2 expression are somehow protected against HU treatment and ATR inhibitors, indicating that even in mammalian cells one of the function of the S-phase checkpoint is to increase the levels of nucleotides [204].

Third, activation of S-phase checkpoint inhibits late origin firing. This avoids cells experiencing a replication stress to conclude replication in

non-permissive conditions. Mec1/ATR can regulate origin firing by different ways; for example, in yeast, Rad53 inhibits both CDK- and DDK-dependent pathways, both required for origin firing [205]. This is also true for mammalian cells, where, in addition, ATR blocks origin firing by blocking the interaction of CDC45 with MCM helicases, that unwind DNA for replication initiation [192].

Lastly, S-phase checkpoint supports replisome stabilization. This is one of the still debated functions of the Mec1/ATR mediated checkpoint. In fact, different studies conducted in yeast have observed that *rad53* mutants treated with HU or MMS show abnormal DNA structures and are defective in DNA replication completion [206,207]. This phenotype leads to infer that, when the checkpoint is not functional, the replisome is unstable ad prone to collapse. In addition, chromatin immunoprecipitation (ChIP) assays performed in checkpoint mutants treated with HU, reported a reduced binding of Polε at early active Autonomously Replicating Sequences (ARSs) [199,200,208]. Anyway, two genome-wide studies conducted first in yeast and then in human cells have demonstrated that in Mec1/ATR defective cells the replisome stability is not altered [209,210]. Furthermore, Dungrawala and colleagues have established that even if the replisome stability is not altered, inhibiting ATR results in a recruitment of HR and NHEJ processing factor that can account for forks collapse [209]. In this context, in yeast, have been observed that viability of *mec1* cells relies on homologous recombination factors like Rad52 and the Sgs1 helicase [211,212]. An interpretation of these data could be that

Mec1/ATR, even without influencing the replisome composition and association to DNA, can regulate fork processing with a protective effect that avoids fork collapse.

Other roles have been assigned to the S-phase checkpoint, like controlling RNA-gating, avoiding the exhaustion of replication factor, regulating replisome function and promoting fork restart [191,192,213].

Going beyond models, what is extremely evident is that S-phase checkpoint has an huge impact on cell survival after replication stress. In fact, at least in yeast, *RAD53* mutations result in a very strong sensitivity to HU. On the contrary, inactivation of Rad53 has a weak effect on other genotoxic agents, indicating that Rad53 has an higher influence upon replication stress than upon DSB inducing treatment.

5.2 DNA end resection at stalled replication fork

In both yeast and mammals, nucleases have been implicated in the processing of stalled replication fork intermediates [190,191].

In yeast, resection of stalled replication forks is observed only in checkpoint deficient mutant. Moreover, *rad53* mutant cells treated with high concentration of HU revealed that around 40% of forks had experienced extensive resection. The 5% of them are in a bubble conformation with one side of the replication bubble being completely single stranded [214]. While extensive resection is associated with fork collapse and, thus, with poor survival after replication stress, controlled nucleolytic degradation can be beneficial for replication fork stability. In this context, yeast checkpoint deficient mutants accumulate reversed

fork intermediated that are considered to be pathological intermediates [191]. Different studies have analyzed the effect of deleting Exo1 nuclease in *rad53* mutant. Cotta-Ramusino and colleagues demonstrated that Exo1 is recruited at HU stalled replication forks. Moreover, combining molecular biology and EM approaches they discovered that the double mutant *rad53 exo1* accumulates aberrant replication fork structures that correlates with an increase in reversed forks, respect to the wild type strain [215]. Interestingly, deletion of *EXO1* diminished the number of replication bubbles with gapped molecules and hemi replicated bubbles with a completely single stranded region. This data indicate that checkpoint mutants accumulate detrimental ssDNA at replication fork in a Exo1 dependent manner. Anyway, abrogating Exo1 activity results in an increase in reversed fork. To correctly analyze this data, it must be taken in account that Rad53 inhibits Exo1 action [185]. In this context, in checkpoint mutants where Exo1 could be hyperactive, excessive resection induces degradation of stalled replication forks. On the contrary, deletion of the nuclease increases pathological fork reversal indicating that both over-processing and inefficient processing of replication intermediates are detrimental to cell survival upon replication stress. Thus, controlled resection of replication intermediate is important for replication fork stabilization. In this context, it has been shown that deletion of Exo1 is able to suppress sensitivity to MMS, UV and IR treated *rad53* mutant cells. On the contrary, deletion of Exo1 neither increases nor suppresses HU sensitivity of *rad53* cells [216].

This can be justified by the fact that while MMS, UV and IR induce fork stalling without leading to fork reversal, HU treated mutant cells accumulates pathological reversed forks. Consequently, Exo1 mediated resection could be detrimental in presence of stalled replication forks but has a sort of beneficial effect in avoiding reversal of replication fork. in this regard, it has been recently shown that Exo1, Dna2 and Sae2 dependent processing has a positive effect in avoiding reversed replication fork formation [217]. In particular, Exo1 and Dna2 can resect reversed nascent strand. This counteracts the formation of reversed replication forks that, once formed, can be processed by endonucleases like Mus81, Yen1 and Slx1 that induce DSB creation. Furthermore, it is conceivable that, at least in yeast, Exo1 and Dna2 can be involved in avoiding regression of stalled replication forks by digesting either the reversed arm or ssDNA generated by two replicative helicase, Rrm3 and Pif1, whose regulation is dependent on Rad53 activity [214].

The control of resection is important both at DSB and at replication fork. Nevertheless, while the molecular mechanism underpinning resection control at DSBs has been analyzed in depth, how resection is controlled at stalled replication forks and if DSB proteins share their function even at replication forks remains to be determined. In this thesis, I provided evidences that Rad9 is able to control resection at stalled replication forks, when the S-phase checkpoint is not fully functional.

In this direction, different studies conducted in mammalian cells have highlighted that proteins implicated in DSB resection can be responsible for fork processing and protection.

Differently from what is currently supposed in yeast, replication fork reversal in mammalian cells is considered a physiological event that supports cell survival after replication stress [190]. In this context, unscheduled resection conducted by the MRE11 nuclease has been associated to replication fork collapse [218–220]. Resection by MRE11 was firstly observed in BRCA1/2 or RAD51 deficient cells. In fact, BRCA1 and BRCA2 protect against MRE11 resection by promoting and stabilizing the RAD51 filament formation [218]. This conclusion has been supported by biochemical studies conducted in *Xenopus* eggs extract where the absence of RAD51 induces the formation of ssDNA gaps at replication forks [195]. *In vivo*, replication fork reversal mediated by SMARCAL1 and RAD52, creates the right substrate for MRE11 dependent resection [221,222]. In the absence of BRCA1, BRCA2 or RAD51, MRE11, together with CtIP and EXO1, is responsible for the over-processing that induces fork degradation [220]. Furthermore, other nucleases have been implicated in fork processing like DNA2, acting in a parallel pathway respect the one of MRE11, or FAN1 which, instead, acts downstream of it [190,197].

As observed in yeast, nucleolytic degradation is a double edge sword. In fact, if uncontrolled can lead to fork degradation and genome instability. On the contrary, a physiological activity of all the nucleases described above is required for replication fork restart and thus for

maintaining genome stability. For example, limited MRE11 activity avoids DSBs formation and promotes the removal of stalled polymerases supporting fork repriming mechanisms [119]. Furthermore, a limited resection is required for MUS81 processing that, in turn, promotes fork rescue [220].

In this context, WRN has been shown to both protect stalled replication fork from excessive resection and to support physiological processing by DNA2, enabling fork restart [223]. In particular, upon WRN nuclease inhibition, MRE11 and EXO1 dependent resection affects the ability to resume replication after replication stress. It has been proposed that, in the presence of replication stress, DNA processing by WRN could create a particular conformation of nascent strand that is resistant to MRE11 processing. Alternatively, the gaps created by the nuclease activity of WRN could promote RAD51 association. In this context, WRN can support RAD51 filament creation by its interacting partner WRNIP1 [224]. Furthermore, a non- enzymatic role of WRN has been demonstrated in protecting stalled replication fork from MRE11 activity [225]. Importantly, in wild type cells, the combined activity of WRN and DNA2 is important to create limited ssDNA necessary for fork restart [223].

Recently, another player in fork protection has been found. BOD1L associates with replication fork. Ablation of BOD1L increases resection at replication fork inducing genome instability. Moreover, genetical analysis have demonstrated that BOD1L acts in a parallel pathway respect the one of BRCA1 and BRCA2 in supporting RAD51 protection

function. In fact, it has been proposed that BOD1L, by physically interacting with BLM helicase, can inhibit its ability to dismantle RAD51 filament. In this context, in BOD1L depleted cells, the over-processing at stalled replication forks depends on the BLM-DNA2 axis [226].

It is evident that in both yeast and mammals the resection process must be tightly controlled at both DSB and stalled replication fork. In fact, the right balance between pro-resection factor and anti-resection factor is necessary to preserve genome stability in both contexts. Synthetic lethal approaches are a very promising tool to increase the power of chemotherapeutic treatments. Furthermore, agents that induce DNA damage or replication stress are currently the elicit therapies for cancer treatment. In this context, the identification of new pathways and the deep understanding of the molecular mechanisms that control repair upon DSB and replication stress inducing treatments will be of high importance to open new chances in cancer treatment.

Results

EMBO reports **(Bonetti, Villa *et al*., 2015)**
2015 Mar;16(3):351-61
doi:10.15252/embr.20143976

Escape of Sgs1 from Rad9 inhibition reduces the requirement for Sae2 and functional MRX in DNA end resection

Diego Bonetti *, Matteo Villa *, Elisa Gobbini, Corinne Cassani, Giulia Tedeschi & Maria Pia Longhese

Dipartimento di Biotecnologie e Bioscienze, Università di Milano-Bicocca, Italy.

* These authors contributed equally to this work

DNA double-strand breaks (DSBs) can be repaired by homologous recombination (HR), which uses undamaged homologous DNA sequences as a template for repair in a mostly error-free manner. The first step in HR is the processing of DNA ends by 5' to 3' nucleolytic degradation (resection) to generate 30 -ended single-stranded DNA (ssDNA) that can invade a homologous template [111]. This ssDNA generation also induces activation of the DNA damage checkpoint, whose key players are the protein kinases ATM and ATR in mammals as well as their functional orthologs Tel1 and Mec1 in *Saccharomyces cerevisiae* [27].

Initiation of DSB resection requires the conserved MRX/MRN complex (Mre11/Rad50/Xrs2 in yeast; Mre11/Rad50/Nbs1 in mammals) that, together with Sae2, catalyzes an endonucleolytic cleavage of the 50 strands [125,129,156]. More extensive resection of the 5' strands depends on two pathways, which require the 5' to 3' double-stranded DNA exonuclease Exo1 and the nuclease Dna2 working in concert with the 30 to 50 helicase Sgs1 [125,156]. Double-strand break resection is controlled by the activity of cyclin-dependent kinases (Cdk1 in yeast) [161], which promotes DSB resection by phosphorylating Sae2 [127] and Dna2 [163], as well as by ATP-dependent nucleosome remodeling complexes [227]. Recently, the chromatin remodeler Fun30 has been shown to be required for extensive resection [172,173,228], possibly because it overcomes the resection barrier exerted by the histone-bound checkpoint protein Rad9 [170,172,229]. The MRX/Sae2-mediated initial endonucleolytic cleavage becomes essential to initiate

DSB resection when covalent modifications or bulky adducts are present at the DSB ends and prevent the access of the long-range Exo1 and Dna2/Sgs1 resection machinery. For example, Sae2 and the MRX nuclease activity are essential during meiosis to remove Spo11 from the 50 -ended strand of the DSBs [230,231]. Furthermore, both *sae2Δ* and *mre11* nuclease-defective (*mre11-nd*) mutants exhibit a marked sensitivity to methyl methanesulfonate (MMS) and ionizing radiation (IR), which can generate chemically complex DNA termini, and to camptothecin (CPT), which extends the half-life of topoisomerase I (Top1)–DNA cleavable complexes [232]. CPT-induced DNA lesions need to be processed by Sae2 and MRX unless the Ku heterodimer is absent. In fact, elimination of Ku restores partial resistance to CPT in both *sae2Δ* and *mre11-nd* cells [167,233]. This suppression requires Exo1, indicating that Ku increases the requirement for MRX/Sae2 activities in DSB resection by inhibiting Exo1. To identify other possible mechanisms regulating MRX/Sae2 requirement in DSB resection, we searched for extragenic mutations that suppressed the sensitivity to DNA damaging agents of *sae2Δ* cells. This search allowed the identification of the SGS1-ss allele, which suppresses the resection defect of *sae2Δ* cells by escaping Rad9-mediated inhibition of DSB resection. The Sgs1-ss variant is robustly associated with the DSB ends both in the presence and in the absence of Rad9 and resects the DSB more efficiently than wildtype Sgs1. Moreover, we found that Rad9 limits the binding at the DSB of Sgs1, which is in turn responsible for rapid resection in *rad9Δ* cells. We

propose that Rad9 limits the activity in DSB resection of Sgs1/Dna2 and the escape from this inhibition can reduce the requirement of Sae2 and functional MRX in DSB resection.

Sgs1-ss suppresses the sensitivity to DNA damaging agents of sae2Δ and mre11-nd mutants

SAE2 deletion causes hypersensitivity to CPT, which creates replication-associated DSBs. The lack of Ku suppresses CPT hypersensitivity of *sae2Δ* mutants, and this rescue requires Exo1 [167,233], indicating that Ku prevents Exo1 from initiating DSB resection.

To identify other possible pathways bypassing Sae2 function in DSB resection, we searched for extragenic mutations that suppress the CPT sensitivity of *sae2Δ* cells. CPT-resistant *sae2Δ* candidates were crossed to each other and to the wild-type strain to identify, by tetrad analysis, 15 single-gene suppressor mutants that fell into 11 distinct allelism groups. Genome sequencing of the five non-allelic suppressor clones that stood from the others for the best suppression phenotype identified single-base pair substitutions either in the *TOP1* gene, encoding the CPT target topoisomerase I, or in the *PDR3*, *PDR10* and *SAP185* genes, which encode for proteins involved in multi-drug resistance. The mutation responsible for the suppression in the fifth clone was a single-base pair substitution in the *SGS1* gene (*SGS1-ss*), causing the amino acid change G1298R in the HRDC domain that is

conserved in the RecQ helicase family. The identity of the genes that are mutated in the six remaining suppressor clones remained to be determined.

The *SGS1-ss* allele suppressed the sensitivity of the *sae2Δ* mutant not only to CPT, but also to phleomycin (phleo) and MMS, resulting in almost wild-type survival of *sae2Δ SGS1-ss* cells treated with these drugs (**Figure 6A**). The ability of Sgs1-ss to suppress the sensitivity of *sae2Δ* to genotoxic agents was dominant, as *sae2Δ/sae2Δ SGS1/SGS1-ss* diploid cells were less sensitive to CPT, phleomycin and MMS compared to *sae2Δ/sae2Δ SGS1/SGS1* diploid cells (**Figure 6B**).

Besides providing the endonuclease activity to initiate DSB resection, MRX also promotes stable association of Exo1, Sgs1 and Dna2 at the DSB ends [234], thus explaining the severe resection defect of cells lacking the MRX complex compared to cells lacking either Sae2 or the Mre11 nuclease activity. Sgs1-ss suppressed the hypersensitivity to genotoxic agents of *mre11-H125N* cells, which were specifically defective in Mre11 nuclease activity (**Figure 6A**). By contrast, *mre11Δ SGS1-ss* double-mutant cells were as sensitive to genotoxic agents as the *mre11Δ* single mutant (**Figure 6A**). Altogether, these findings indicate that Sgs1-ss can bypass the requirement of Sae2 or MRX nuclease activity for survival to genotoxic agents, but it still requires the physical integrity of the MRX complex to exert its function.

Sgs1 promotes DSB resection by acting as a helicase [125,156], prompting us to investigate whether Sgs1-ss requires its helicase

activity to exert the suppression effect. Both the lack of Sgs1 and its helicase-dead Sgs1-hd variant, carrying the K706A amino acid substitution [235], impaired viability of *sae2Δ* cells [156] (**Figure 6C**). This synthetic sickness is likely due to poor DSB resection, as it is known to be alleviated by making DNA ends accessible to the Exo1 nuclease [167,233]. The K706A substitution was therefore introduced in Sgs1-ss, thus generating the Sgs1-hd-ss variant, and meiotic tetrads from diploid strains double heterozygous for *sae2Δ* and *sgs1-hd-ss* were analysed for spore viability on YEPD plates. All *sae2Δ sgs1-hd-ss* double-mutant spores formed much smaller colonies than each single-mutant spore (**Figure 6D**), with a colony size similar to that obtained from *sae2Δ sgs1-hd* double-mutant spores (**Figure 6C**). Thus, Sgs1-ss appears to require its helicase activity to suppress the lack of Sae2 function.

Suppression of sae2Δ by Sgs1-ss requires Dna2, but not Exo1

The ssDNA formed by Sgs1 unwinding is degraded by the nuclease Dna2, which acts in DSB resection in a parallel pathway with respect to Exo1 [156]. Thus, we asked whether the suppression of *sae2Δ* hypersensitivity to DNA damaging agents by Sgs1-ss requires Exo1 and/or Dna2. Although the lack of Exo1 exacerbated the sensitivity of *sae2Δ* cells to some DNA damaging agents (**Figure 6E**), the *SGS1-ss* allele was still capable to suppress the sensitivity to CPT, phleomycin

and MMS of *sae2Δ exo1Δ* double-mutant cells (**Figure 6E**), indicating the suppression of *sae2Δ* by Sgs1-ss is independent of Exo1. As DNA2 is essential for cell viability, *dna2Δ* cells were kept viable by the *pif1-M2* mutation, which impairs the ability of Pif1 to promote formation of long flaps that are substrates for Dna2 [236]. Diploids homozygous for the *pif1-M2* mutation and heterozygous for *sae2Δ*, *dna2Δ* and *SGS1-ss* were generated, followed by sporulation and tetrads dissection. No viable *sae2Δ dna2Δ pif1-M2* cells could be recovered, and the presence of the *SGS1-ss* allele did not restore viability of *sae2Δ dna2Δ pif1-M2* triple-mutant spores (**Figure 6F**). By contrast, tetrads from a diploid homozygous for the *pif1-M2* mutation and heterozygous for *sae2Δ*, *dna2Δ* and *ku70Δ* showed that the lack of Ku70, which relieved Exo1 inhibition [167,233], restored viability of *sae2Δ dna2Δ pif1-M2* spores (**Figure 6G**). These findings indicate that Sgs1-ss requires Dna2 to bypass Sae2 requirement.

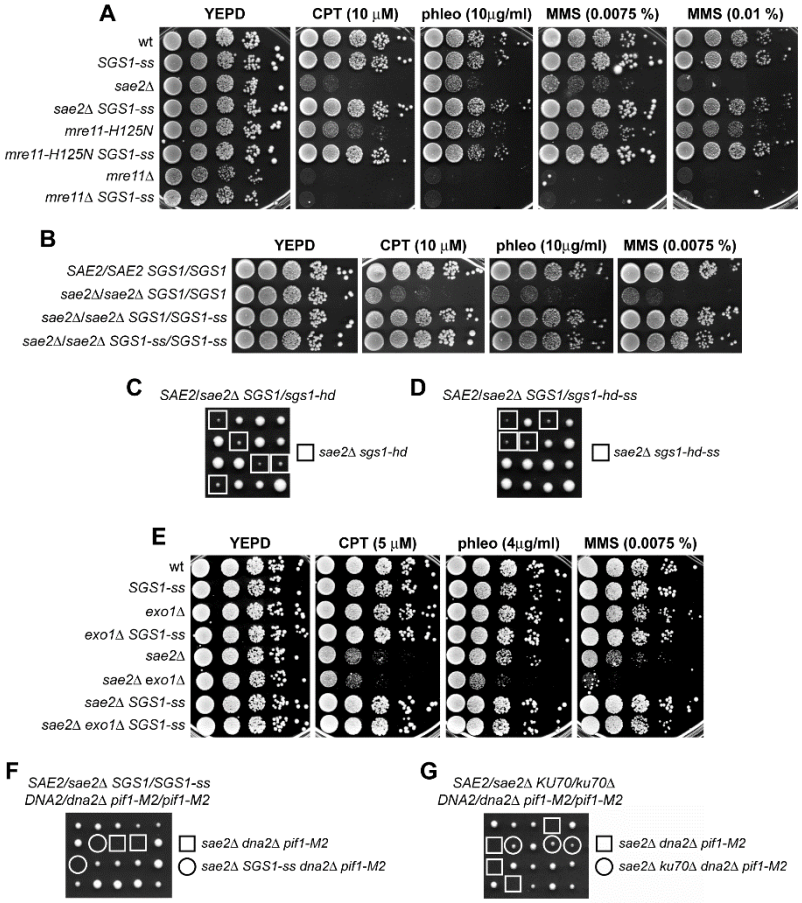

Figure 6 Suppression of the sensitivity to genotoxic agents of *sae2*Δ and *mre11* nuclease defective mutants by Sgs1-ss.

(A, B) Exponentially growing cells were serially diluted (1:10), and each dilution was spotted out onto YEPD plates with or without camptothecin (CPT), phleomycin or MMS. (C,D) Meiotic tetrads were dissected on YEPD plates that were incubated at 25°C, followed by spore genotyping. (E) Exponentially growing cells were serially diluted (1:10), and each dilution was spotted out onto YEPD plates with or without CPT, phleomycin or MMS. (F, G) Meiotic tetrads were dissected on YEPD plates that were incubated at 25°C, followed by spore genotyping.

Sgs1-ss suppresses the adaptation defect of sae2Δ cells

A single irreparable DSB triggers a checkpoint-mediated cell cycle arrest. Yeast cells can escape an extended checkpoint arrest and resume cell cycle progression even with an unrepaired DSB (adaptation) [237,238]. Sae2 lacking cells, like other resection deficient mutants, fail to turn off the checkpoint triggered by an unrepaired DSB and remain arrested at G2/M as large budded cells [58,132,228,239]. To investigate whether Sgs1-ss suppresses the adaptation defect of *sae2Δ* cells, we used JKM139 derivative strains carrying the *HO* endonuclease gene under the control of a galactose-inducible promoter. Galactose addition leads to generation at the *MAT* locus of a single DSB that cannot be repaired by HR, because the homologous donor loci *HML* or *HMR* are deleted [237]. When G1-arrested cell cultures were spotted on galactose-containing plates, *sae2Δ SGS1-ss* cells formed microcolonies with more than two cells more efficiently than *sae2Δ* cells, which were still arrested at the two-cell dumbbell stage after 24 h (**Figure 7A**). Checkpoint activation was monitored also by following Rad53 phosphorylation, which is required for Rad53 activation and is detectable as a decrease of its electrophoretic mobility. When galactose was added to exponentially growing cell cultures of the same strains, *sae2Δ* and *sae2Δ SGS1-ss* mutant cells showed similar amounts of phosphorylated Rad53 after HO induction (**Figure 7B**), indicating that Sgs1-ss did not affect checkpoint

activation. However, Rad53 phosphorylation decreased in *sae2Δ SGS1-ss* double-mutant cells within 12–14 h after galactose addition, whereas it persisted longer in *sae2Δ* cells that were defective in re-entering the cell cycle (**Figure 7B**). Thus, Sgs1-ss suppresses the inability of *sae2Δ* cells to turn off the checkpoint in the presence of an unrepaired DSB. The adaptation defect of *sae2Δ* cells has been proposed to be due to an increased persistence at DSBs of the MRX complex, which in turn causes unscheduled Tel1 activation [58,132]. We then asked by chromatin immunoprecipitation (ChIP) and quantitative real-time PCR (qPCR) analysis whether Sgs1-ss can reduce the binding of MRX to the DSB ends in *sae2Δ* cells. When HO was induced in exponentially growing cells, the amount of Mre11 bound at the HO-induced DSB end was lower in *sae2Δ SGS1-ss* than in *sae2Δ* cells (**Figure 7C**). As MRX persistence at the DSB in *sae2Δ* cells has been proposed to be due to defective DSB resection, this finding suggests that Sgs1-ss suppresses the resection defect of *sae2Δ* cells.

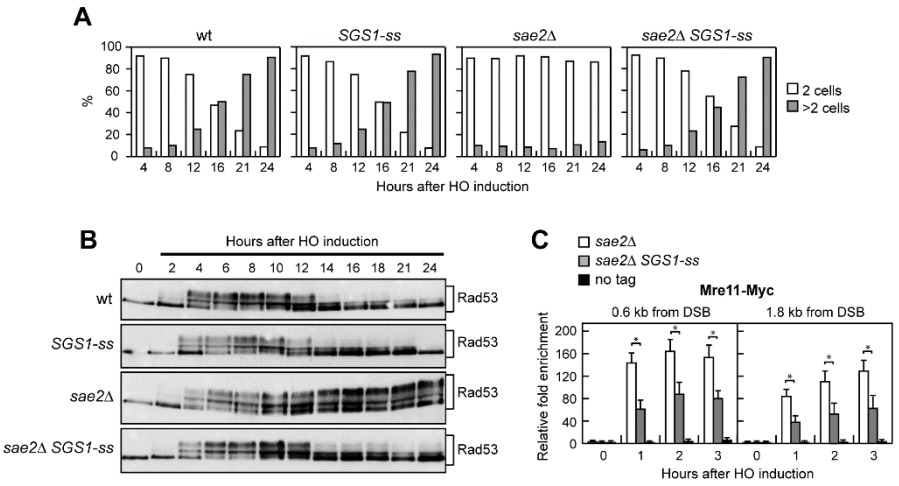

Figure 7 Suppression of the adaptation defect of *sae2Δ* cells by Sgs1-ss.
(A) YEPR G1-arrested cell cultures of wild-type JKM139 and otherwise isogenic derivative strains were plated on galactose-containing plates (time zero). At the indicated time points, 200 cells for each strain were analyzed to determine the frequency of large budded cells and of cells forming microcolonies of more than two cells. The mean values from three independent experiments are represented (n = 3). (B) Exponentially growing YEPR cultures of the strains in (A) were transferred to YEPRG (time zero), followed by Western blot analysis with anti-Rad53 antibodies. (C) ChIP analysis. Exponentially growing YEPR cell cultures of JKM139 derivative strains were transferred to YEPRG, followed by ChIP analysis of the recruitment of Mre11–Myc at the indicated distance from the HO-cut compared to untagged Mre11 (no tag). In all diagrams, the ChIP signals were normalized for each time point to the corresponding input signal. The mean values are represented with error bars denoting s.d. (n = 3). *P < 0.01, t-test.

Sgs1-ss suppresses the resection defect of sae2Δ cells

To investigate whether Sgs1-ss suppresses the sensitivity to genotoxic agents and the adaptation defect of *sae2Δ* cells by restoring DSB resection, we used JKM139 derivative strains to monitor directly generation of ssDNA at the DSB ends [237]. Because ssDNA is resistant to cleavage by restriction enzymes, we directly monitored ssDNA formation at the irreparable HO-cut by following the loss of SspI restriction fragments after galactose addition by Southern blot analysis under alkaline conditions, using a single-stranded probe that anneals to the 3' end at one side of the break (**Figure 8A**). Resection in *sae2Δ SGS1-ss* cells was markedly increased compared to *sae2Δ* cells, indicating that Sgs1-ss suppresses the resection defect caused by the lack of Sae2 (**Figure 8B and C**). Repair of a DSB flanked by direct repeats occurs primarily by single-strand annealing (SSA), which requires nucleolytic degradation of the 5' DSB ends to reach the complementary DNA sequences that can then anneal [240]. To assess whether the Sgs1- ss-mediated suppression of the resection defect caused by the lack of Sae2 was physiologically relevant, we asked whether Sgs1-ss suppresses the SSA defect of *sae2Δ* cells. To this end, we introduced the *SGS1-ss* allele in YMV45 strain, which carries two tandem *leu2* repeats located 4.6 kb apart, with a HO recognition site adjacent to one of the repeats [28]. This strain also harbours a *GAL-HO* construct for galactose-inducible *HO* expression. As

expected, accumulation of the repair product was reduced in *sae2Δ* compared to wild-type cells, whereas it occurred with almost wildtype kinetics in *sae2Δ SGS1-ss* double-mutant cells (**Figure 8D and E**), indicating that Sgs1-ss improves SSA-mediated DSB repair in the absence of Sae2. Altogether, these findings indicate that Sgs1-ss suppresses both the sensitivity to genotoxic agents of *sae2Δ* cells and the MRX persistence at DSBs by restoring DSB resection. Interestingly, the effects of the *SGS1-ss* mutation are opposite to those of the separation-of-function *sgs1-D664Δ* allele, which specifically impairs viability of *sae2Δ* cells and DSB resection without affecting other Sgs1 functions [241].

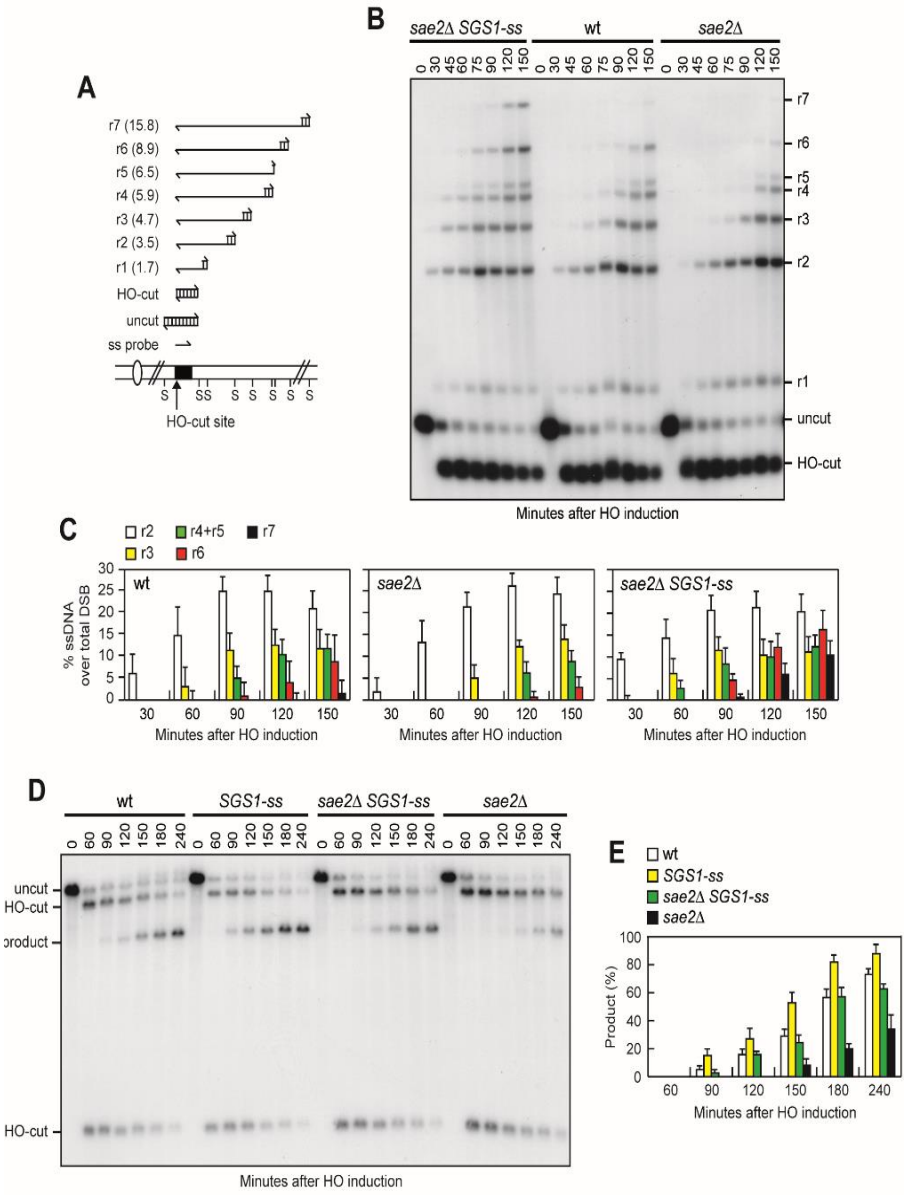
A
r7 (15.8)
r6 (8.9)
r5 (6.5)
r4 (5.9)
r3 (4.7)
r2 (3.5)
r1 (1.7)
HO-cut
uncut
ss probe
HO-cut site
B
sae2Δ SGS1-ss
wt
sae2Δ
r7
r6
r5
r4
r3
r2
r1
uncut
HO-cut
Minutes after HO induction
C
r2
r4+r5
r7
r3
r6
wt
sae2Δ
sae2Δ SGS1-ss
% ssDNA over total DSB
Minutes after HO induction
D
wt
SGS1-ss
sae2Δ SGS1-ss
sae2Δ
uncut
HO-cut
product
HO-cut
Minutes after HO induction
E
wt
SGS1-ss
sae2Δ SGS1-ss
sae2Δ
Product (%)
Minutes after HO induction

Figure 8 Sgs1-ss suppresses the resection defect of *sae2Δ* cells.
(A) Method to measure double-strand break (DSB) resection. Gel blots of SspI-digested genomic DNA separated on alkaline agarose gel were hybridized with a single-stranded MAT probe (ss probe) that anneals to the unresected strand. 50 –30 resection progressively eliminates SspI sites (S), producing larger SspI fragments (r1 through r7) detected by the probe. (B) DSB resection. YEPR exponentially growing cell cultures of JKM139 derivative strains were transferred to YEPRG at time zero. Genomic DNA was analysed for ssDNA formation at the indicated times after HO induction as described in (A). (C) Densitometric analyses. The experiment as in (B) has been independently repeated three times, and the mean values are represented with error bars denoting s.d. (n = 3). (D) DSB repair by single-strand annealing (SSA). In YMV45 strain, the HO-cut site is flanked by homologous leu2 sequences that are 4.6 kb apart. HO-induced DSB formation results in generation of 12- and 2.5-kb DNA fragments (HO-cut) that can be detected by Southern blot analysis with a LEU2 probe of KpnI-digested genomic DNA. DSB repair by SSA generates an 8-kb fragment (product). (E) Densitometric analysis of the product band signals. The intensity of each band was normalized with respect to a loading control (not shown). The mean values are represented with error bars denoting s.d. (n = 3).

Sgs1-ss accelerates DSB resection by escaping Rad9 inhibition

The Sgs1-ss mutant variant can bypass Sae2 requirement in initiation of DSB resection either because it allows Dna2 to substitute for Sae2/MRX endonuclease activity or because it increases the resection efficiency. To distinguish between these two possibilities, we asked whether Sgs1-ss could bypass Sae2 requirement in resecting meiotic DSBs, where the Sae2/MRX-mediated endonucleolytic cleavage is absolutely required to initiate DSB resection by allowing the removal of Spo11 from the DSB ends [230,231]. A *sae2Δ/sae2Δ SGS1-ss/SGS1-ss* diploid strain was constructed and its kinetics of processing/repair of meiotic DSBs generated at the *THR4* hotspot was compared to those of a *sae2Δ/sae2Δ* diploid. DSBs disappeared in both wild-type and *SGS1-ss/SGS1-ss* cells about 4 h after transfer to sporulation medium, while they persisted until the end of the experiment in both *sae2Δ/sae2Δ* and *sae2Δ/sae2Δ SGS1-ss/SGS1-ss* diploid cells (**Figure 9A**). Thus, Sgs1-ss cannot substitute the endonucleolytic clipping by Sae2/MRX when this is absolutely required to initiate DSB resection. Interestingly, the Sgs1-ss mutant variant accelerates both DSB resection and SSA compared to wild-type Sgs1 (**Figure 8B-E**), suggesting that Sgs1-ss might increase the resection efficiency by escaping the effect of negative regulators of this process. In particular, Rad9 provides a barrier to resection through an unknown mechanism [170,229]. As shown in **Figure 10A and B**, both *SGS1-ss* and *rad9Δ*

mutant cells accumulated the resection products more efficiently than wildtype cells, and the presence of Sgs1-ss did not accelerate further the generation of ssDNA in *rad9Δ* cells. Thus, the lack of Rad9 and the presence of Sgs1-ss appear to increase the efficiency of DSB resection through the same mechanism. Furthermore, cells lacking Rad9 displayed sensitivity to CPT and phleomycin (**Figure 10C**). Consistent with the finding that the *SGS1-ss* and *rad9Δ* alleles affect the same process, *rad9Δ* was epistatic to *SGS1-ss* with respect to the survival to genotoxic agents, as *sae2Δ rad9Δ SGS1-ss* cells were as sensitive to CPT and phleomycin as *sae2Δ rad9Δ* and *rad9Δ* cells (**Figure 10C**). Double-strand break resection in the G1 phase of the cell cycle is specifically inhibited by the Ku complex, whose lack allows nucleolytic processing in G1 cells independently of Cdk1 activity [242]. *RAD9* deletion does not allow DSB resection in G1, but it enhances resection in G1-arrested *kuΔ* cells [243], indicating that Rad9 inhibits DSB resection in G1, but this function becomes apparent only when Ku is absent. To investigate whether Sgs1-ss was capable to counteract the inhibitory function of Rad9 in G1, we monitored DSB resection in *SGS1-ss* and *ku70Δ SGS1-ss* cells that were kept arrested in G1 by a-factor during HO induction. Consistent with the requirement of Cdk1 activity for efficient DSB resection, the 3'-ended resection products were barely detectable in wild-type G1 cells, whereas their amount increased in *ku70Δ* G1 cells that, as previously reported [242], accumulated mostly 1.7-, 3.5- and 4.7-kb ssDNA products (r1, r2, r3) (**Figure 9B and C**). By contrast, DSB resection in *SGS1-ss* cells was

undistinguishable from that observed in wild-type cells (**Figure 9 B and C**), indicating that Sgs1-ss does not allow DSB resection in G1. Furthermore, while *RAD9* deletion enhanced the resection efficiency of *ku70Δ* G1 cells, G1-arrested *ku70Δ* and *ku70Δ SGS1-ss* cells accumulated resection products with similar kinetics (**Figure 10D and E**). Altogether, these findings indicate that Sgs1-ss is not capable to allow DSB resection in G1 either in the presence or in the absence of Ku. As Sgs1-ss function in DSB resection depends on Dna2, whose activity requires Cdk1-mediated phosphorylation [163], the inability of Sgs1-ss to overcome both Ku- and Rad9-mediated inhibition in G1 may be due to the requirement of Cdk1 activity to support Dna2 and therefore Sgs1-ss function in DSB resection.

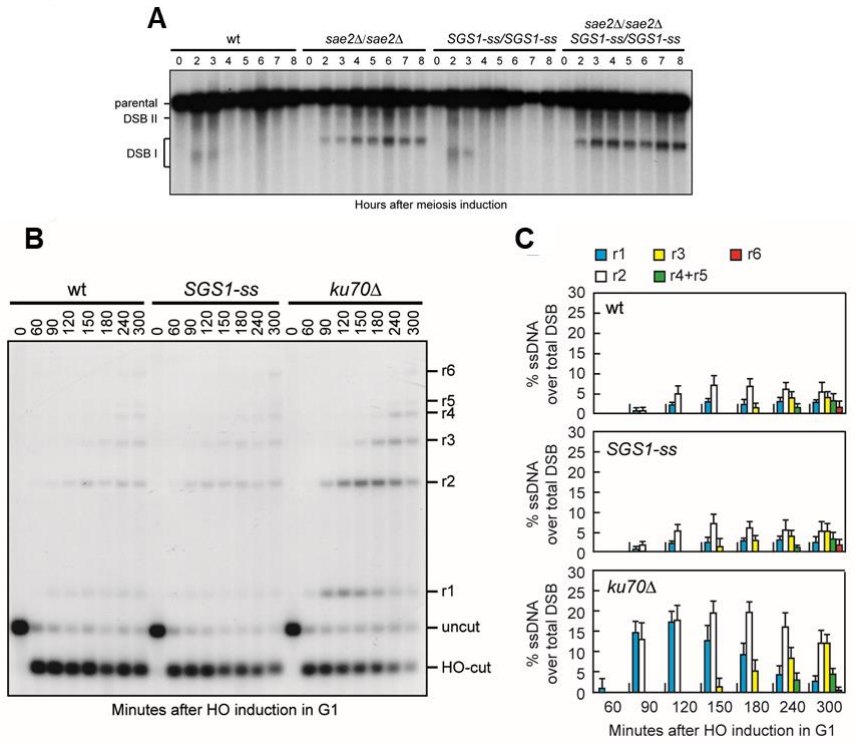

Figure 9 Sgs1-SS cannot compensate for the absence of Sae2 in meiosis and does not allow resection in G1.

(A) Diploid cells were grown to stationary phase in YPA medium and then resuspended in SPM at time zero. Cells sample were collected at the indicated time points after transfer to SPM to analyze meiotic DSB formation by Southern blot analysis. Southern blot was performed on EcoRI-digested genomic DNA run on a native agarose gel and the filter was hybridized with a probe complementary to the 5' non coding region of the THR4 gene. This probe reveals an intact EcoRI fragment (parental) of 7.9 kb and two bands of 5.7 and 7.1 kb corresponding to the prominent meiotic DSB sites (DSB1 and DSBII). (B and C) DSB resection. HO was induced at time zero in α-factor-arrested JKM139 derivative cells that were kept arrested in G1 with α-factor throughout the experiment. Genomic DNA was analyzed for ssDNA formation at the indicated times after HO induction. Densitometric analyses. The experiment as in (B) has been independently repeated three times and the mean values are represented with error bars denoting s.d. (n=3).

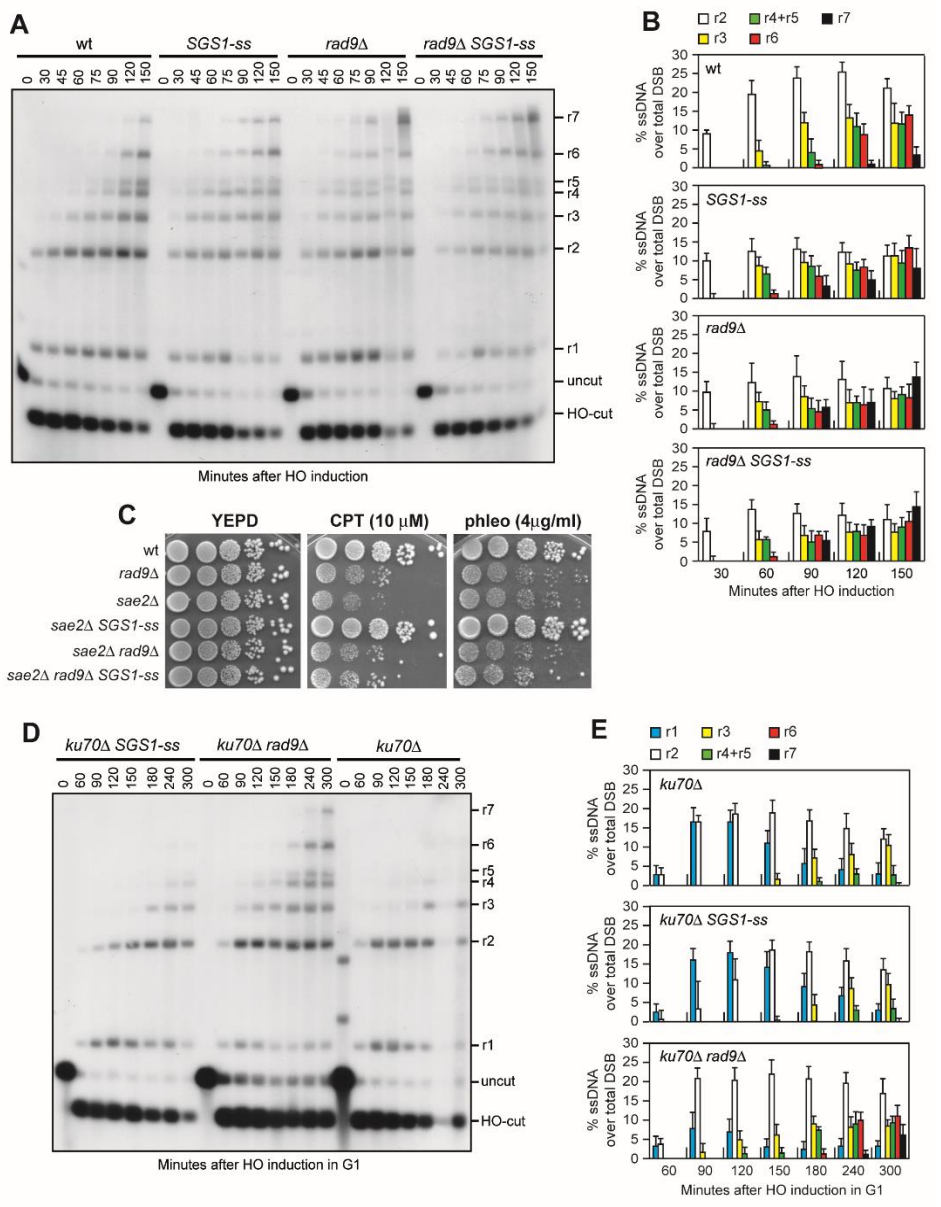
A
wt
SGS1-ss
rad9Δ
rad9Δ SGS1-ss
0 30 45 60 75 90 120 150
r7
r6
r5
r4
r3
r2
r1
uncut
HO-cut
Minutes after HO induction
B
r2
r4+r5
r7
r3
r6
wt
SGS1-ss
rad9Δ
rad9Δ SGS1-ss
% ssDNA over total DSB
30 60 90 120 150
Minutes after HO induction
C
YEPD
CPT (10 μM)
phleo (4μg/ml)
wt
rad9Δ
sae2Δ
sae2Δ SGS1-ss
sae2Δ rad9Δ
sae2Δ rad9Δ SGS1-ss
D
ku70Δ SGS1-ss
ku70Δ rad9Δ
ku70Δ
0 60 90 120 150 180 240 300
r7
r6
r5
r4
r3
r2
r1
uncut
HO-cut
Minutes after HO induction in G1
E
r1
r3
r6
r2
r4+r5
r7
ku70Δ
ku70Δ SGS1-ss
ku70Δ rad9Δ
% ssDNA over total DSB
60 90 120 150 180 240 300
Minutes after HO induction in G1

Figure 10 Double-strand break (DSB) resection is accelerated by the same mechanism in SGS1-ss and *rad9Δ* cells.
(A) DSB resection. YEPR exponentially growing cell cultures of JKM139 derivative strains were transferred to YEPRG at time zero. Genomic DNA was analyzed for ssDNA formation as described in Figure 8A (B) Densitometric analyses. The experiment as in (A) has been independently repeated three times, and the mean values are represented with error bars denoting s.d.(n = 3) (C) Exponentially growing cells were serially diluted (1:10), and each dilution was spotted out onto YEPD plates with or without camptothecin (CPT) or phleomycin (D) DSB resection. HO was induced at time zero in a-factor-arrested JKM139 derivative cells that were kept arrested in G1 with a-factor throughout the experiment Genomic DNA was analyzed for ssDNA formation as described in Figure 8A (E) Densitometric analyses. The experiment as in (D) has been independently repeated three times, and the mean values are represented with error bars denoting s.d.(n = 3).

Rapid DSB resection in rad9Δ cells depends mainly on Sgs1

Generation of ssDNA at uncapped telomeres in *rad9Δ* cells has been shown to be more dependent on Dna2/Sgs1 than on Exo1 [141]. This observation, together with the finding that *SGS1-ss* does not accelerate further the generation of ssDNA in *rad9Δ* cells (**Figure 10A and B**), raises the possibility that Rad9 inhibits DSB resection by limiting Sgs1 activity and that the Sgs1-ss variant can escape this inhibition. We tested this hypothesis by investigating the contribution of Sgs1 and Exo1 to the accelerated DSB resection displayed by rad9Δ cells. As shown in **Figure 11A and B**, *sgs1Δ* was epistatic to *rad9Δ* with respect to DSB resection, as *sgs1Δ rad9Δ* double-mutant and *sgs1Δ* single mutant cells resected the HO-induced DSB with similar kinetics. By contrast, DSB resection in *exo1Δ rad9Δ* cells was more efficient than in *exo1Δ* cells, although it was delayed compared to *rad9Δ* cells (**Figure 11C and D**). Thus, the rapid resection in the absence of Rad9 depends mainly on Sgs1, although also Exo1 contributes to resect the DSB in the absence of Rad9. Consistent with the finding that Sgs1-ss overrides Rad9 inhibition, *SGS1-ss exo1Δ* cells resected the DSB with kinetics similar to that of *rad9Δ exo1Δ* cells (**Figure 12A and B**).

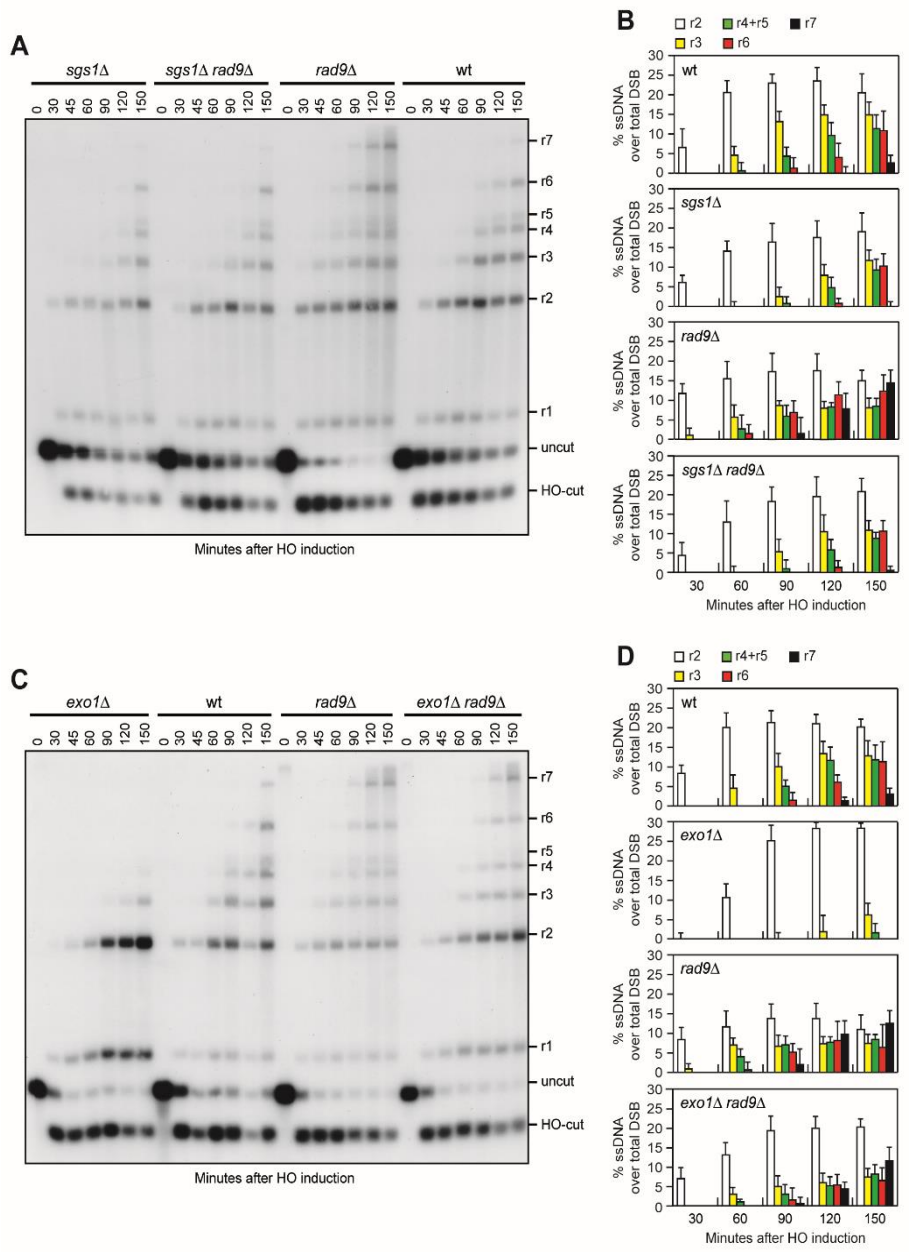
A
sgs1Δ
sgs1Δ rad9Δ
rad9Δ
wt
0 30 45 60 90 120 150
r7
r6
r5
r4
r3
r2
r1
uncut
HO-cut
Minutes after HO induction
B
r2
r4+r5
r7
r3
r6
wt
sgs1Δ
rad9Δ
sgs1Δ rad9Δ
% ssDNA over total DSB
30 60 90 120 150
Minutes after HO induction
C
exo1Δ
wt
rad9Δ
exo1Δ rad9Δ
0 30 45 60 90 120 150
r7
r6
r5
r4
r3
r2
r1
uncut
HO-cut
Minutes after HO induction
D
r2
r4+r5
r7
r3
r6
wt
exo1Δ
rad9Δ
exo1Δ rad9Δ
% ssDNA over total DSB
30 60 90 120 150
Minutes after HO induction

Figure 11. Rapid resection in *rad9Δ* cells depends mainly on Sgs1.
(A) Double-strand break (DSB) resection. YEPR exponentially growing cell cultures of JKM139 derivative strains were transferred to YEPRG at time zero. Genomic DNA wasanalysed for ssDNA formation as described in Figure 8A. (B) Densitometric analyses. The experiment as in (A) has been independently repeated three times, and the mean values are represented with error bars denoting s.d.(n = 3). (C) DSB resection. The experiment was performed as in (A). (D) Densitometric analyses. The experiment as in (C) has been independently repeated three times, and the mean values are represented with error bars denoting s.d. (n = 3).

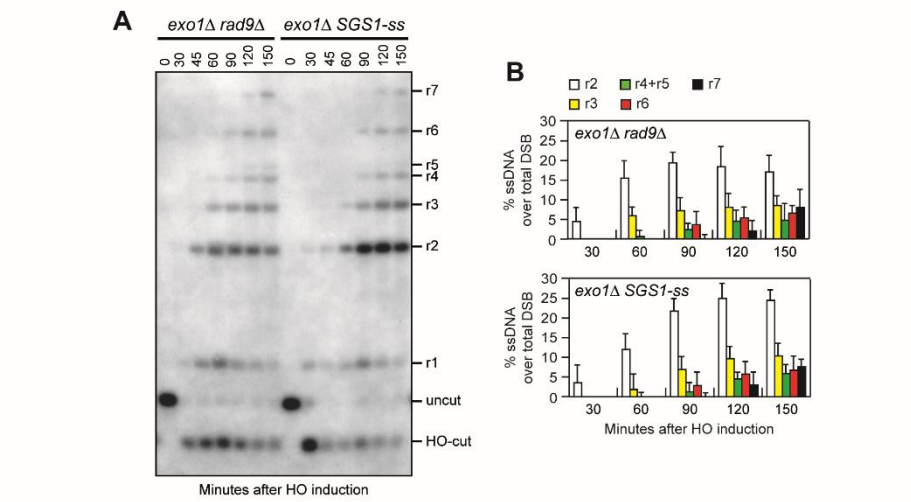

Figure 12 *exo1Δ rad9Δ* and *exo1Δ SGS1-ss* resect the DSB with similar kinetics.
(A) DSB resection. YEPR exponentially growing cells cultures of JKM 139 derivative strains were transferred to YEPRG at time zero. Genomic DNA was analysed for ssDNA formation at the indicated times after HO induction. (B) Densiometric analyses. The experiment as in (A) has been independently repeated three times and the mean values are represented with error bars denoting s.d (n=3).

Rad9 inhibits DSB resection by limiting Sgs1 association at DNA break

If loss of end protection by Rad9 allowed Sgs1 to initiate DSB resection, which normally requires Sae2, then *RAD9* deletion, like Sgs1-ss, should suppress the resection defect of sae2Δ cells. Indeed, DSB resection in *sae2Δ rad9Δ* cells was as fast as in *rad9Δ* cells, which resected the DSB more efficiently than wild-type and *sae2Δ* cells (**Figure 13A and B**), indicating that the lack of Rad9 bypasses Sae2 function in DSB resection. We then asked by ChIP and qPCR analysis whether Rad9 limits Sgs1 activity by regulating Sgs1 binding/persistence to the DSB ends. When *HO* was induced in exponentially growing cells, the amount of Sgs1 bound at the HO-induced DSB was higher in *rad9Δ* than in wild-type cells (**Figure 13F**), indicating that Rad9 counteracts Sgs1 recruitment to the DSB. Interestingly, the Sgs1-ss variant was recruited at the DSB with equivalent efficiencies in both exponentially growing wild-type and *rad9Δ* cells (**Figure 13C**). These differences were not due to different resection kinetics, as we obtained similar results also when the HO-induced DSB was generated in G1-arrested cells (**Figure 13D**), which resected the DSB very poorly due to the low Cdk1 activity [161]. Interestingly, the amount of Sgs1-ss bound to the DSB was higher than the amount of wild-type Sgs1 in *rad9Δ* cells (**Figure 13C and D**), suggesting that Sgs1-ss has a higher intrinsic ability to bind/persist at the DSB. Altogether, these results indicate that Rad9 limits the

association of Sgs1 to the DSB ends and that the Sgs1-ss variant escapes this inhibition possibly because it binds more tightly the DSB. Interestingly, the robust association of Sgs1-ss to the DSB in G1-arrested cells (low Cdk1 activity) did not result in DSB resection (**Figure 9B and C**) possibly because Sgs1 acts in DSB resection together with Dna2, whose activity requires Cdk1- mediated phosphorylation [163]. Consistent with a contribution of Exo1 in promoting DSB resection in the absence of Rad9, *rad9Δ* cells showed an increased Exo1 recruitment to the DSB compared to wild-type cells (**Figure 13E**).

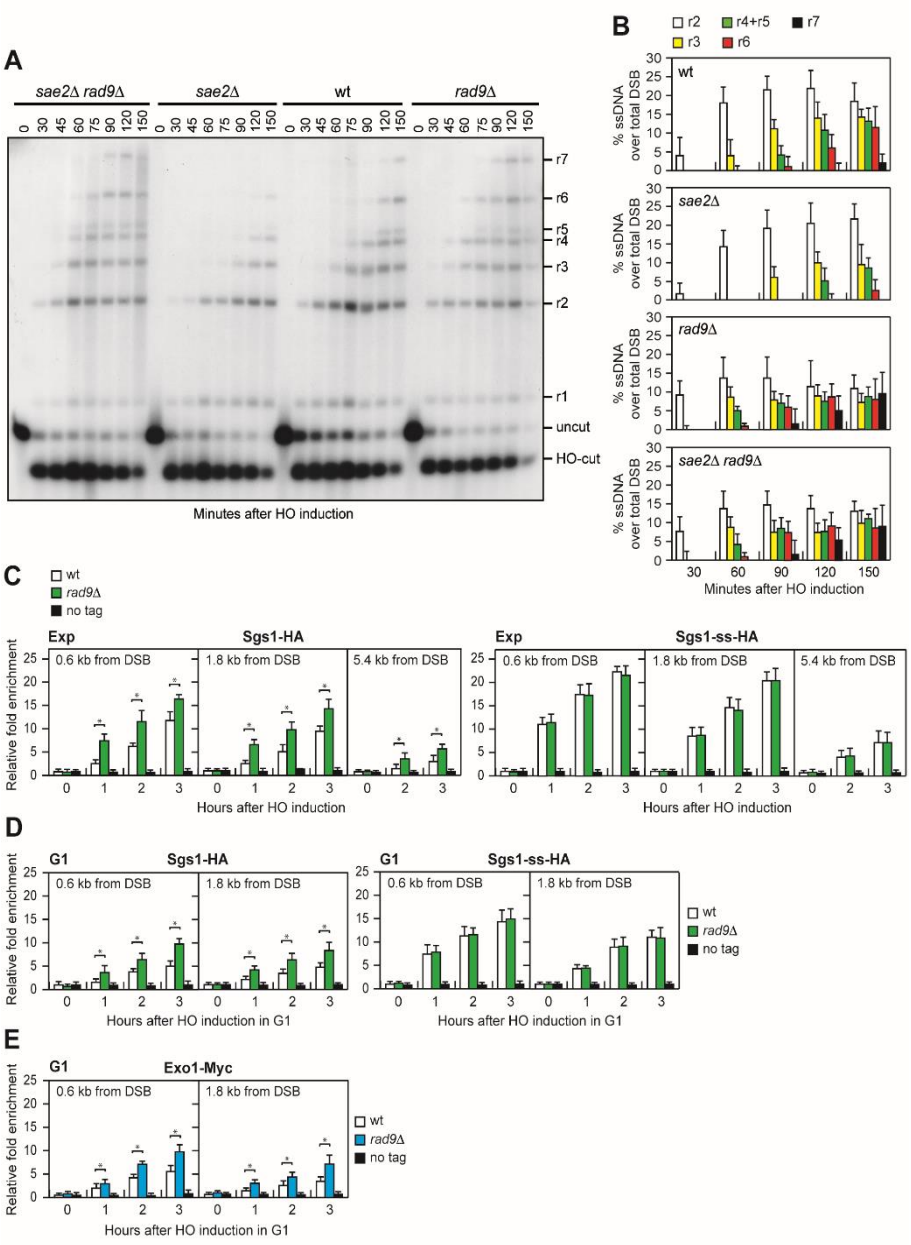
A
sae2Δ rad9Δ
sae2Δ
wt
rad9Δ
0 30 45 60 75 90 120 150
r7
r6
r5
r4
r3
r2
r1
uncut
HO-cut
Minutes after HO induction
B
r2
r4+r5
r7
r3
r6
wt
sae2Δ
rad9Δ
sae2Δ rad9Δ
% ssDNA over total DSB
30 60 90 120 150
Minutes after HO induction
C
wt
rad9Δ
no tag
Exp
Sgs1-HA
Sgs1-ss-HA
0.6 kb from DSB
1.8 kb from DSB
5.4 kb from DSB
Relative fold enrichment
Hours after HO induction
D
G1
Sgs1-HA
Sgs1-ss-HA
Hours after HO induction in G1
E
G1
Exo1-Myc

Figure 13 Rad9 inhibits Sgs1 association at the double-strand breaks (DSBs).
(A) DSB resection. YEPR exponentially growing cell cultures of JKM139 derivative strains were transferred to YEPRG at time zero. Genomic DNA was analyzed for ssDNA formation as described in Figure 8A. (B) Densitometric analyses. The experiment as in (A) has been independently repeated three times, and the mean values are represented with error bars denoting s.d.(n = 3). (C) ChIP analysis. Exponentially growing YEPR cell cultures of JKM139 derivative strains were transferred to YEPRG, followed by ChIP analysis of the recruitment of Sgs1-HA and Sgs1-ss-HA at the indicated distance from the HO-cut compared to untagged Sgs1 (no tag). In all diagrams, the ChIP signals were normalized for each time point to the corresponding input signal. The mean values are represented with error bars denoting s.d. (n = 3). *P < 0.01, t-test. (D) ChIP analysis in G1-arrested cells. As in (C), but showing ChIP analysis of the recruitment of Sgs1-HA and Sgs1-ss-HA in cells that were kept arrested in G1 by a-factor. The mean values are represented with error bars denoting s.d. (n = 3). *P < 0.01, t-test. (E) ChIP analysis in G1-arrested cells. As in (C), but showing ChIP analysis of the recruitment of Exo1–Myc in cells that were kept arrested in G1 by a-factor. The mean values are represented with error bars denoting s.d. (n = 3). *P < 0.01, t-test.

PLOS GENETICS **(Gobbini, Villa *et al*., 2015)**
2015 Nov19;11(11):e1005685.
doi:10.1371/journal.pgen.1005685

Sae2 function at DNA double-strand breaks is bypassed by dampening Tel1 or Rad53 activity

Elisa Gobbini *, Matteo Villa *, Marco Gnugnoli, Luca Menin, Michela Clerici & Maria Pia Longhese

Dipartimento di Biotecnologie e Bioscienze, Università di Milano-Bicocca, Italy.

* These authors contributed equally to this work

Programmed DNA double-strand breaks (DSBs) are formed during meiotic recombination and rearrangement of the immunoglobulin genes in lymphocytes. Furthermore, potentially harmful DSBs can arise by exposure to environmental factors, such as ionizing radiations and radiomimetic chemicals, or by failures in DNA replication. DSB generation elicits a checkpoint response that depends on the mammalian protein kinases ATM and ATR, whose functional orthologs in *Saccharomyces cerevisiae* are Tel1 and Mec1, respectively [26]. Tel1/ATM is recruited to DSBs by the MRX (Mre11-Rad50-Xrs2)/MRN (Mre11-Rad50-Nbs1) complex, whereas Mec1/ATR recognizes single-stranded DNA (ssDNA) covered by Replication Protein A (RPA) [27]. Once activated, Tel1/ATM and Mec1/ATR propagate their checkpoint signals by phosphorylating the downstream checkpoint kinases Rad53 (Chk2 in mammals) and Chk1, to couple cell cycle progression with DNA repair [27].

Repair of DSBs can occur by either non-homologous end joining (NHEJ) or homologous recombination (HR). Whereas NHEJ directly joins the DNA ends, HR uses the sister chromatid or the homologous chromosome to repair DSBs. HR requires that the 5’ ends of a DSB are nucleolytically processed (resected) to generate 3’-ended ssDNA that can invade an undamaged homologous DNA template [24,111]. In *Saccharomyces cerevisiae*, recent characterization of core resection proteins has revealed that DSB resection is initiated by the MRX complex, which catalyzes an endonucleolytic cleavage near a DSB [111], with the Sae2 protein (CtIP in mammals) promoting MRX

endonucleolytic activity [129]. This MRX-Sae2-mediated DNA clipping generates 5' DNA ends that are optimal substrates for the nucleases Exo1 and Dna2, the latter working in concert with the helicase Sgs1 [125,150,156,159]. In addition, the MRX complex recruits Exo1, Sgs1 and Dna2 to DSBs independently of the Mre11 nuclease activity [234]. DSB resection is also negatively regulated by Ku and Rad9, which inhibit the access to DSBs of Exo1 and Sgs1-Dna2, respectively [167,178,233,244]

The MRX-Sae2-mediated endonucleolytic cleavage is particularly important to initiate resection at DNA ends that are not easily accessible to Exo1 and Dna2-Sgs1. For instance, both *sae2*Δ and *mre11* nuclease defective mutants are completely unable to resect meiotic DSBs, where the Spo11 topoisomerase-like protein remains covalently attached to the 5'-terminated strands [230,231]. Furthermore, the same mutants exhibit a marked sensitivity to camptothecin (CPT), which extends the half-life of DNA-topoisomerase I cleavable complexes [232,245], and to methylmethane sulfonate (MMS), which can generate chemically complex DNA termini. The lack of Rad9 or Ku suppresses both the hypersensitivity to DSB-inducing agents and the resection defect of *sae2*Δ cells [167,178,233,234,244]. These suppression events require Dna2-Sgs1 and Exo1, respectively, indicating that Rad9 increases the requirement for MRX-Sae2 activity in DSB resection by inhibiting Sgs1-Dna2 [178,244], while Ku mainly limits the action of Exo1 [167,233,234]. By contrast, elimination of either Rad9 or Ku does not bypass Sae2/MRX function in resecting

meiotic DSBs [167,244], likely because Sgs1-Dna2 and Exo1 cannot substitute for the Sae2/MRX mediated endonucleolytic cleavage when this event is absolutely required to generate accessible 5'-terminated DNA strands.

Sae2 plays an important role also in modulating the checkpoint response. Checkpoint activation in response to DSBs depends primarily on Mec1, with Tel1 playing a minor role [186]. On the other hand, impaired Mre11 endonuclease activity caused by the lack of Sae2 leads to increased MRX persistence at the DSB ends. The enhanced MRX signaling in turn causes unscheduled Tel1-dependent checkpoint activation that is associated to prolonged Rad53 phosphorylation [29,132,239]. Mutant *mre11* alleles that reduce MRX binding to DSBs restore DNA damage resistance in *sae2*Δ cells and reduce their persistent checkpoint activation without restoring efficient DSB resection [133,246], suggesting that enhanced MRX association to DSBs contributes to the DNA damage hypersensitivity caused by the lack of Sae2. Persistently bound MRX might increase the sensitivity to DNA damaging agents of *sae2*Δ cells by hyperactivating the DNA damage checkpoint. If this were the case, then the DNA damage hypersensitivity of *sae2*Δ cells should be restored by the lack of Tel1 or of its downstream effector Rad53, as they are responsible for the *sae2*Δ enhanced checkpoint signaling [132,239]. However, while Rad53 inactivation has never been tested, *TEL1* deletion not only fails to restore DNA damage resistance in *sae2*Δ cells, but also it exacerbates their sensitivity to DNA damaging agents [133,246].

Therefore, other studies are required to understand whether the Tel1- and Rad53-mediated checkpoint signaling has any role in determining the DNA damage sensitivity of *sae2*Δ cells.

By performing a genetic screen, we identified *rad53* and *tel1* mutant alleles that suppress both the hypersensitivity to DNA damaging agents and the resection defect of *sae2*Δ cells by reducing the amount of Rad9 at DSBs. Decreased Rad9 binding at DNA ends bypasses Sae2 function in DNA damage resistance and resection by relieving the inhibition of the Sgs1-Dna2 resection machinery. Altogether our data suggest that the primary cause of the resection defect of *sae2*Δ cells is Rad9 association to DSBs, which is promoted by persistent Tel1 and Rad53 signaling activities in these cells.

*The Rad53-H88Y and Tel1-N2021D variants suppress the DNA damage hypersensitivity of sae2*Δ *cells*

We have previously described our search for extragenic mutations that suppress the CPT hypersensitivity of *sae2*Δ cells [244]. This genetic screen identified 15 single-gene suppressor mutants belonging to 11 distinct allelism groups. Analysis of genomic DNA by next-generation Illumina sequencing of 5 non allelic suppressor mutants revealed that the DNA damage resistance was due to single base pair substitutions in the genes encoding Sgs1, Top1, or the multidrug resistance proteins Pdr3, Pdr10 and Sap185 [244]. Subsequent genome sequencing and genetic analysis of 2 more non allelic suppressor mutants allowed to

link suppression to either the *rad53-H88Y* mutant allele, causing the replacement of Rad53 amino acid residue His88 by Tyr, or the *tel1-N2021D* allele, resulting in the replacement of Tel1 amino acid residue Asn2021 by Asp. Both *rad53-H88Y* and *tel1-N2021D* alleles restored resistance of *sae2*Δ cells not only to CPT, but also to phleomycin (phleo) and MMS (**Figure 14A**). While both *rad53-H88Y* and *tel1-N2021D* fully rescued the hypersensitivity of *sae2*Δ cells to phleomycin and MMS, the CPT hypersensitivity of *sae2*Δ cells was only partially suppressed by the same alleles (**Figure 14A**), suggesting that they did not bypass all Sae2 functions.

Both *rad53-H88Y* and *tel1-N2021D* suppressor alleles were recessive, as the sensitivity to genotoxic agents of *sae2*Δ*/sae2*Δ *RAD53/rad53-H88Y* and *sae2*Δ*/sae2*Δ *TEL1/tel1-N2021D* diploid cells was similar to that of *sae2*Δ*/sae2*Δ *RAD53/RAD53 TEL1/TEL1* diploid cells (**Figure 15**), suggesting that *rad53-H88Y* and *tel1-N2021D* alleles encode hypomorphic variants. Furthermore, both variants suppressed the hypersensitivity to DNA damaging agents of *sae2*Δ cells by altering the same mechanism, as *sae2*Δ *rad53-H88Y tel1-N2021D* triple mutant cells survived in the presence of DNA damaging agents to the same extent as *sae2*Δ *rad53-H88Y* and *sae2*Δ *tel1-N2021D* double mutant cells (**Figure 14B**).

The MRX complex not only provides the nuclease activity for initiation of DSB resection, but also it promotes the binding of Exo1, Sgs1 and Dna2 at the DSB ends [234]. These MRX multiple roles explain the severe DNA damage hypersensitivity and resection defect of cells

lacking any of the MRX subunits compared to cells lacking either Sae2 or the Mre11 nuclease activity. As Sae2 has been proposed to activate Mre11 nuclease activity [129], we asked whether the suppression of *sae2*Δ DNA damage hypersensitivity by Rad53-H88Y and Tel1-N2021D requires Mre11 nuclease activity. Both *rad53-H88Y* and t*el1-N2021D* alleles suppressed the hypersensitivity to DNA damaging agents of *sae2*Δ cells carrying the nuclease defective *mre11-H125N* allele (**Figure 14C**). By contrast, *sae2*Δ *mre11*Δ *rad53-H88Y* and *sae2*Δ *mre11*Δ *tel1-N2021D* triple mutant cells were as sensitive to genotoxic agents as *sae2*Δ *mre11*Δ double mutant cells (**Figure 14D**) indicating that neither the *rad53-H88Y* nor the *tel1-N2021D* allele can suppress the hypersensitivity to DNA damaging agents of *sae2*Δ *mre11*Δ cells. Altogether, these findings indicate that both Rad53-H88Y and Tel1-N2021D require the physical presence of the MRX complex, but not its nuclease activity, to bypass Sae2 function in cell survival to genotoxic agents.

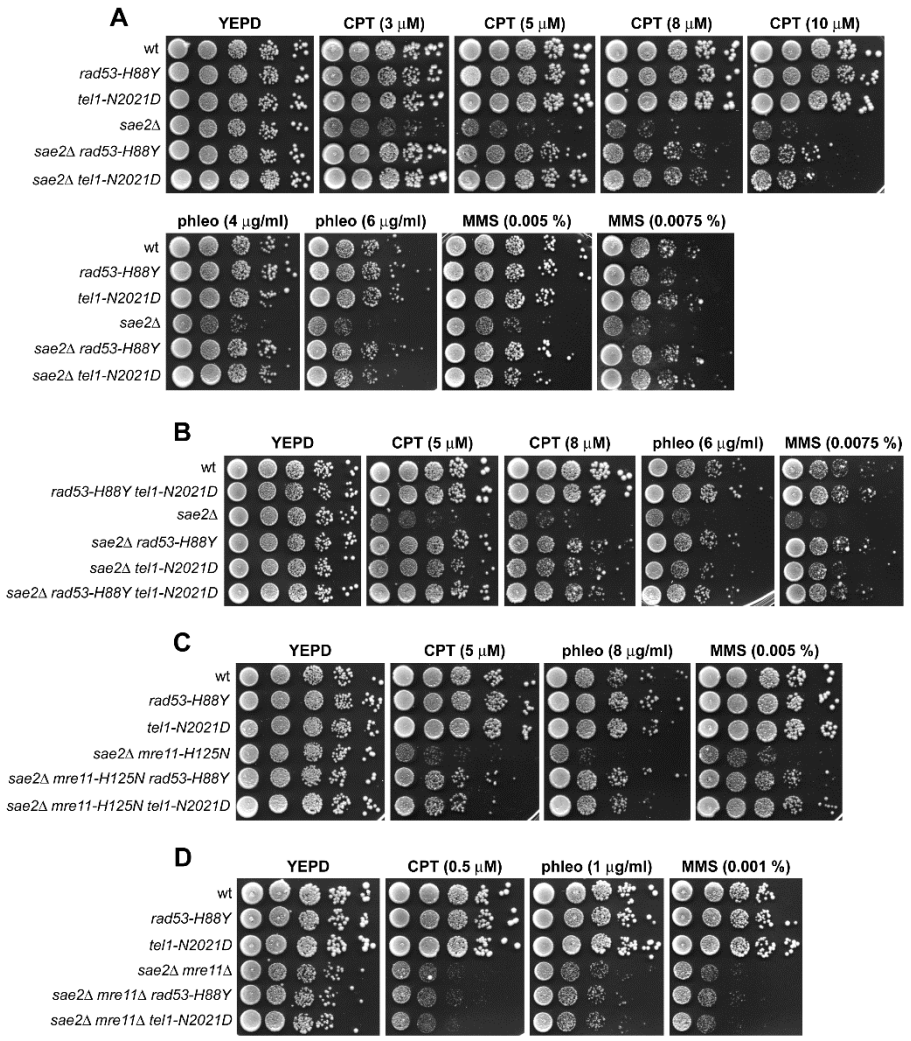

Figure 14. Rad53-H88Y and Tel1-N2021D suppress the hypersensitivity to genotoxic agents of *sae2*Δ cells.
(A-D) Exponentially growing cells were serially diluted (1:10) and each dilution was spotted out onto YEPD plates with or without camptothecin (CPT), phleomycin or MMS.

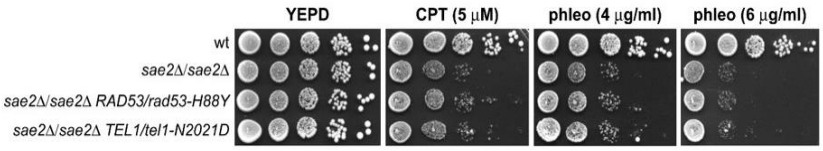

Figure 15 *rad53-H88Y* and *tel11-N2021D* suppressor alleles are recessive. Exponentially growing cells were serially diluted (1:10) and each dilution was spotted out onto YEPD plates with or without camptothecin (CPT) or phleomycin.

The Rad53-H88Y variant is defective in the interaction with Rad9 and bypasses the adaptation defect of sae2Δ cells by impairing checkpoint activation

A single unrepairable DSB induces a DNA damage checkpoint that depends primarily on Mec1, with Tel1 playing a minor role [186]. This checkpoint response can be eventually turned off, allowing cells to resume cell cycle progression through a process that is called adaptation [237,247,248]. In the absence of Sae2, cells display heightened checkpoint activation that prevents cells from adapting to an unrepaired DSB [132,239]. This persistent checkpoint activation is due to increased MRX amount/persistence at the DSB that in turn causes enhanced and prolonged Tel1 activation that is associated with persistent Rad53 phosphorylation [29,50,132,239].

If the *rad53-H88Y* mutation impaired Rad53 activity, then it is expected to suppress the adaptation defect of *sae2*Δ cells by lowering checkpoint activation. We addressed this point by using JKM139 derivative strains, where a single DSB at the *MAT* locus can be generated by expression of the HO endonuclease gene under the control of a galactose-dependent promoter. This DSB cannot be repaired by HR because of the deletion of the homologous donor loci *HML* and *HMR* [237]. We measured checkpoint activation by monitoring the ability of cells to arrest the cell cycle and to phosphorylate Rad53 after HO induction. Both *rad53-H88Y* and *sae2*Δ *rad53-H88Y* cells formed microcolonies of more than 2 cells with higher

efficiency than either wild type or *sae2*Δ cells (**Figure 16A**). Furthermore, the Rad53-H88Y variant was poorly phosphorylated after HO induction both in the presence and in the absence of Sae2 (**Figure 16B**). Thus, the *rad53-H88Y* mutation suppresses the adaptation defect of *sae2*Δ cells by impairing Rad53 activation.

DNA damage-dependent activation of Rad53 requires its phospho-dependent interaction with Rad9, which acts as a scaffold to allow Rad53 intermolecular autophosphorylation and activation [78,97,249]. Interestingly, the His88 residue, which is replaced by Tyr in the Rad53-H88Y variant, is localized in the forkhead-associated domain 1 of the protein and has been implicated in mediating Rad9-Rad53 interaction [250]. Thus, we asked whether the Rad53-H88Y variant was defective in the interaction with Rad9.

When HA-tagged Rad9 was immunoprecipitated with anti-HA antibodies from wild type and *rad53-H88Y* cells grown for 4 hours in the presence of galactose to induce HO, wild type Rad53 could be detected in Rad9-HA immunoprecipitates, whereas Rad53-H88Y did not (**Figure 16C**). This defective interaction of Rad53-H88Y with Rad9 could explain the impaired checkpoint activation in *sae2*Δ *rad53-H88Y* double mutant cells.

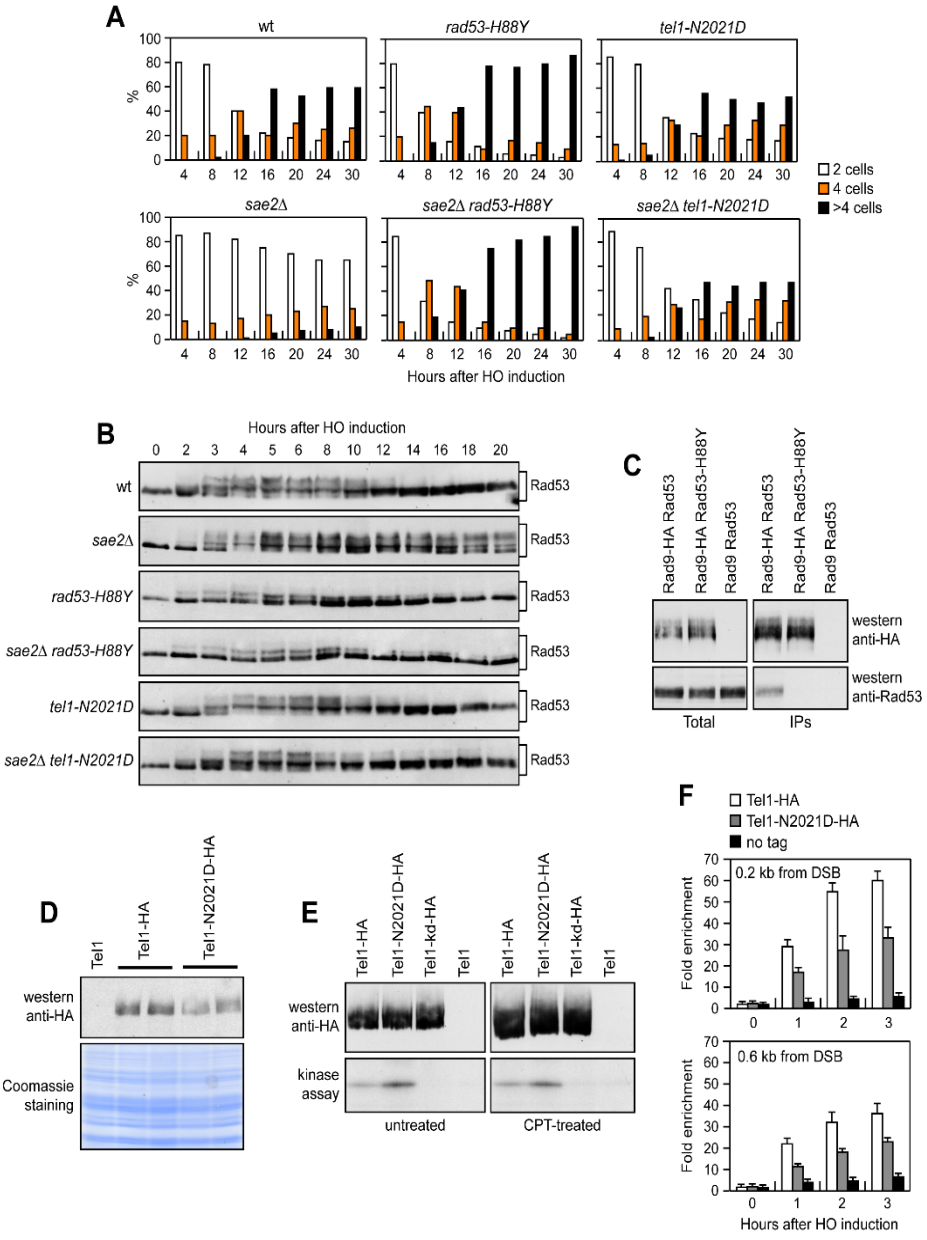
A
wt
rad53-H88Y
tel1-N2021D
sae2Δ
sae2Δ rad53-H88Y
sae2Δ tel1-N2021D
%
2 cells
4 cells
>4 cells
Hours after HO induction
B
Hours after HO induction
wt
sae2Δ
rad53-H88Y
sae2Δ rad53-H88Y
tel1-N2021D
sae2Δ tel1-N2021D
Rad53
C
Rad9-HA Rad53
Rad9-HA Rad53-H88Y
Rad9 Rad53
western anti-HA
western anti-Rad53
Total
IPs
D
Tel1
Tel1-HA
Tel1-N2021D-HA
western anti-HA
Coomassie staining
E
Tel1-HA
Tel1-N2021D-HA
Tel1-kd-HA
Tel1
western anti-HA
kinase assay
untreated
CPT-treated
F
Tel1-HA
Tel1-N2021D-HA
no tag
0.2 kb from DSB
0.6 kb from DSB
Fold enrichment
Hours after HO induction

Figure 16 Rad53-H88Y and Tel1-N2021D suppress the checkpoint shut off defect of *sae2*Δ cells.
(A) YEPR G1-arrested cell cultures of JKM139 derivative strains were plated on galactose-containing plates (time zero). At the indicated time points, 200 cells for each strain were analyzed to determine the frequency of large budded cells (2 cells) and of cells forming microcolonies of 4 or more than 4 cells. (B) Exponentially growing YEPR cultures of the strains in (A) were transferred to YEPRG (time zero), followed by western blot analysis with anti-Rad53 antibodies. (C) Protein extracts were analyzed by western blot with anti-HA or anti-Rad53 antibodies either directly (Total) or after Rad9-HA immunoprecipitation (IPs) with anti-HA antibodies. (D) Protein extracts from exponentially growing cells were analyzed by western blotting with anti-HA antibodies. The same amounts of protein extracts were separated by SDS-PAGE and stained with Coomassie as loading control. (E) Kinase assay was performed on equal amounts of anti-HA immunoprecipitates of protein extracts from cells either exponentially growing in YEPD or after treatment with 50 μM CPT for 1 hour. All the immunoprecipitates were also subjected to western blot analysis using anti-HA antibodies. (F) Relative fold enrichment of Tel1-HA and Tel1-N2021D-HA compared to untagged Tel1 (no tag) at the indicated distance from the HO cleavage site was evaluated after ChIP with anti-HA antibodies and qPCR analysis. In all diagrams, the ChIP signals were normalized for each time point to the amount of the corresponding immunoprecipitated protein and input signal. The mean values are represented with error bars denoting s.d. (n=3).

The Tel1-N2021D variant binds poorly to DSBs and bypasses the adaptation defect of sae2Δ cells by reducing persistent Rad53 activation

Tel1 signaling activity is responsible for the prolonged Rad53 activation that prevents *sae2*Δ cells to adapt to the checkpoint triggered by an unrepairable DSB [132,239]. Although telomere length in *tel1-N2021D* mutant cells was unaffected both in the presence and in the absence of Sae2 (**Figure 17**), the recessivity of *tel1-N2021D* suppressor effect on *sae2*Δ DNA damage hypersensitivity suggests that the Asn2021Asp substitution impairs Tel1 function. If this were the case, Tel1-N2021D might suppress the adaptation defect of *sae2*Δ cells by reducing the DSB-induced persistent Rad53 phosphorylation. When G1-arrested cell cultures were spotted on galactose containing plates to induce HO, wild type, *sae2*Δ, *tel1-N2021D* and *sae2*Δ *tel1-N2021D* cells accumulated large budded cells within 4 hours (**Figure 16A**). This cell cycle arrest is due to checkpoint activation. In fact, when the same cells exponentially growing in raffinose were transferred to galactose, Rad53 phosphorylation was detectable about 2-3 hours after galactose addition (**Figure 16B**). However, while *sae2*Δ cells remained arrested as large budded cells for at least 30 hours (**Figure 16A**) and showed persistent Rad53 phosphorylation (**Figure 16B**), wild type, *tel1-N2021D* and *sae2*Δ *tel1-N2021D* cells formed microcolonies with more than 2 cells (**Figure 16A**) and decreased the amounts of phosphorylated Rad53 (**Figure 16B**) with similar kinetics 10-12 hours

after HO induction. Therefore, the Tel1-N2021D variant impairs Tel1 signaling activity, as it rescues the *sae2*Δ adaptation defect by reducing the persistent Rad53 phosphorylation.

The Asn2021Asp substitution resides in the Tel1 FAT domain, a helical solenoid that encircles the kinase domain of all the phosphoinositide 3-kinase (PI3K)-related kinases (PIKKs) [251,252], suggesting that this amino acid change might reduce Tel1 kinase activity. Western blot analysis revealed that the amount of Tel1-N2021D was slightly lower than that of wild type Tel1 (**Figure 16D**). We then immunoprecipitated equivalent amounts of Tel1-HA and Tel1-N2021D-HA variants from both untreated and CPT-treated cells (**Figure 16E, top**), and we measured their kinase activity *in vitro* using the known artificial substrate of the PIKKs family PHAS-I (Phosphorylated Heat and Acid Stable protein) [253]. Both Tel1-HA and Tel1-N2021D-HA were capable to phosphorylate PHAS-I, with the amount of phosphorylated substrate being slightly higher in Tel1-N2021D-HA than in Tel1-HA immunoprecipitates (**Figure 16E, bottom**). This PHAS-I phosphorylation was dependent on Tel1 kinase activity, as it was not detectable when the immunoprecipitates were prepared from strains expressing either kinase dead Tel1-kd-HA or untagged Tel1 (**Figure 16E, bottom**). Thus, the *tel1-N2021D* mutation does not affect Tel1 kinase activity.

Interestingly, the FAT domain is in close proximity to the FATC domain, which was shown to be important for Tel1 recruitment to DNA ends [254], suggesting that the Tel1-N2021D variant might be defective in

recruitment/association to DSBs. Strikingly, when we analyzed Tel1 and Tel1-N2021D binding at the HO-induced DSB by chromatin immunoprecipitation (ChIP) and quantitative real time PCR (qPCR), the amount of Tel1-N2021D bound at the DSB turned out to be lower than that of wild type Tel1 (**Figure 16F**) This decreased Tel1-N2021D association was not due to lower Tel1-N2021D levels, as the ChIP signals were normalized for each time point to the amount of immunoprecipitated protein. Thus, the inability of *sae2*Δ *tel1-N2021D* cells to sustain persistent Rad53 phosphorylation after DSB generation can be explained by a decreased association of Tel1-N2021D to DSBs.

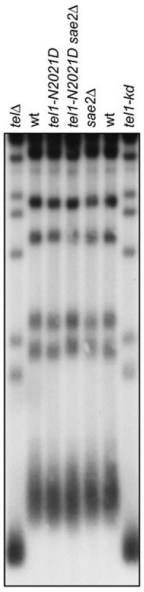

Figure 17 The Tel1-N2021D variant does not affect telomere length**.**
Genomic DNA prepared from exponentially growing cells was digested with XhoI and hybridized with a poly(GT) telomere-specific probe.

Checkpoint-mediated cell cycle arrest is not responsible for the DNA damage hypersensitivity of sae2Δ cells

As both Rad53-H88Y and Tel1-N2021D reduce checkpoint signaling in *sae2*Δ cells, we asked whether the increased DNA damage resistance of *sae2*Δ *rad53-H88Y* and *sae2*Δ *tel1-N2021D* cells was due to the elimination of the checkpoint-mediated cell cycle arrest. This hypothesis could not be tested by deleting the *MEC1*, *DDC1*, *RAD24*, *MEC3* or *RAD9* checkpoint genes, because they also regulate DSB resection [140,229,255]. On the other hand, an HO-induced DSB activates also the Chk1 checkpoint kinase [238], which contributes to arrest the cell cycle in response to DSBs by controlling a pathway that is independent of Rad53 [256]. Importantly, *chk1*Δ cells do not display DNA damage hypersensitivity and are not defective in resection of uncapped telomeres [255,256]. We therefore asked whether *CHK1* deletion restores DNA damage resistance in *sae2*Δ cells. Consistent with the finding that Chk1 contributes to arrest the cell cycle after DNA damage independently of Rad53 [256], Rad53 was phosphorylated with wild type kinetics after HO induction in both *chk1*Δ and *sae2*Δ *chk1*Δ cells (**Figure 18A**). Furthermore, *CHK1* deletion suppresses the adaptation defect of *sae2*Δ cells. In fact, both *chk1*Δ and *sae2*Δ *chk1*Δ cells spotted on galactose-containing plates formed microcolonies of more than 2 cells with higher efficiency than wild type and *sae2*Δ cells (**Figure 18B**), although they did it less efficiently than *mec1*Δ cells,

where both Rad53 and Chk1 signaling were abrogated [256]. Strikingly, the lack of Chk1 did not suppress the hypersensitivity to DNA damaging agents of *sae2*Δ cells (**Figure 18C**), although it overrides the checkpoint-mediated cell cycle arrest.

To rule out the possibility that *CHK1* deletion failed to restore DNA damage resistance in *sae2*Δ cells because it impairs DSB resection, we used JKM139 derivative strains to monitor directly generation of ssDNA at the DSB ends in the absence of Chk1. As ssDNA is resistant to cleavage by restriction enzymes, we followed loss of SspI restriction sites as a measure of resection by Southern blot analysis under alkaline conditions, using a single-stranded probe that anneals to the 3' end at one side of the break. Consistent with previous indications that Chk1 is not involved in DNA-end resection [255], *chk1*Δ single mutant cells resected the DSB with wild type kinetics (**Figure 18D**). Furthermore, *CHK1* deletion did not exacerbate the resection defect of *sae2*Δ cells (**Figure 18E**). Altogether, these data indicate that the prolonged checkpoint-mediated cell cycle arrest of *sae2*Δ cells is not responsible for their hypersensitivity to DNA damaging agents.

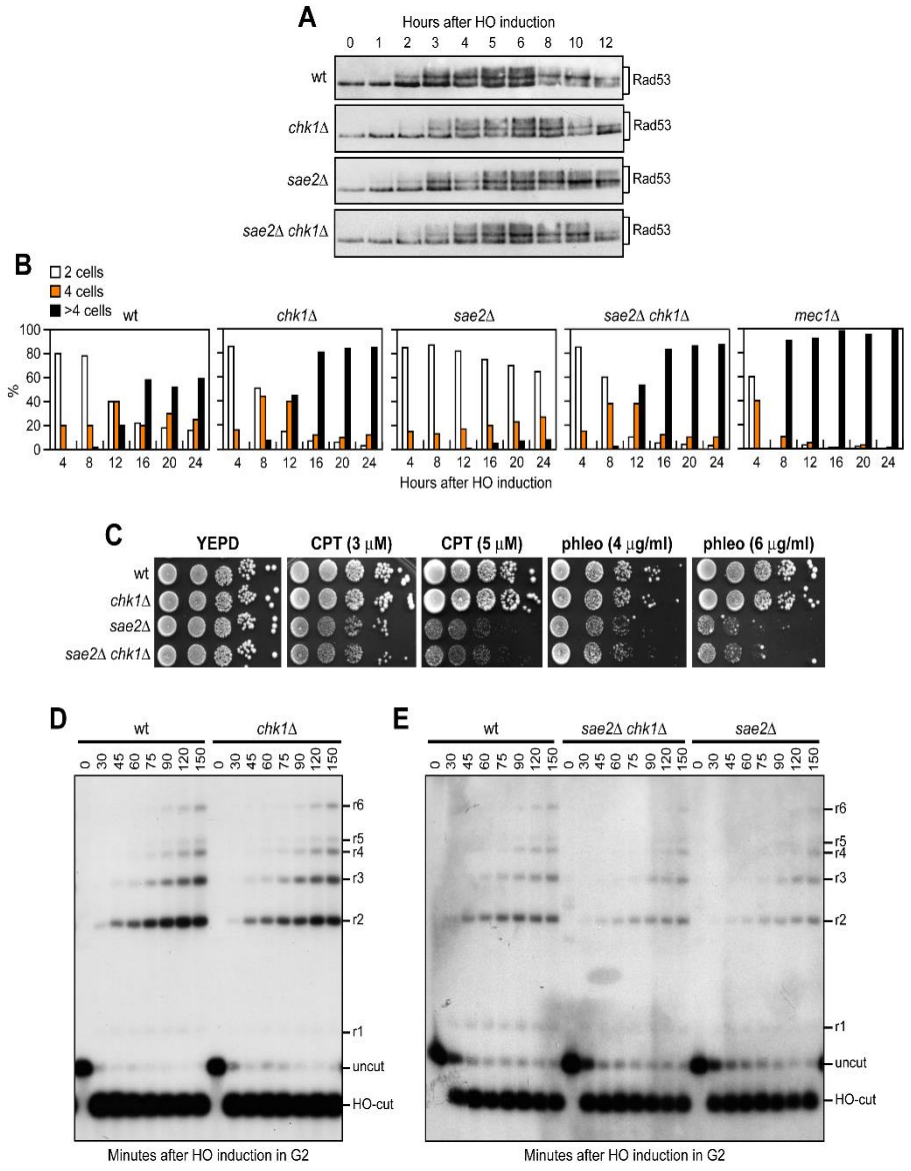
A
Hours after HO induction
0 1 2 3 4 5 6 8 10 12
wt
chk1Δ
sae2Δ
sae2Δ chk1Δ
Rad53
B
2 cells
4 cells
>4 cells
wt
chk1Δ
sae2Δ
sae2Δ chk1Δ
mec1Δ
%
Hours after HO induction
C
YEPD
CPT (3 μM)
CPT (5 μM)
phleo (4 μg/ml)
phleo (6 μg/ml)
wt
chk1Δ
sae2Δ
sae2Δ chk1Δ
D
wt
chk1Δ
0 30 45 60 75 90 120 150
r6
r5
r4
r3
r2
r1
uncut
HO-cut
Minutes after HO induction in G2
E
wt
sae2Δ chk1Δ
sae2Δ
0 30 45 60 75 90 120 150
r6
r5
r4
r3
r2
r1
uncut
HO-cut
Minutes after HO induction in G2

Figure 18. The lack of Chk1 does not suppress the hypersensitivity to DNA damaging agents of *sae2*Δ cells**.**
(A) Exponentially growing YEPR cultures of JKM139 derivative strains were transferred to YEPRG (time zero), followed by western blot analysis with anti-Rad53 antibodies. (B) YEPR G1-arrested cell cultures of JKM139 derivative strains were plated on galactose-containing plates (time zero). At the indicated time points, 200 cells for each strain were analyzed to determine the frequency of large budded cells (2 cells) and of cells forming microcolonies of 4 or more than 4 cells. (C) Exponentially growing cells were serially diluted (1:10) and each dilution was spotted out onto YEPD plates with or without camptothecin (CPT) and phleomycin. (D, E) DSB resection. YEPR exponentially growing cultures of JKM139 derivative cells were arrested in G2 with nocodazole and transferred to YEPRG in the presence of nocodazole at time zero. Gel blots of SspI-digested genomic DNA separated on alkaline agarose gel were hybridized with a single-stranded MAT probe that anneals to the unresected strand on one side of the break. 5'-3' resection progressively eliminates SspI sites, producing larger SspI fragments (r1 through r6) detected by the probe.

The Rad53-H88Y and Tel1-N2021D variants restore resection and SSA in sae2Δ cells

As the checkpoint-mediated cell cycle arrest was not responsible for the DNA damage hypersensitivity of *sae2*Δ cells, we asked whether Rad53-H88Y and/or Tel1-N2021D suppressed the *sae2*Δ resection defect. We first measured the efficiency of Single-Strand Annealing (SSA), a mechanism that repairs a DSB flanked by direct DNA repeats when sufficient resection exposes the complementary DNA sequences, which can then anneal to each other [24]. The *rad53-H88Y* and *tel1-N2021D* alleles were introduced in the YMV45 strain, which carries two tandem *leu2* gene repeats located 4.6 kb apart on chromosome III, with a HO recognition site adjacent to one of the repeats [240]. This strain also harbors a GAL-HO construct for galactose-inducible HO expression. Both Rad53-H88Y and Tel1-N2021D bypass Sae2 function in SSA-mediated DSB repair. In fact, accumulation of the SSA repair product after HO induction occurred more efficiently in both *sae2*Δ *rad53-H88Y* (**Figure 19A and B**) and *sae2*Δ *tel1-N2021D* (**Figure 19C and D**) than in *sae2*Δ cells, where it was delayed compared to wild type.

To confirm that Rad53-H88Y and Tel1-N2021D suppress the SSA defect of *sae2*Δ cells by restoring DSB resection, we used JKM139 derivative strains to monitor directly generation of ssDNA at the DSB ends. Indeed, *sae2*Δ *rad53-H88Y* (**Figure 20A**) and *sae2*Δ *tel1-N2021D* (**Figure 20B**) cells resected the HO-induced DSB more

efficiently than *sae2*Δ cells, indicating that both Rad53-H88Y and Tel1-N2021D suppress the resection defect of *sae2*Δ cells.

The DSB resection defect of sae2Δ cells is thought to be responsible for the increased persistence of MRX at the DSB [58]. Because Rad53-H88Y and Tel1-N2021D restore DSB resection in *sae2*Δ cells, we expected that the same variants also reduce the amount of MRX bound at the DSB. The amount of Mre11 bound at the HO-induced DSB end turned out to be lower in both *sae2*Δ *rad53-H88Y* and *sae2*Δ *tel1-N2021D* than in *sae2*Δ cells (**Figure 20C**). Therefore, the Rad53-H88Y and Tel1-N2021D variants restore DSB resection in *sae2*Δ cells and reduce MRX association/persistence at the DSB.

Consistent with the finding that Rad53-H88Y and Tel1-N2021D do not fully restore CPT resistance in *sae2*Δ cells (**Figure 14A**), and therefore do not bypass completely all Sae2 functions, the *rad53-H88Y* and *tel1-N2021D* mutations were unable to suppress the sporulation defects of *sae2*Δ/ *sae2*Δ diploid cells (**Figure 20D**), suggesting that they cannot bypass the requirement for Sae2/MRX endonucleolytic cleavage to remove Spo11 from meiotic DSBs.

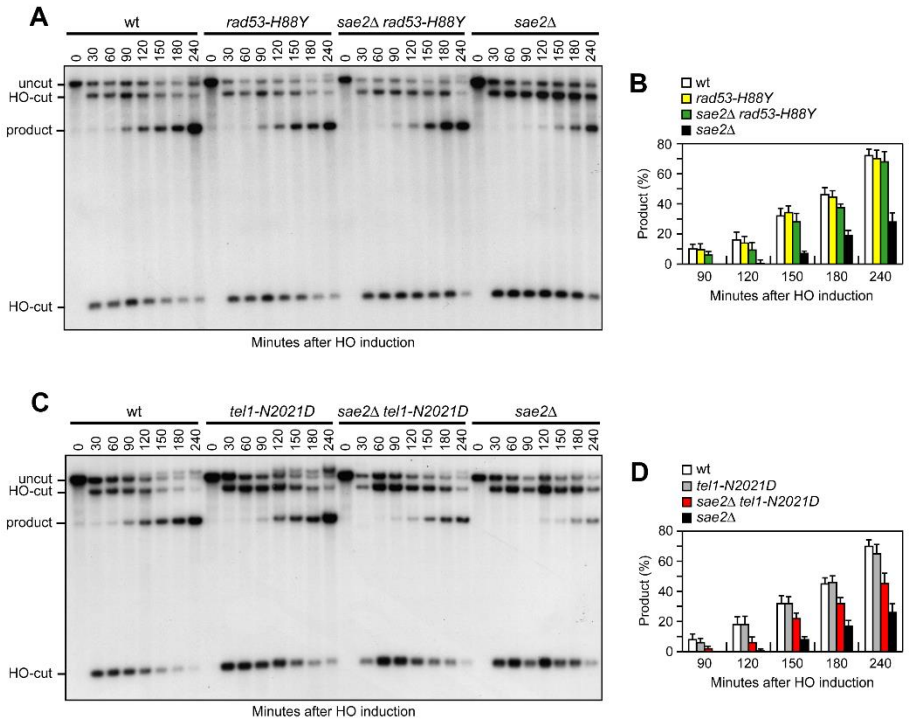

Figure 19 Rad53-H88Y and Tel1-N2021D suppress the SSA defect of *sae2*Δ cells**.** (A) DSB repair by SSA. YEPR exponentially growing cell cultures of YMV45 derivative strains, carrying the HO-cut site flanked by homologous leu2 sequences that are 4.6 kb apart, were transferred to YEPRG at time zero. HO-induced DSB formation results in generation of 12 kb and 2.5 kb DNA fragments (HO-cut) that can be detected by Southern blot analysis with a LEU2 probe of KpnI-digested genomic DNA. DSB repair by SSA generates an 8 kb fragment (product). (B) Densitometric analysis of the product band signals. The experiment as in (A) has been independently repeated three times and the mean values are represented with error bars denoting s.d. (n=3). (C) DSB repair by SSA was analyzed as in (A). (D) Densitometric analysis of the product band signals. The experiment as in (C) has been independently repeated three times and the mean values are represented with error bars denoting s.d. (n=3).

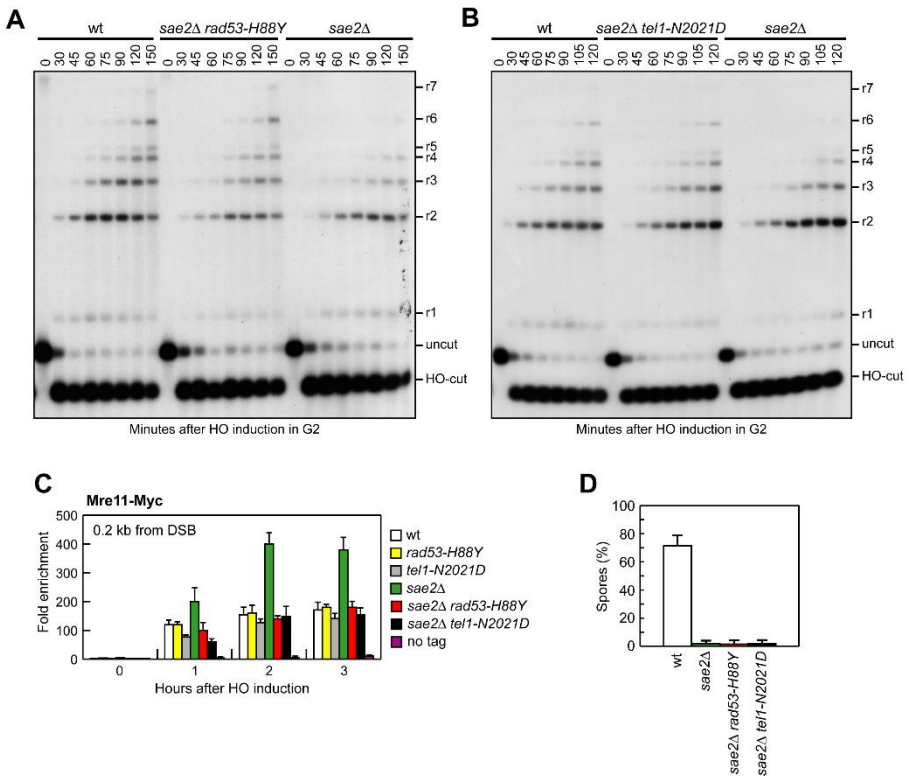

Figure 20 Rad53-H88Y and Tel1-N2021D suppress the resection defect of *sae2*Δ cells**.**

(A, B) DSB resection. YEPR exponentially growing cultures of JKM139 derivative strains were arrested in G2 with nocodazole and transferred to YEPRG in the presence of nocodazole at time zero. Detection of ssDNA was carried out as described in Figure 18D . 5'-3' resection produces SspI fragments indicated as r1 to r7. (C) ChIP analysis. Exponentially growing YEPR cell cultures of JKM139 derivative strains were transferred to YEPRG. Relative fold enrichment of Mre11-Myc at 0.2 kb from the HO cleavage site was evaluated after ChIP with anti-Myc antibodies and qPCR analysis compared to untagged Mre11 (no tag). In all diagrams, the ChIP signals were normalized for each time point to the amount of the corresponding input signal. The mean values are represented with error bars denoting s.d. (n=3). (D) Sporulation efficiency. Spores after 24 hours in sporulation medium of diploid cells homozygous for the indicated mutations.

Suppression of the DNA damage hypersensitivity of sae2Δ cells by Rad53-H88Y and Tel1-N2021D variants requires Sgs1-Dna2

The MRX complex not only provides the nuclease activity for initiation of DSB resection, but also allows extensive resection by promoting the binding at the DSB ends of the resection proteins Exo1 and Sgs1-Dna2 [156,167,234]. Suppression of the DNA damage hypersensitivity of *sae2*Δ cells by Rad53-H88Y and Tel1-N2021D requires the physical presence of the MRX complex but not its nuclease activity (**Figure 14C and D**). As the loading of Exo1, Sgs1-Dna2 at DSBs depends on the MRX complex independently of its nuclease activity [234], we asked whether the investigated suppression events require Exo1, Sgs1 and/or Dna2. This question was particularly interesting, as Rad53 was shown to inhibit resection at uncapped telomeres through phosphorylation and inhibition of Exo1 [185,255]. As shown in Fig. 23A, *sae2*Δ suppression by Rad53-H88Y and Tel1-N2021D was Exo1-independent. In fact, although the lack of Exo1 exacerbated the sensitivity to DNA damaging agents of *sae2*Δ cells, both *sae2*Δ *exo1*Δ *rad53-H88Y* and *sae2*Δ *exo1*Δ *tel1-N2021D* triple mutants were more resistant to genotoxic agents than *sae2*Δ *exo1*Δ double mutant cells (**Figure 21A**).

By contrast, neither Rad53-H88Y nor Tel1-N2021D were able to suppress the sensitivity to DNA damaging agents of *sae2*Δ cells carrying the temperature sensitive *dna2-1* allele (**Figure 21B**),

suggesting that Dna2 activity is required for their suppressor effect. Dna2, in concert with the helicase Sgs1, functions as a nuclease in DSB resection [156]. The *dna2-E675A* allele abolishes Dna2 nuclease activity, which is essential for cell viability and whose requirement is bypassed by the *pif1-M2* mutation that impairs the nuclear activity of the Pif1 helicase [257]. The lack of Sgs1 or expression of the Dna2-E675A variant in the presence of the *pif1-M2* allele impaired viability of *sae2*Δ cells even in the absence of genotoxic agents. The synthetic lethality of *sae2*Δ *sgs1*Δ cells, and possibly of *sae2*Δ *dna2-E675A pif1-M2*, is likely due to defects in DSB resection, as it is known to be suppressed by either *EXO1* overexpression or *KU* deletion [167]. Thus, we asked whether Rad53-H88Y and/or Tel1-N2021D could restore viability of *sae2*Δ *sgs1*Δ and/or *sae2*Δ *dna2-E675A pif1-M2* cells. Tetrad dissection of diploid cells did not allow to find viable spores with the *sae2*Δ *dna2-E675A pif1-M2 rad53-H88Y* (**Figure 21C**) or *sae2*Δ *dna2-E675A pif1-M2 tel1-N2021D* genotypes (**Figure 21D**), indicating that neither Rad53-H88Y nor Tel1-N2021D can restore the viability of *sae2*Δ *dna2-E675A pif1-M2* cells. Similarly, no viable *sae2*Δ *sgs1*Δ spores could be recovered, while *sae2*Δ *sgs1*Δ *rad53-H88Y* and *sae2*Δ *sgs1*Δ *tel1-N2021D* triple mutant spores formed very small colonies that could not be further propagated (**Figure 21E and F**). Finally, neither Rad53-H88Y nor Tel1-N2021D, which allowed DNA damage resistance in *sae2*Δ *exo1*Δ cells (**Figure 21A**), were able to suppress the growth defect of *sgs1*Δ *exo1*Δ double mutant cells even in the absence of genotoxic agents (**Figure 21G**). Altogether, these findings

indicate that suppression by Rad53-H88Y and Tel1-N2021D of the DNA damage hypersensitivity caused by the absence of Sae2 is dependent on Sgs1-Dna2.

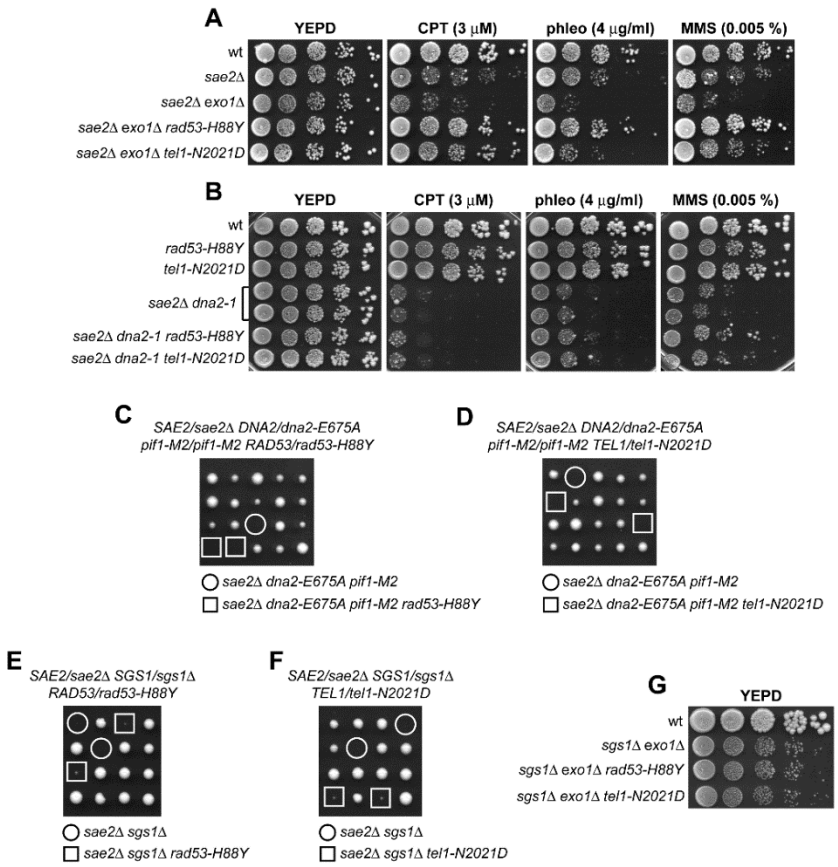

Figure 21 The Rad53-H88Y and Tel1-N2021D bypass of Sae2 function is Sgs1-Dna2-dependent.

(A, B) Exponentially growing cells were serially diluted (1:10) and each dilution was spotted out onto YEPD plates with or without camptothecin (CPT), phleomycin or MMS. (C-F) Meiotic tetrads were dissected on YEPD plates that were incubated at 25°C, followed by spore genotyping. (G) Exponentially growing cells were serially diluted (1:10) and each dilution was spotted out onto YEPD plates.

The lack of Rad53 kinase activity suppresses the DNA damage hypersensitivity and the resection defect of sae2Δ cells

The Rad53-H88Y protein is defective in interaction with Rad9 (**Figure 16C**) and therefore fails to undergo autophosphorylation and activation, prompting us to test whether other mutations affecting Rad53 activity can bypass Sae2 functions. To this end, we could not use *rad53Δ* cells because they show growth defects even when the lethal effect of *RAD53* deletion is suppressed by the lack of Sml1 [258]. We then substituted the chromosomal wild type *RAD53* allele with the kinase-defective *rad53-K227A* allele (*rad53-kd*), which does not impair cell viability in the absence of genotoxic agents but affects checkpoint activation [259]. The *rad53-kd* allele rescued the sensitivity of *sae2Δ* cells to CPT and MMS to an extent similar to Rad53-H88Y (**Figure 22A**). Furthermore, accumulation of the SSA repair products occurred more efficiently in *sae2Δ rad53-kd* cells than in *sae2Δ* (**Figure 22B and C**), indicating that the lack of Rad53 kinase activity bypasses Sae2 function in SSA-mediated DSB repair.

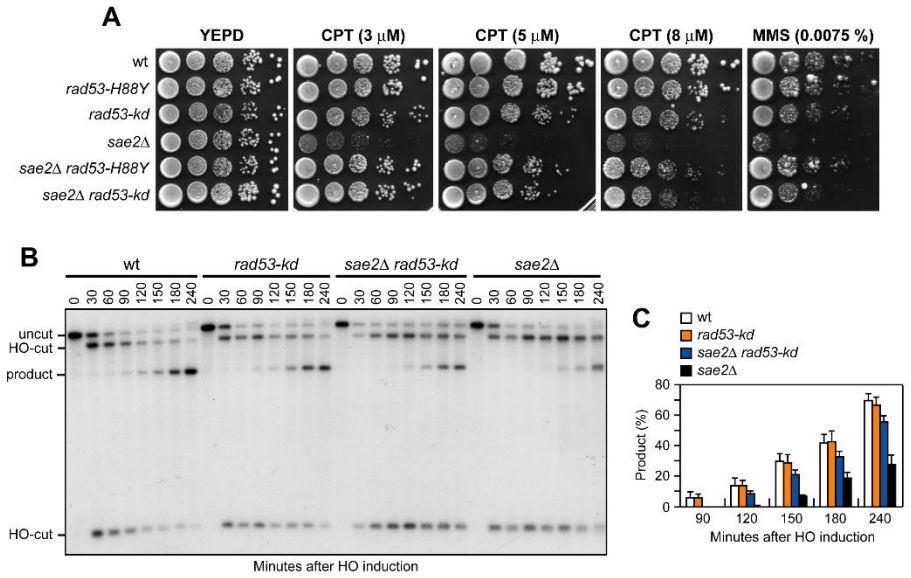

Figure 22 The Rad53-kd variant restores DNA damage resistance and SSA in *sae2*Δ cells.

(A) Exponentially growing cells were serially diluted (1:10) and each dilution was spotted out onto YEPD plates with or without camptothecin (CPT) or MMS. (B) DSB repair by SSA. The analysis was performed as described in Fig. 21A. (C) Densitometric analysis of the product band signals. The experiment as in (B) has been independently repeated three times and the mean values are represented with error bars denoting s.d. (n=3).

The lack of Tel1 kinase activity bypasses Sae2 function at DSBs, whereas Tel1 hyperactivation increases Sae2 requirement

Suppression of *sae2*Δ may be peculiar to Tel1-N2021D, which is poorly recruited to DSBs (**Figure 16F**), or it might be performed also by *TEL1* deletion (*tel1*Δ) or by expression of a Tel1 kinase defective variant (Tel1-kd). Indeed, the Tel1-kd variant, carrying the Gly2611Asp, Asp2612Ala, Asn2616Lys, and Asp2631Glu amino acid substitutions that abolish Tel1 kinase activity *in vitro* (**Figure 16E**) [253], rescued the hypersensitivity of *sae2*Δ cells to genotoxic agents to an extent similar to Tel1-N2021D (**Figure 23A**). The lack of Tel1 kinase activity bypassed also Sae2 function in DSB resection, because *sae2*Δ *tel1-kd* cells repaired a DSB by SSA more efficiently than *sae2*Δ cells (**Figure 23B and C**). By contrast, and consistent with previous studies [133,246] *TEL1* deletion was not capable to suppress the hypersensitivity to DNA damaging agents of *sae2*Δ cells (**Figure 23A**). Rather, *tel1*Δ *sae2*Δ double mutant cells displayed higher sensitivity to CPT than *sae2*Δ cell (**Figure 23A**). Altogether, these data indicate that the lack of Tel1 kinase activity can bypass Sae2 function both in DNA damage resistance and DSB resection, but these suppression events require the physical presence of the Tel1 protein.

As impairment of Tel1 function rescued the *sae2*Δ defects, we asked whether Tel1 hyperactivation exacerbates the DNA damage hypersensitivity of *sae2*Δ cells. We previously isolated the *TEL1-hy909*

allele, which encodes a Tel1 mutant variant with enhanced kinase activity that causes an impressive telomere over-elongation [260]. As shown in **Figure 23D**, *sae2*Δ *TEL1-hy909* double mutant cells were more sensitive to DNA damaging agents than *sae2*Δ single mutant cells. This enhanced DNA damage sensitivity was likely due to Tel1 kinase activity, as *sae2*Δ cells expressing a kinase defective Tel1-hy909-kd variant were as sensitive to DNA damaging agents as *sae2*Δ cells (**Figure 23D**). Thus, impairment of Tel1 activity bypasses Sae2 function at DSBs, whereas Tel1 hyperactivation increases the requirement for Sae2 in survival to genotoxic stress.

The absence of Tel1 failed not only to restore DNA damage resistance in *sae2*Δ cells (**Figure 23A**), but also to suppress their SSA defect (**Figure 24A and B**). The difference in the effects of *tel1*Δ and *tel1-kd* was not due to checkpoint signaling, as Rad53 phosphorylation decreased with similar kinetics in both *sae2*Δ *tel1-kd* and *sae2*Δ *tel1*Δ double mutant cells 10-12 hours after HO induction (**Figure 24C**). Interestingly, SSA-mediated DSB repair occurred with wild type kinetics in *tel1-kd* mutant cells (**Figure 23B and C**), while *tel1*Δ cells repaired a DSB by SSA less efficiently than wild type cells (**Figure 24A and B**), suggesting that Tel1 might have a function at DSBs that does not require its kinase activity. Indeed, *TEL1* deletion was shown to slight impair DSB resection [186]. Furthermore, it did not exacerbate the resection defect and the hypersensitivity to DNA damaging agents of *mre11*Δ cells (**Figure 24D**), suggesting that the absence of Tel1 can impair MRX function. Tel1 was also shown to promote MRX

association at DNA ends flanked by telomeric DNA repeats independently of its kinase activity [261], and we are showing that suppression of *sae2*Δ by Tel1-N2021D requires the physical presence of the MRX complex (**Figure 14D**). Thus, it is possible that the lack of Tel1 fails to bypass Sae2 function at DSBs because it reduces MRX association at DSBs to a level that is not sufficient to restore DNA damage resistance and DSB resection in *sae2*Δ cells. Indeed, the amount of Mre11 bound at the HO-induced DSB was decreased in *tel1*Δ, but not in *tel1-kd* cells, compared to wild type (**Figure 24E**). In agreement with a partial loss of Tel1 function, the Tel1-N2021D variant, whose association to DSBs is diminished compared to wild type Tel1 but not abolished (**Figure 16F**), only slightly decreased Mre11 association to the DSB (**Figure 24E**). As the rescue of *sae2*Δ by Tel1-N2021D requires the physical presence of the MRX complex, this Tel1 function in promoting MRX association to DSBs can explain the inability of *tel1*Δ to bypass Sae2 function in DNA damage resistance and resection.

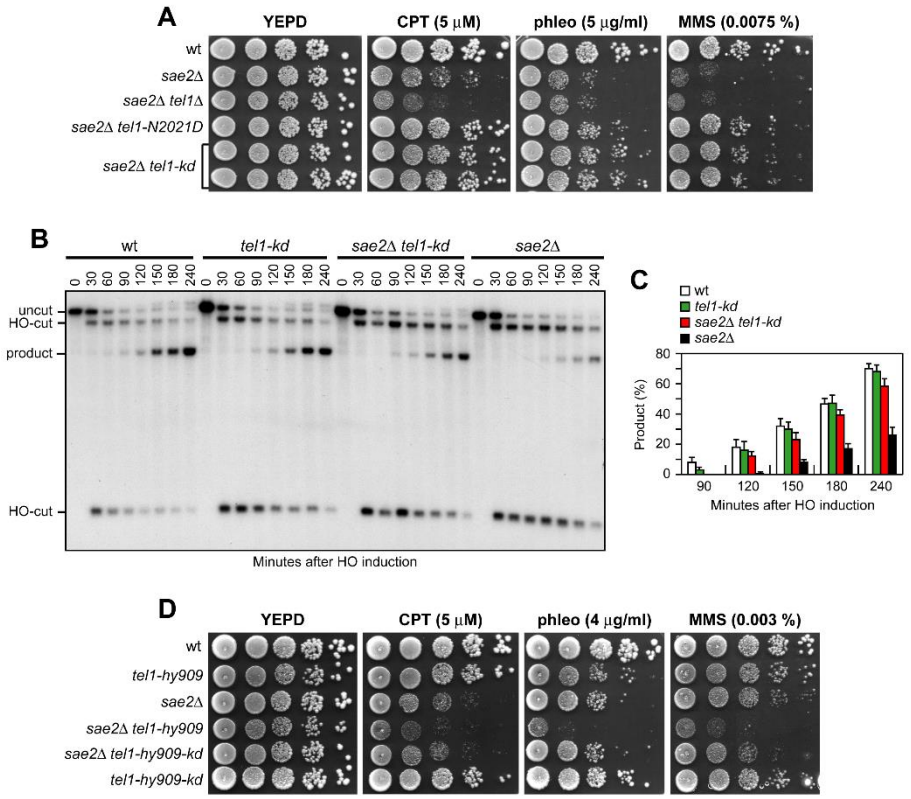

Figure 23 The Tel1-kd variant restores DNA damage resistance and SSA in *sae2*Δ cells.

(A) Exponentially growing cells were serially diluted (1:10) and each dilution was spotted out onto YEPD plates with or without camptothecin (CPT), phleomycin or MMS. (B) DSB repair by SSA. The analysis was performed as described in Fig. 21A. (C) Densitometric analysis of the product band signals. The experiment as in (B) has been independently repeated three times and the mean values are represented with error bars denoting s.d. (n=3). (D) Exponentially growing cells were serially diluted (1:10) and each dilution was spotted out onto YEPD plates with or without camptothecin (CPT), phleomycin or MMS.

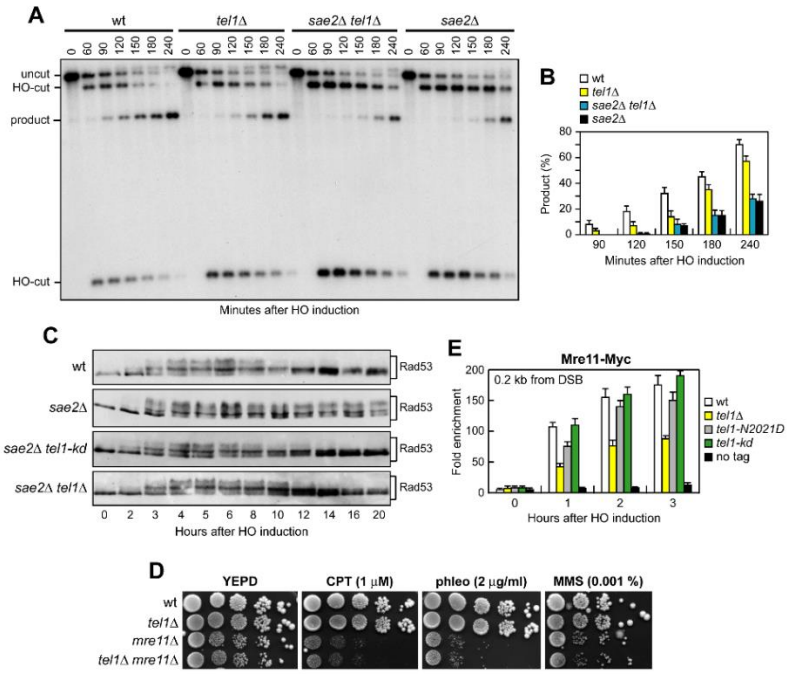

Figure 24 The lack of Tel1 does not restore DNA damage resistance and SSA in *sae2*Δ cells.

*(*A) DSB repair by SSA. The analysis was performed as described in Figure 19A. (B) Densitometric analysis of the product band signals. The experiment as in (A) has been independently repeated three times and the mean values are represented with error bars denoting s.d. (n=3). (C) Exponentially growing YEPR cell cultures of JKM139 derivative strains were transferred to YEPRG (time zero), followed by western blot analysis with anti-Rad53 antibodies of protein extracts prepared at the indicated time points. (D) Exponentially growing cells were serially diluted (1:10) and each dilution was spotted out onto YEPD plates with or without camptothecin (CPT), phleomycin or MMS. (E) ChIP analysis. Exponentially growing YEPR cell cultures of JKM139 derivative strains were transferred to YEPRG. Recruitment of Mre11-Myc compared to untagged Mre11 (no tag) at 0.2 kb from the HO-cut was determined by ChIP analysis and qPCR. In all diagrams, the ChIP signals were normalized for each time point to the amount of the corresponding input signal. The mean values are represented with error bars denoting s.d. (n=3).

Tel1 and Rad53 kinase activities promote Rad9 binding to the DSB ends

The suppression of the DNA damage hypersensitivity of *sae2*Δ cells by Rad53-H88Y and Tel1-N2021D requires Dna2-Sgs1 (**Figure 21**). Because Sgs1-Dna2 activity is counteracted by Rad9, whose lack restores DSB resection in *sae2*Δ cells [178,244], we asked whether suppression of the DSB resection defect of *sae2*Δ cells by Rad53 or Tel1 dysfunction might be due to decreased Rad9 association to the DSB ends. We have previously shown that wild type and *sae2*Δ cells have similar amounts of Rad9 bound at 1.8 kb from the DSB (**Figure 25A**) [58]. However, a robust increase in the amount of Rad9 bound at 0.2 kb and 0.6 kb from the DSB was detected in *sae2*Δ cells compared to wild type (**Figure 25A**) [178]. Strikingly, this enhanced Rad9 accumulation in *sae2*Δ cells was reduced in the presence of the Rad53-kd or Tel1-kd variant, which both decreased the amount of Rad9 bound at the DSB also in otherwise wild type cells (**Figure 25A**). Thus, Rad9 association close to the DSB depends on Rad53 and Tel1 kinase activity. Rad9 inhibits DSB resection by counteracting Sgs1 recruitment to DSBs [244] and, as expected, Sgs1 binding to DSBs was lower in *sae2*Δ cells than in wild type (**Figure 25B**). By contrast, the presence of Rad53-kd or Tel1-kd variants increased the amount of Sgs1 at the DSB in both wild type and *sae2*Δ cells (**Figure 25B**). Together with the observation that the suppression of *sae2*Δ hypersensitivity to genotoxic agents by Rad53 and Tel1 dysfunctions

requires Sgs1-Dna2, these findings indicate that the lack of Rad53 or Tel1 kinase activity restores DSB resection in *sae2*Δ cells by decreasing Rad9 association close to the DSB and therefore by relieving Sgs1-Dna2 inhibition. Although both *rad53-kd* and *tel1-kd* cells showed some lowering of Rad9 binding at DSBs compared to wild type cells (**Figure 25A**), they did not appear to accelerate SSA, suggesting that this extent of Rad9 binding is anyhow sufficient to limit resection in a wild type context. Rad9 is known to be enriched at the sites of damage by interaction with histone H2A that has been phosphorylated on Serine 129 (γH2A) by Mec1 and Tel1 [73,81,262,263]. As the lack of γH2A suppresses the SSA defect of *sae2*Δ cells [178], Tel1 activity might increase the amount of Rad9 bound at the DSB in *sae2*Δ cells by promoting generation of γH2A. Indeed, the *hta1-S129A* allele, which encodes a H2A variant where Ser129 is replaced by a non-phosphorylatable Alanine residue, thus causing the lack of γH2A, suppressed the resection defect of *sae2*Δ cells (**Figure 26**). Furthermore, γH2A formation turned out to be responsible for the enhanced Rad9 binding close to the break site, as *sae2*Δ *hta1-S129A* cells showed wild type levels of Rad9 bound at the DSB (**Figure 25C**). Finally, γH2A formation close to the DSB depends on Tel1 kinase activity, as γH2A at the DSB was not detectable in *sae2*Δ *tel1-kd* cells (**Figure 26D**). Altogether, these data indicate that Tel1 promotes Rad9 association to DSB in *sae2*Δ cells through γH2A generation.

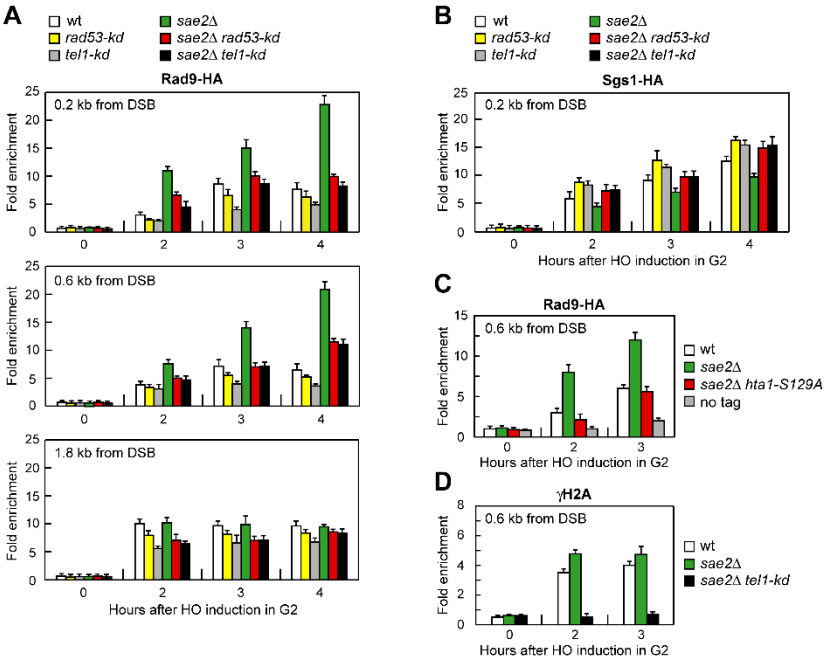

Figure 25 Rad53-kd and Tel1-kd prevent Rad9 association at DSBs.
(A) ChIP analysis. Exponentially growing YEPR cell cultures of JKM139 derivative strains were arrested in G2 with nocodazole and transferred to YEPRG in the presence of nocodazole. Recruitment of Rad9-HA at the indicated distance from the HO-cut was determined by ChIP and qPCR. In all diagrams, the ChIP signals were normalized for each time point to the amount of the corresponding input signal. The mean values are represented with error bars denoting s.d. (n=3). (B) As in (A), but showing Sgs1-HA binding. (C) As in (A). All strains carried also the deletion of HTA2 gene. D) As in (A), but showing γH2A binding.

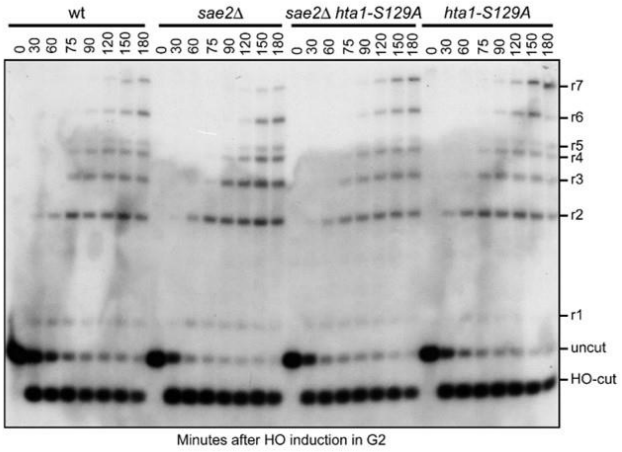

Figure 26 The lack of γH2A suppresses the resection defect of sae2Δ cells. DSB resection.
YEPR exponentially growing cultures of JKM139 derivative cells with the indicated genotypes were arrested in G2 with nocodazole and transferred to YEPRG in the presence of nocodazole at time zero. All strains carried also the deletion of HTA2 gene. Resection is analyzed as in Figure 18D.

EMBO reports **(Villa *et al*., 2018)**
EMBO Rep. 2018 Jan 4.
doi:10.15252/embr.201744910**.**

Rad9/53BP1 protects stalled replication forks from degradation in Mec1/ATR-defective cells

Matteo Villa, Diego Bonetti, Massimo Carraro & Maria Pia Longhese

Dipartimento di Biotecnologie e Bioscienze, Università di Milano-Bicocca, Italy.

DNA replication stress is an important source of genomic instability and can be induced by a transient slowing or stalling of replication forks due to damaged DNA, unusual DNA structures, repetitive sequences or nucleotide depletion [190,191]. Stalled replication forks generally result in the uncoupling either of leading from lagging strand polymerases or of polymerases from replicative helicases. These events cause generation of tracts of Replication Protein A (RPA)-covered single stranded DNA (ssDNA) that recruits the checkpoint kinase Mec1 (ATR in mammals) [60]. Once activated, Mec1/ATR propagates the checkpoint signal to the downstream checkpoint kinase Rad53 (CHK2 in mammals), whose activation requires the interaction with the mediator protein Mrc1 [190,191]. Rad53 activation in turn prevents entry into mitosis, increases the intracellular dNTP pools, represses late origins firing and prevents fork collapse through poorly identified pathways [190,191].

Replication stress can be experimentally induced by treatment with the ribonucleotide reductase inhibitor hydroxyurea (HU), which globally blocks active replication forks by depleting the cellular pool of deoxynucleotide triphosphates (dNTPs) [190,191]. Although the molecular mechanism is still unclear, a key function of the S-phase checkpoint in ensuring cell survival to replication stress is to maintain the ability of the replisome to resume DNA synthesis once the block to fork progression is relieved [206,207,264,265]. Replisome components appear to be no longer associated with the replicative sites in Mec1- and Rad53-defective mutants [208,212,266], although the replication

proteins might still remain bound to chromatin but unable to resume replication [267].

The RecQ helicase Sgs1 (BLM in mammals) acts synergistically with Mec1 in resuming DNA replication upon replication stress, possibly by promoting the resolution of recombination structures that accumulate at damaged replication forks [211,212,241,266]. Furthermore, it contributes to initiate the checkpoint in response to stalled forks by promoting the recruitment of Rad53 into close proximity of Mec1-Ddc2 [200]. Finally, in both yeast and mammals, Sgs1 and some nucleases like Mre11, Sae2 (CtIP in mammals), Exo1 and Dna2 have been implicated in the nucleolytic processing of intrachromosomal DNA double-strand breaks (DSBs). In particular, Sae2-dependent Mre11 endonuclease activity generates a nick in the 5'-terminated strand that provides the access for Exo1 and Dna2 nucleases that can degrade DNA in the 5'-3' direction [125,129,150,152,156,159]. The helicase activity of Sgs1 unwinds double-stranded DNA and generates a substrate for Dna2 that cleaves ssDNA overhangs adjoining a duplex DNA [150,152,156,159,268]. The resection activity of Sgs1-Dna2 is thought to be inhibited by the checkpoint protein Rad9 (53BP1 in mammals) [178,244], which provides a barrier to DNA end resection [170,229].

The above yeast and mammalian nucleases have key roles also in the processing of replication intermediates to allow repair/restart of stalled replication forks and/or to prevent accumulation of replication-associated DSBs [190,191,269]. However, unrestricted nuclease

access to replication forks could destroy the fork structure and prevent continued DNA synthesis, leading to genome instability. In the absence of the intra-S-phase checkpoint, the genome of HU-treated yeast cells is subjected to degradation by Exo1 [193,215–217] and Sae2 [217]. Furthermore, replication stress in ATR-defective *S. pombe* and mammalian cells results in MRE11- and EXO1-dependent ssDNA accumulation [270,271], suggesting that the checkpoint plays a role in protecting replication forks from aberrant nuclease activity. Consistent with this hypothesis, phospho-proteomic screens have identified Exo1 as a target of Rad53, which negatively regulates Exo1 activity through phosphorylation events [185,272]. Furthermore, the fission yeast ortholog of Rad53, Cds1, phosphorylates and regulates Dna2 activity [273], which is involved in the processing and restart of reversed forks in both yeast and mammals [197,274].

Mammalian proteins involved in homologous recombination (HR) or in the Fanconi Anaemia (FA) network, including FANCD2, RAD51, BRCA1 and BRCA2, have been shown to prevent excessive fork degradation by antagonizing MRE11 and DNA2 actions [195,219,275–280]. Furthermore, loss of the WRN exonuclease activity enhances degradation at nascent DNA strands by EXO1 and MRE1 [223,225], whereas cells depleted of BOD1L protein exhibit a DNA2-dependent degradation of stalled/damaged replication forks [226].

Here we show that the *Saccharomyces cerevisiae* checkpoint protein Rad9, ortholog of mammalian 53BP1, is important to restrain uncontrolled nucleolytic degradation of damaged replication forks

when Mec1 is not fully functional. Loss of Rad9 or expression of a Sgs1 variant (Sgs1-G1298R), which escapes Rad9-mediated inhibition of DNA-end resection, exacerbates the sensitivity to dNTP depletion of cells expressing the Mec1-100 defective variant. This protective function of Rad9 is independent of checkpoint activation and is mainly due to Rad9-Dpb11 interaction. The severe HU sensitivity of *rad9*Δ *mec1-100* and *sgs1-G1298R mec1-100* cells is accompanied by increased ssDNA generation at stalled replication forks and impaired DNA replication recovery upon dNTP depletion. These findings, together with the observation that Dna2 inactivation decreases the amount of ssDNA at stalled replication forks in both *rad9*Δ *mec1-100* and *sgs1-G1298R mec1-100* cells, indicate a role for Rad9 in supporting viability of Mec1-defective cells by protecting replication forks from degradation.

Both Sgs1-G1298R and the lack of Rad9 exacerbate the sensitivity to HU of mec1-100 cells

The RecQ helicase Sgs1 is involved in resection of DNA DSBs [125,156]. The lack of Sgs1 causes cell death in *sae2*Δ cells and this synthetic lethality can be due to defective DSB resection, as it is suppressed by either *EXO1* overexpression or elimination of the resection inhibitor Ku complex [167]. We have previously described the *sgs1-G1298R* allele that fully suppresses the hypersensitivity to genotoxic agents (**Figure 27A**) and the resection defect of *sae2*Δ cells [244].

Unlike *SGS1* deletion, the Sgs1-G1298R variant did not cause by itself hypersensitivity to hidroxyurea (HU), camptothecin (CPT) or methyl methanesulfonate (MMS) (**Figure 27B**).

Sgs1 is thought to work together with the recombination protein Mus81 in the processing of repair intermediates that occur at the replication forks [281]. The lack of Mus81 causes cell death in a *sgs1*Δ background [200], presumably because Sgs1 is implicated in the resolution of, or recovery from, recombination events that arise in the absence of Mus81. We found that *sgs1-G1298R* did not impair cell viability when combined with the lack of Mus81 (**Figure 27C**), supporting further the finding that Sgs1-G1298R maintains most if not all Sgs1 functions.

In addition to its role in promoting DSB resection, Sgs1 is constitutively associated to replications forks, where it acts synergistically with Mec1

in fork maintenance under replication stress [212,266]. To understand how Sgs1 functions in DSB resection and DNA replication under stress conditions are connected to each other, we analyzed the effects of the *sgs1-G1298R* allele in cells defective for the Mec1 checkpoint kinase. As *mec1*-null cells (kept viable by deleting *SML1*) die even in the presence of very low HU doses and experience extensive fork degradation after exposure to replication stress [206,216,282], we took advantage of the *mec1-100* mutant allele that causes less severe sensitivity to HU compared to the *mec1*-null allele [283]. Furthermore, unlike *mec1*-null cells, *mec1-100* cells are partially defective in the intra-S checkpoint but not in the G2/M checkpoint and are able to resume DNA replication after HU removal, although less efficiently than wild type cells [282,284]. Similar to *sgs1*Δ *mec1-100* cells, *sgs1-G1298R mec1-100* double mutant cells were more sensitive to HU treatment compared to *mec1-100* single mutant cells (**Figure 27D**), indicating that Sgs1-G1298R becomes detrimental for cell viability when the intra-S checkpoint is not fully functional.

The resection activity of Sgs1/Dna2 is inhibited by the checkpoint protein Rad9 [178,244], which is known to limit resection of DNA DSBs [170,229]. We have previously demonstrated that Sgs1-G1298R not only suppresses the resection defect of *sae2*Δ cells (**Figure 27A**), but it also accelerates the resection process by escaping the Rad9-mediated inhibition of DSB resection [244]. This finding prompted us to investigate the effect of deleting *RAD9* in *mec1-100* cells. The lack of Rad9, which did not cause HU hypersensitivity by itself, exacerbated

the sensitivity to HU of *mec1-100* cells, with *mec1-100 rad9*Δ cells being more sensitive to HU than *sgs1-G1298R mec1-100* cells (**Figure 27E**). The HU sensitivity of *sgs1-G1298R rad9*Δ *mec1-100* triple mutant cells was similar to that of *rad9*Δ *mec1-100* double mutant cells (**Figure 27F**), indicating that the lack of Rad9 or the presence of Sgs1-G1298R impair viability of HU-treated *mec1-100* cells by affecting the same mechanism.

These synthetic effects on HU are not specific for a *mec1-100* background. In fact, the lack of Rad9 or the presence of Sgs1-G1298R exacerbated the HU sensitivity of cells carrying either *MEC1* deletion (kept viable by *SML1* deletion) (**Figure 28A**) or the hypomorphic *mec1-14* allele (**Figure 28B**). *RAD9* deletion also increased the HU sensitivity of cells carrying a Rad53 kinase defective variant (*rad53-K227A*) (**Figure 28C**), whereas it had no effect on cells lacking the downstream checkpoint kinase Chk1 (**Figure 28D**).

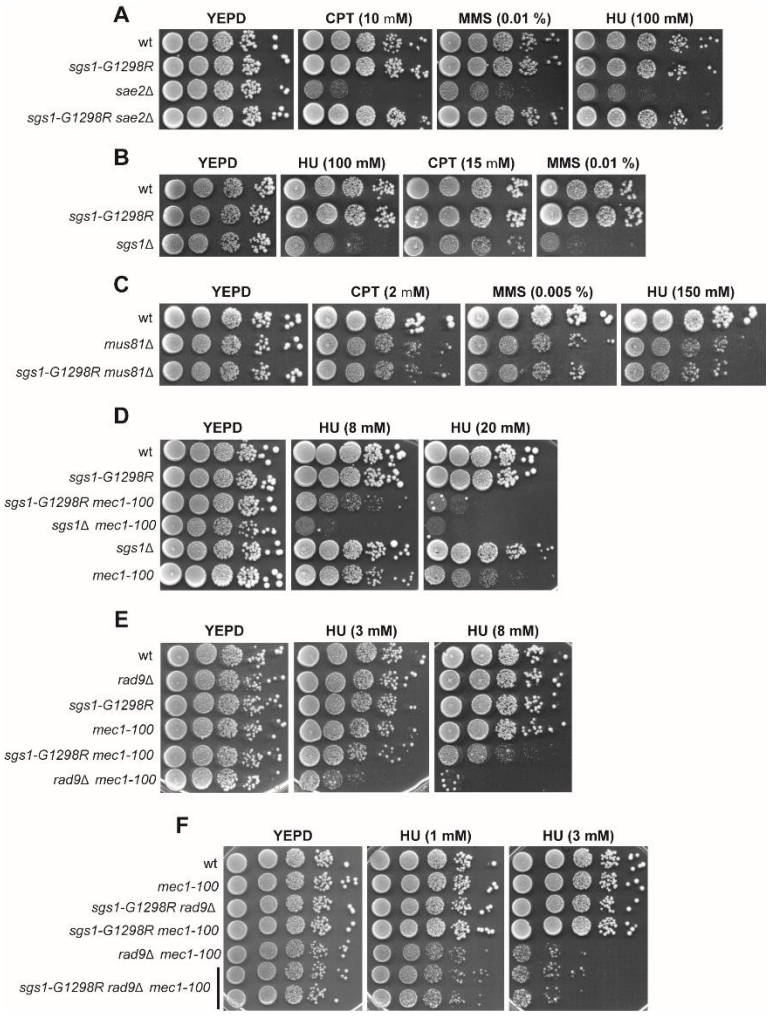

Figure 27 The HU sensitivity of *mec1-100* cells is exacerbated by either Sgs1-G1298R or the lack of Rad9**.**

(A-F) Exponentially growing cell cultures were serially diluted (1:10) and each dilution was spotted out onto YEPD plates with or without CPT, MMS or HU at the indicated concentrations.

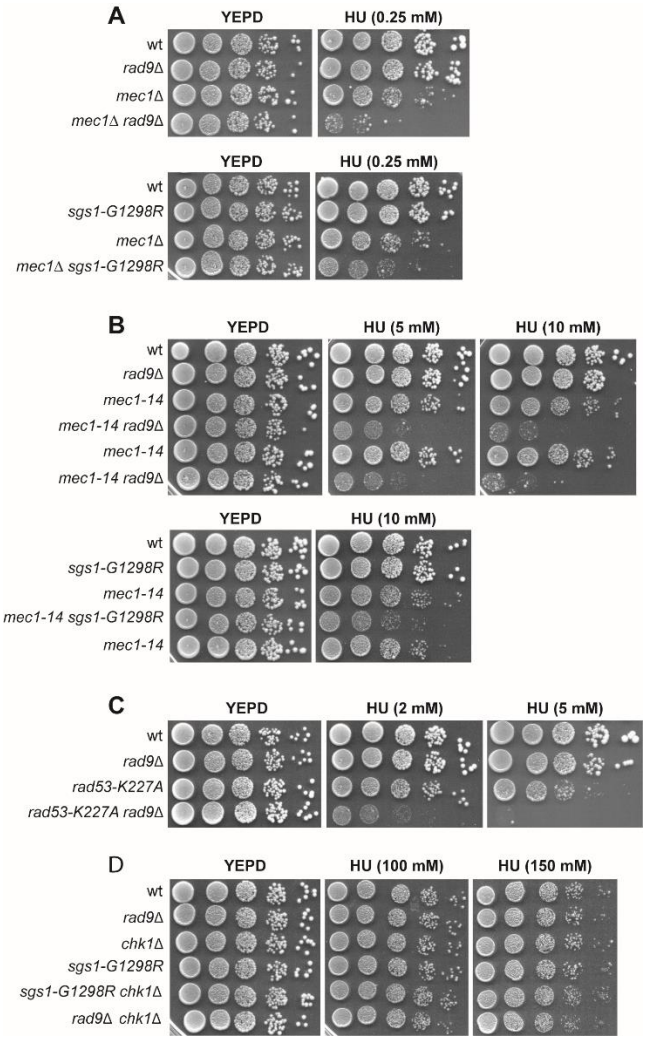

Figure 28 The synthetic effects of *rad9Δ* and *sgs1-G129R* on HU are not specific for *mec1-100*.
(A-D) Exponentially growing cultures were serially diluted (1:10) and each dilution was spotted out onto YEPD plates with or without HU at the indicated concentrations.

Both Sgs1-G1298R and the lack of Rad9 impair the ability of mec1-100 cells to resume DNA replication under replicative stress

We examined the effects caused by either the lack of Rad9 or the presence of Sgs1-G1298R on the ability of *mec1-100* cells to resume DNA replication after transient HU arrest by measuring DNA content by flow cytometry. Cells were blocked in G1 with α-factor and released into medium containing HU. After 2 hr, cells were transferred to medium lacking HU but containing nocodazole to prevent passage through mitosis. Wild type, *rad9*Δ and *sgs1-G1298R* cells completed replication in 40-50 minutes after release, whereas *mec1-100* cells reached significant amounts of DNA synthesis 20-30 minutes later (**Figure 29A**). By contrast, *rad9*Δ *mec1-100* and *sgs1-G1298R mec1-100* double mutant cells were unable to reach 2C DNA content even after 90 minutes (**Figure 29A**), indicating a severe defect in resuming DNA replication after transient HU exposure. Furthermore, both *rad9*Δ *mec1-100* and *sgs1-G1298R mec1-100* cells exhibited a rapid loss of viability when synchronously released from a G1 arrest into S phase in the presence of HU (**Figure 29B**).

To follow the fate of stalled replication forks in a more direct way, we used bromodeoxyuridine (BrdU) pulse-chase experiments to label nascent strands during DNA replication in HU. We used strains that can incorporate BrdU into DNA because they express both the nucleoside transporter hENT and a thymidine kinase from Herpes

Simplex virus. Cells were synchronized in G1 with α-factor and released into medium containing HU and BrdU (**Figure 29C**). After the nascent DNA was labeled, the BrdU was chased by transferring cells to medium lacking both HU and BrdU and containing thymidine (**Figure 29C**). As previously reported [216], labeled nascent DNA replication intermediates detected by using anti-BrdU antibody appeared as a smear in all HU-treated strains (**Figure 29D**). After release, most of the incorporated BrdU had been chased into high-molecular-weight within 20 and 40 minutes in wild type and *mec1-100* cells, respectively (**Figure 29D**). By contrast, the majority of the nascent DNA in both *rad9*Δ *mec1-100* and *sgs1-G1298R mec1-100* cells remained at the same position even after 60 minutes after release (**Figure 29D**), indicating a failure to resume DNA replication after HU-induced fork stalling.

Next, we measured the association to the early ARS607 and ARS305 replication origins of Myc-tagged DNA Polε by chromatin immunoprecipitation (ChIP) and quantitative PCR (qPCR) in cells synchronously released from a G1 arrest into S phase in the presence of HU. DNA Polε in wild type cells was efficiently bound to ARS607 and ARS305 about 20 minutes after release in HU (**Figure 29E**). By contrast, both ARS607- and ARS305-Polε association diminished in *mec1-100* cells compared to wild type and decreased further in both *sgs1-G1298R mec1-100* and *rad9*Δ *mec1-100* cells (**Figure 29E**).

To understand the possible impact of the *sgs1-G1298R* and *rad9*Δ mutations on checkpoint activation, we monitored Rad53

phosphorylation in cells synchronously released from a G1 arrest into S phase in the presence of HU. According to the finding that Mec1-100 does not completely abolish checkpoint activation [283], *mec1-100* cells showed a delay in Rad53 phosphorylation compared to wild type cells and residual Rad53 phosphorylation was under detection level in *rad9*Δ *mec1-100* cells (**Figure 29F**). By contrast, the presence of the *sgs1-G1298R* allele did not decrease the amount of Rad53 phosphorylated forms in *mec1-100* cells (**Figure 29F**), indicating that the increased HU hypersensitivity of *sgs1-G1298R mec1-100* double mutant cells cannot be ascribed to impaired checkpoint activation.

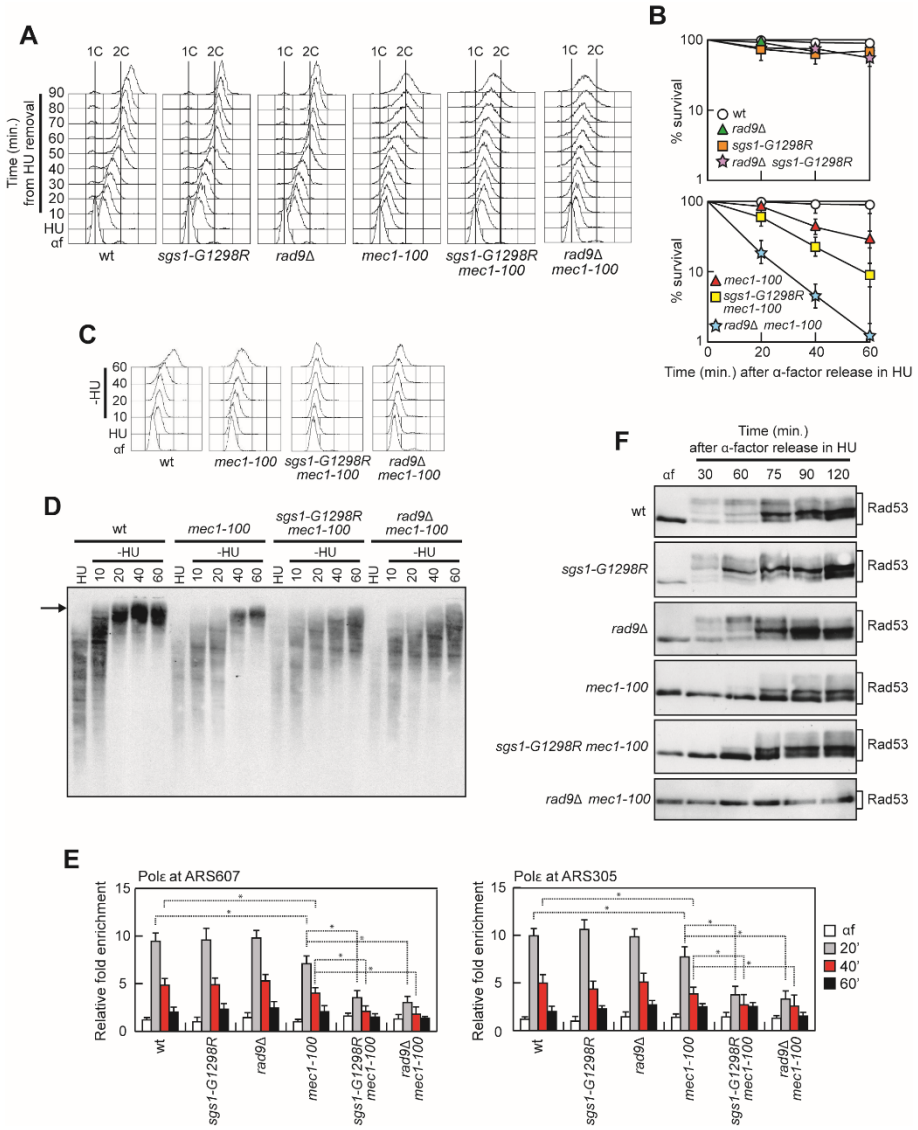
A
1C 2C
Time (min.) from HU removal
90
80
70
60
50
40
30
20
10
HU
αf
wt
sgs1-G1298R
rad9Δ
mec1-100
sgs1-G1298R mec1-100
rad9Δ mec1-100
B
% survival
wt
rad9Δ
sgs1-G1298R
rad9Δ sgs1-G1298R
mec1-100
sgs1-G1298R mec1-100
rad9Δ mec1-100
Time (min.) after α-factor release in HU
C
-HU
HU
αf
D
-HU
HU
10
20
40
60
E
Polε at ARS607
Polε at ARS305
Relative fold enrichment
αf
20'
40'
60'
F
Time (min.) after α-factor release in HU
αf
30
60
75
90
120
Rad53

Figure 29 The ability of *mec1-100* cells to resume DNA replication under replicative stress is impaired by either Sgs1-G1298R or the lack of Rad9
(A) Cells were arrested in G1 with α-factor (αf) and then released in YEPD containing 0.2M HU at time zero. After 2 hr (HU), cells were transferred to medium lacking HU but containing nocodazole to prevent passage through mitosis. Aliquots of each culture were harvested at the indicated times after HU removal to determine DNA content by flow cytometry. (B) Cell viability. Cells were arrested in G1 with α-factor and then released in YEPD containing 0.2M HU at time zero. Cells taken at the indicated time points after release in HU were tested for colony forming units on YEPD plates. Plotted values are the mean values with error bars denoting s.d. (n=3). (C, D) Immunodetection of BrdU-pulsed DNA. Cells were arrested in G1 with α-factor (αf) and released into YEPD containing 0.2M HU + 25μM BrdU. After 1 hour (HU), cells were chased with 2 mM thymidine into fresh medium and samples were taken at the indicated times after chase (-HU). DNA content during the time course was measured by flow cytometry (C). BrdU-labeled DNA was detected with anti-BrdU antibody (D). High molecular weight DNA molecules are indicated by an arrow. (E) ChIP analysis. Cells were arrested in G1 with α-factor and then released in YEPD containing 0.2M HU at time zero. Relative fold enrichment of Myc-tagged DNA Polε at ARS607 and ARS305 replication origins was determined after ChIP with anti-Myc antibodies and subsequent qPCR analysis. Plotted values are the mean values with error bars denoting s.d. (n=3). *P<0.05 (Student's t-test). (F) Cells were arrested in G1 with α-factor (αf) and then released in YEPD containing 0.2M HU.

Dna2 dysfunction is epistatic to rad9Δ and sgs1-G1298R with respect to the HU sensitivity of mec1-100 cells

Extensive DSB resection can be carried out by either of two pathways dependent on the enzymatic activities of the nucleases Exo1 and Dna2, respectively [125,150,152,156,159]. While Exo1 does not require a helicase activity to resect DNA ends, Sgs1 helicase is known to support the nuclease activity of Dna2 that degrades DNA endonucleolytically [150,152,156,159,268]. Thus, we analyzed the consequences of inactivating Exo1 or Dna2 on the HU sensitivity of *rad9Δ mec1-100* and *sgs1-G1298R mec1-100* double mutant cells. As expected [216], *EXO1* deletion exacerbated the HU sensitivity of *mec1-100* cells and the presence of *sgs1-G1298R* increased further the HU hypersensitivity of *exo1Δ mec1-100* cells (**Figure 30A**), indicating that *sgs1-G1298R* and *exo1Δ* increase the HU sensitivity of *mec1-100* cells by altering two different pathways.

As Dna2 is essential for cell viability [285], we used the hypomorphic *dna2-1* allele, which increased the HU sensitivity of *mec1-100* cells possibly due to defects in DNA replication (**Figure 30B**). The presence of the *dna2-1* allele was epistatic to both *sgs1-G1298R* and *rad9Δ* with respect to the HU sensitivity of *mec1-100* cells. In fact, the HU sensitivity of *sgs1-G1298R dna2-1 mec1-100* cells was similar to that *dna2-1 mec1-100* (**Figure 30B**), suggesting that Sgs1-G1298R and Dna2-1 increase the HU sensitivity of *mec1-100* by altering the same

pathway. Furthermore, the HU sensitivity of *rad9*Δ *dna2-1 mec1-100* cells was similar to that of *dna2-1 mec1-100* cells and less severe than that of *rad9*Δ *mec1-100* cells (**Figure 30C**), suggesting that the lack of Rad9 requires Dna2 to exacerbate the HU sensitivity of *mec1-100* cells.

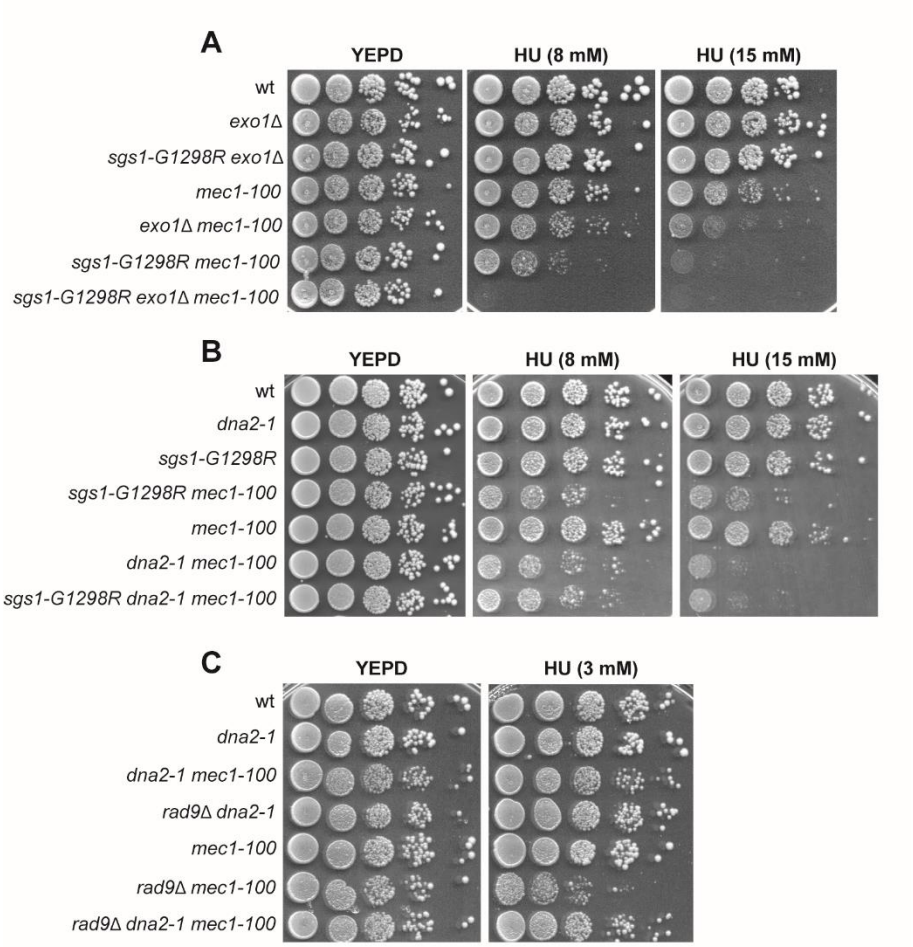

Figure 30 Epistatic relationships between *rad9Δ*, *sgs1-G1298R*, *exo1Δ* and *dna2-1* with respect of the HU sensitivity of mec1-100 cells.
(A-C) Exponentially growing cultures were serially diluted (1:10) and each dilution was spotted out onto YEPD plates with or without HU at the indicated concentrations.

Dpb11-mediated recruitment of Rad9 plays the major role in supporting mec1-100 survival to replicative stress

We investigated whether Rad9 is recruited at stalled replication forks by ChIP and qPCR in cells synchronously released from a G1 arrest into S phase in the presence of HU. Transient Rad9 association to ARS607 replication origin was detected in both wild type and *mec1-100* cells about 30 minutes after release in the presence of HU, with *mec1-100* cells showing a stronger Rad9 association (**Figure 31A**).

Recruitment of Rad9 to chromatin involves multiple pathways. In both yeast and mammals, Rad9 is constitutively bound to chromatin even in the absence of DNA damage through the interaction between its Tudor domain and histone H3 methylated at K79 (H3-K79me) [79,80,286–288]. In addition, Rad9 binding to the damaged sites is further strengthened through the interaction of its BRCT domain with histone H2A phosphorylated at S129 (γH2A) by Mec1 and Tel1 checkpoint kinases [262,263]. Finally, phosphorylation of the S462 and T474 Rad9 residues by cyclin-dependent kinase (Cdk1) leads to Rad9 interaction with the multi-BRCT domain protein Dpb11 (TopBP1 in mammals), which is a replication factor that mediates histone-independent Rad9 recruitment to damaged sites [82,83].

To investigate which of the above pathways could mediate Rad9 function in supporting viability of *mec1-100* cells under replication stress, we analyzed the HU sensitivity of *mec1-100* cells that were

defective in Rad9 binding to H3-K79me, γH2A or Dpb11. The HU sensitivity of *mec1-100* cells was only slightly increased by expression of either the *rad9-Y798A* or the *hta1-S129A* allele (**Figure 31B**), which abolishes γH2A generation and Rad9 association to H3-K79me, respectively [79,80,262,263,288]. By contrast, the HU sensitivity of *mec1-100* cells was dramatically increased by expression of the *rad9-S462A-T474A* allele (*rad9-STAA*) (**Figure 31B**), which lacks the S462 and T474 Cdk1-dependent phosphorylation sites that mediate Rad9-Dpb11 interaction [83]. This finding indicates that Dpb11-dependent recruitment of Rad9 plays the major role in supporting *mec1-100* resistance to replicative stress.

While the lack of Rad9 impairs checkpoint activation in response to DNA damage in G1 and G2, the Rad9-STAA mutant variant is fully able to activate both the G1/S and the G2/M checkpoints [172]. Moreover, the lack of either γH2A or H3-K79me affects only activation of the G1/S checkpoint [57-63]. The increased HU sensitivity of *mec1-100* cells lacking histone-dependent or -independent Rad9 association to DNA cannot be attributed to impaired activation of the downstream kinase Rad53. In fact, unlike *RAD9* deletion that reduces Rad53 phosphorylation in HU-treated *mec1-100* cells (**Figure 29F**), Rad53 phosphorylation in *rad9-Y798A mec1-100*, *hta1-S129A mec1-100* and *rad9-STAA mec1-100* cell cultures synchronously released from a G1 arrest into S phase in the presence of HU was similar to that of *mec1-100* cells (**Figure 31C**). The finding that *rad9*Δ *mec1-100* cells, which displayed an undetectable Rad53 phosphorylation upon replicative

stress (**Figure 29F**), were more sensitive to HU than *rad9-STAA mec1-100* cells and *sgs1-G1298R mec1-100* cells (**Figure 31B**) suggests that part of the *rad9Δ mec1-100* HU hypersensitivity is due to a defect in checkpoint activation

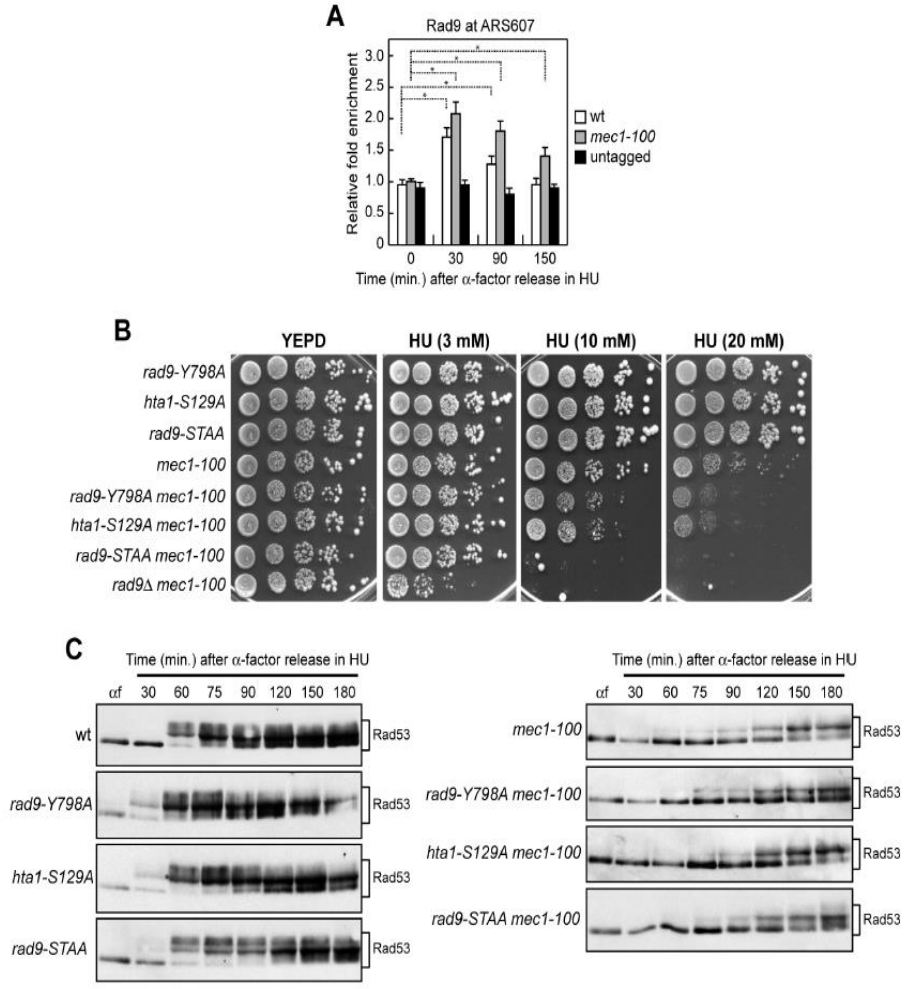

Figure 31 The lack of Rad9-Dbp11 interaction exacerbates HU sensitivity of *mec1-100* cells.
(A) ChIP analysis. Cells were arrested in G1 with α-factor and then released in YEPD containing 0.2M HU at time zero. Relative fold enrichment of Flag-tagged Rad9 at ARS607 replication origin was determined after ChIP with anti-Flag antibodies and subsequent qPCR analysis. Plotted values are the mean values with error bars denoting s.d. (n=3). *P<0.05 (Student's t-test). (B) Exponentially growing cultures were serially diluted (1:10) and each dilution was spotted out onto YEPD plates with or without HU at the indicated concentrations. The hta1-S129A strains also carry HTA2 deletion.(C) Cells were arrested in G1 with α-factor (αf) and then released in YEPD containing 0.2M HU at time zero, followed by western blot analysis of protein extracts with anti-Rad53 antibodies.

The lack of Fun30 or Slx4 suppresses the HU hypersensitivity of mec1-100 cells

The function of Rad9 in inhibition of DSB resection is counteracted by the Swr1-like family remodeler Fun30 (SMARCAD1 in mammals) [171–173,228] and the scaffold protein complex Slx4-Rtt107 [177,187], both of which promote DSB resection by limiting Rad9 accumulation to DNA DSBs [172,177]. Thus, we reasoned that, if Rad9 maintains viability of HU-treated *mec1-100* cells by limiting ssDNA generation, then the lack of Fun30 or Slx4-Rtt107 might suppress the HU hypersensitivity of *mec1-100* cells by increasing Rad9-mediated inhibition of resection. Indeed, both *fun30*Δ *mec1-100* and *slx4*Δ *mec1-100* double mutants were less sensitive to HU compared to *mec1-100* cells (**Figure 32A**). Moreover, the lack of Fun30 or Slx4 did not suppress the HU sensitivity of *rad9*Δ *mec1-100* cells (**Figure 32A**), suggesting that their suppression effect on *mec1-100* requires Rad9.

Slx4 also counteracts the function of Rad9 in allowing Rad53 activation in response to MMS treatment [71]. Suppression of the HU hypersensitivity of *mec1-100* cells by *SLX4* deletion is not due to a more efficient checkpoint activation, as the kinetics of Rad53 phosphorylation in HU-treated *slx4*Δ *mec1-100* cells was similar to that of *mec1-100* cells (**Figure 32B**).

The interaction between Slx4 and Dpb11 is strongly induced by Mec1-dependent Slx4 phosphorylation in response to MMS treatment [187,289]. The dependency on Rad9 for survival of HU-treated *mec1-*

100 cells is likely not due to decreased Slx4 phosphorylation, as HU treatment did not result in changes of Slx4 electrophoretic mobility as it did MMS treatment [290]. Furthermore, the lack of Rad9 exacerbated also the HU sensitivity of cells defective for the Rad53 checkpoint kinase (**Figure 29C**), which is not involved in Slx4 phosphorylation [290].

Fun30 not only promotes DNA end resection by counteracting the resection block imposed by Rad9, but it participates in chromatin organization even in the absence of DNA lesions [291]. Fun30 is phosphorylated by Cdk1 and these phosphorylation events generate a binding site for Dpb11 that targets Fun30 to DSBs [171]. The Fun30-S20A-S28A mutant variant (Fun30-SSAA) cannot be phosphorylated by Cdk1 and is defective in DSB resection but not in silencing [171], indicating that Cdk1-mediated Fun30 phosphorylation is required for Fun30 function in DSB resection but not for its function in chromatin organization. Thus, to rule out the possibility that general changes in chromatin organization could be responsible for suppression of the HU sensitivity of *mec1-100* cells by the lack of Fun30, we asked whether Fun30-SSAA still suppressed the HU sensitivity of *mec1-100* cells. Indeed, *fun30-SSAA mec1-100* cells, similar to *fun30*Δ *mec1-100* cells, were less sensitive to HU compared to *mec1-100* cells (**Figure 32C**), indicating that this suppression effect depends on the lack of Fun30 function in DSB resection.

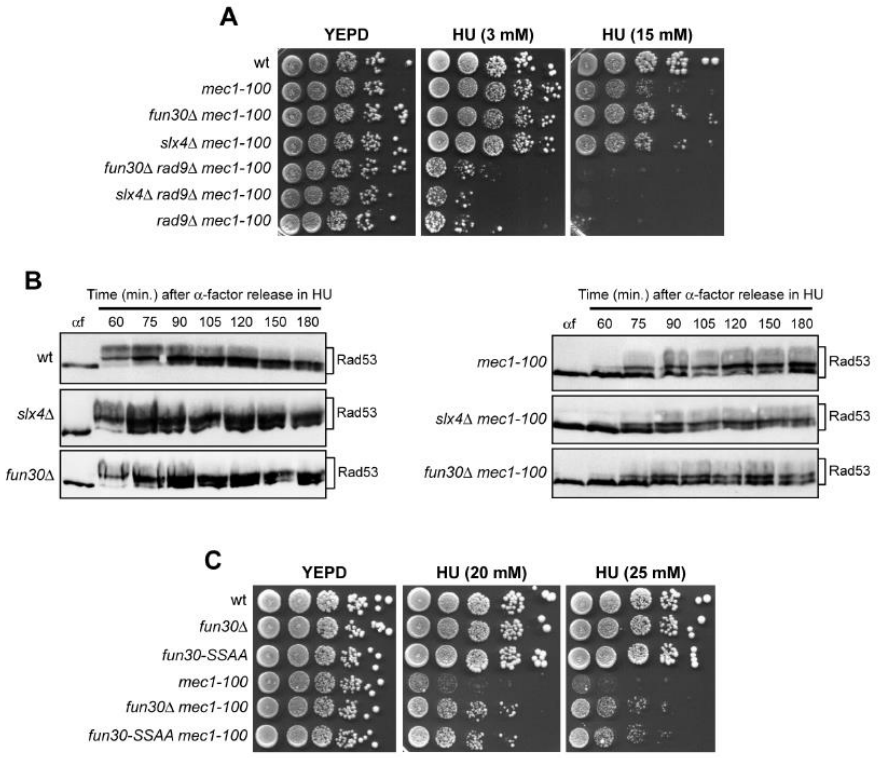

Figure 32 The lack of Slx4 or Fun30 suppresses the HU hypersensitivity of *mec1-100 cells*.
(A, C) Exponentially growing cultures were serially diluted (1:10) and each dilution was spotted out onto YEPD plates with or without HU at the indicated concentrations. (B) Cells were arrested in G1 with α-factor (αf) and then released in YEPD containing 0.2M HU at time zero, followed by western blot analysis of protein extracts with anti-Rad53 antibodies.

Both Sgs1-G1298R and the lack of Rad9 increase ssDNA generation at stalled replication forks in a Dna2-dependent manner

As loss of the inhibition that Rad9 exerts on resection is sufficient to reduce survival of *mec1-100* cells to replication stress, the increased HU hypersensitivity of *sgs1-G1298R mec1-100* and *rad9Δ mec1-100* cells might be due to uncontrolled degradation of stalled replication forks. To evaluate directly the presence of ssDNA at stalled replication forks, we took advantage of a qPCR assay that was previously used to detect ssDNA at DSBs [162] and at terminally arrested replication forks [292]. This assay is based on ssDNA being refractory to digestion by the restriction enzyme SspI, which cleaves double-stranded DNA (dsDNA) but not ssDNA. Ssp1-digested and mock-digested DNAs were amplified by qPCR using primers surrounding Ssp1 restriction sites and the resulting amplification products were then normalized to an amplicon on chromosome XI.

Cells arrested in G1 with α-factor were released into medium containing HU and ssDNA was analyzed by qPCR at different distances from the early efficient ARS607 replication origin. It has been previously reported that replication forks in untreated wild type cells show short gaps of ~220 nt, which likely represent the regions engaged by the replisome during replication [193]. In the presence of HU, the size of these gaps increases by ~100 nt asymmetrically, possibly because of uncoupling events [193]. Consistent with these findings, an

increase in ssDNA above background levels (αf) was detected in HU-treated wild type, *rad9*Δ, *sgs1-G1298R* and *mec1-100* cells at DNA regions closed to the replication origin. Both the amount and the extension of this ssDNA was dramatically increased in *rad9*Δ *mec1-100* and *sgs1-G1298R mec1-100* double mutant cells after release in HU compared to *mec1-100* cells, with *rad9*Δ *mec1-100* cells showing the strongest effect (**Figure 33**). The ssDNA detected in *rad9*Δ *mec1-100* and *sgs1-G1298R mec1-100* cells was specific to DNA regions surrounding the replication origin, as no significant differences above background levels (αf) were observed at a control locus (**Figure 33**). Furthermore, the amount of ssDNA decreased progressively as the distance from the replication origin increased. Strikingly, the presence of the *dna2-1* allele decreased the amount of ssDNA in both *rad9*Δ *mec1-100* and *sgs1-G1298R mec1-100* cells (**Figure 33**), strongly suggesting that the ssDNA accumulated in the above double mutants is caused by Dna2-mediated nucleolytic processing.

As ssDNA is rapidly coated by the RPA complex that coordinates DNA damage signaling [110], we also evaluated the association of Rpa1 at stalled replication forks by ChIP and qPCR in cells synchronously released from a G1 arrest into S phase in the presence of HU. Rpa1 association at both early efficient ARS607 and ARS305 replication origins increased in all cell cultures about 20 minutes after release in the presence of HU and decreased about 40 minutes later, with *sgs1-G1298R mec1-100* and *rad9*Δ *mec1-100* double mutant cells showing a more persistent RPA binding compared to both wild type and each

single mutant (**Figure 34A**). Interestingly, while Rpa1 association at stalled replication forks in wild type, *rad9*Δ, *sgs1-G1298R* and *mec1-100* cells paralleled that of DNA Polε and showed a pick of association at 20 minutes after release in HU (compare **Figure 29E and A**), the amount of ssDNA detected directly by qPCR remained constant at 20, 40 and 60 minutes after release (**Figure 33**). As the ssDNA molecules could re-anneal to each other upon DNA extraction and deproteinization, the signal detected by qPCR could represent preferentially ssDNA gaps generated asymmetrically (which therefore cannot re-anneal), rather than ssDNA regions covered by RPA that are engaged by the replisome during replication.

RPA is subsequently displaced by the recombinase Rad51 to generate Rad51 nucleoprotein filaments that initiate homologous recombination [110]. Consistent with an increase in ssDNA generation, the decrease in Rpa1 binding at the replication origins in *sgs1-G1298R mec1-100* and *rad9*Δ *mec1-100* double mutant cells was concomitant with an increased accumulation of Rad51, whose association and persistence was higher in both *sgs1-G1298R mec1-100* and *rad9*Δ *mec1-100* cells than in *mec1-100* cells (**Figure 34B**). Interestingly, although we could not detect any increase in ssDNA generation at the replication origin in HU-treated *mec1-100* cells (**Figure 33**) [212], Rad51 association appeared to be increased in *mec1-100* cells compared to wild type cells (**Figure 34B**). This finding can be consistent with a role of Mec1 in inhibiting Rad51 activity possibly by controlling its association to DNA that can be partially defective in *mec1-100* cells [293].

Finally, as the recombination protein Rad52 stimulates DNA annealing and Rad51-catalyzed strand invasion reactions to allow recombination-mediated fork restart [110], we analyzed the formation of Rad52 recombination foci. Rad52 foci were not detectable in HU-treated wild type cells, while their frequency increased dramatically after HU treatment in both *sgs1-G1298R mec1-100* and *rad9*Δ *mec1-100* double mutant cells compared to *mec1-100* cells (**Figure 34C**). Collectively, these results show that both *sgs1-G1298R* and the lack of Rad9 increase ssDNA generation at the replication forks when the checkpoint is dysfunctional, pointing to a role for Rad9 in restricting resection at arrested replication forks.

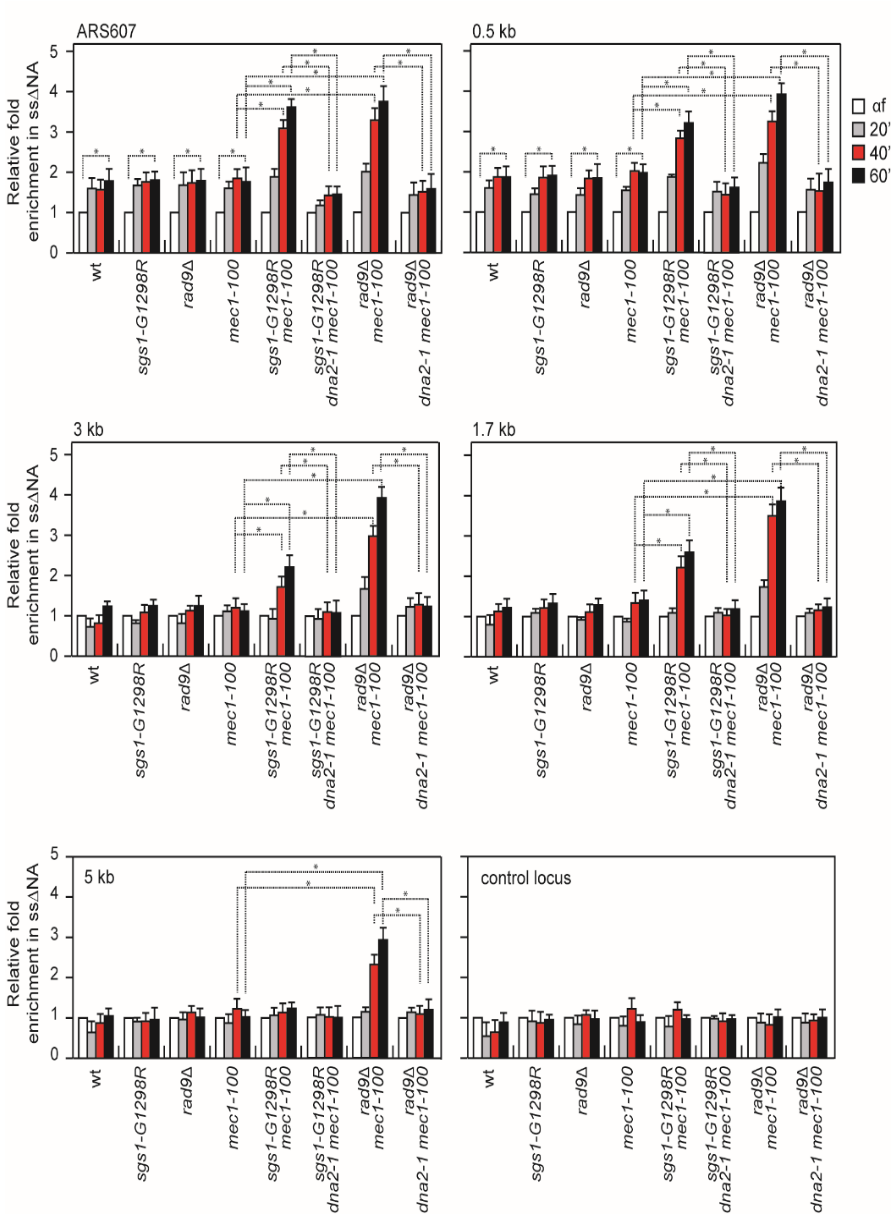
ARS607
0.5 kb
3 kb
1.7 kb
5 kb
control locus
Relative fold enrichment in ssΔNA
af
20'
40'
60'
wt
sgs1-G1298R
rad9Δ
mec1-100
sgs1-G1298R mec1-100
sgs1-G1298R dna2-1 mec1-100
rad9Δ mec1-100
rad9Δ dna2-1 mec1-100

Figure 33 ssDNA generation at stalled forks in *mec1-100* cells is increased by either Sgs1-G1298R or the lack of Rad9 in a Dna2-dependent manner.
Analysis of ssDNA formation at different distances from ARS607 by qPCR. Exponentially growing YEPD cell cultures were arrested in G1 with α-factor (αf) and then released in YEPD containing 0.2M HU. Genomic DNA prepared at different time points after α-factor release was either digested or mock-digested with Ssp1 and used as template in qPCR. The value of Ssp1-digested over non-digested DNAs was determined for each time points after normalization to an amplicon on chromosome XI that does not contain Ssp1 sites. The data shown are expressed as fold enrichments in ssDNA at different time points after α-factor release in HU relative to the α-factor (αf) (set to 1.0). A locus containing Ssp1 sites on chromosome XI is used as a control (control locus). The mean values are represented with error bars denoting s.d. (n=3). *P<0.05 (Student's t-test).

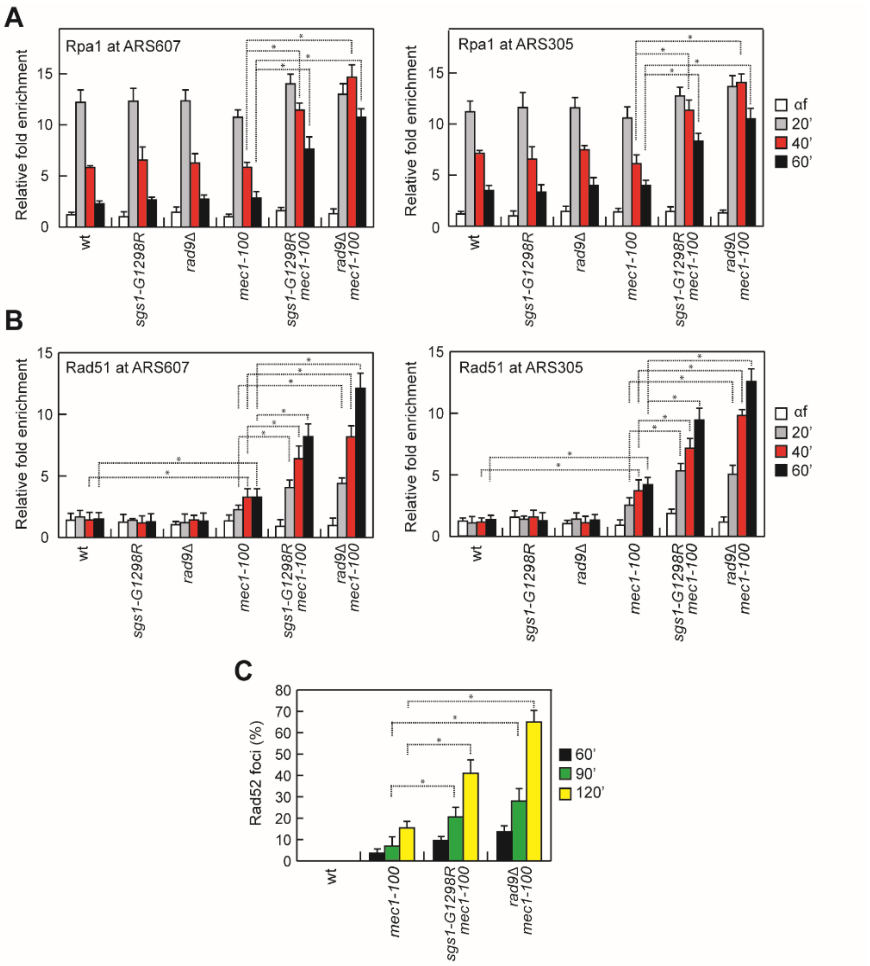

Figure 34 Rpa1, Rad51 and Rad52 association to stalled replication forks is increased by either Sgs1-G1298R or the lack of Rad9.
(A, B) ChIP analysis. Cells were arrested in G1 with α-factor and then released in YEPD containing 0.2M HU at time zero. Relative fold enrichment of Rpa1 and Rad51 at ARS607 and ARS305 replication origins was determined after ChIP with anti-Myc (A) or anti-Rad51 (B) antibodies and subsequent qPCR analysis. Plotted values are the mean values with error bars denoting s.d. (n=3). *P<0.05 (Student's t-test). (C) Rad52 foci at the indicated times after release from a G1 arrest in 0.2M HU. Plotted values are the mean values with error bars denoting s.d. (n=3). *P<0.05 (Student's t-test).

Discussion

Genome instability is one of the most pervasive feature of cancer cells [3]. DNA damage and replication stress are responsible for a significant portion of genome instability [4,6,15]. DNA double strand breaks (DNA DSBs) are the most dangerous damages that cells have to manage. In fact, failure of repairing them can lead to genomic rearrangements and loss of genetic information.

Damaged DNA activates a highly conserved cellular response named DNA Damage Checkpoint (DDC) [8]. DDC is a transduction cascade whose primary objective is to stop the cell cycle and to favor DNA repair. Cells repair DSBs mainly by two distinct pathways: Non Homologous End Joining (NHEJ) and Homologous Recombination (HR). NHEJ repairs DNA DSBs by simply rejoining the two broken ends, with minimal processing. Since no intact template is used for the repair, it is considered an error prone mechanism. On the contrary, HR exploits the intact information on the sister chromatids to fix the break. HR requires nucleolytic degradation (resection) of the DSB ends to create ssDNA that is engaged in the homology search process [112]. In both yeast and mammals, the resection process must be tightly regulate to avoid the creation of excessive ssDNA that could be detrimental for genome stability. Using the budding yeast *S. cerevisiae* as model organism, in this experimental work I have provided data about the regulation of this process at both DNA DSB and stalled replication forks.

In *S. cerevisiae*, the MRX complex and Sae2 are involved in the onset of DSB resection, whereas the extensive resection requires the action of Exo1 and Dna2 nucleases, with the latter working together with the Sgs1 helicase [125,129,294,295]. The absence of Sae2 not only impairs DSB resection, but also causes prolonged MRX binding at the DSB that leads to an unscheduled activation of the DNA damage checkpoint dependent on Tel1 and Rad53.

Furthermore, *sae2*Δ cells are sensitive to genotoxic agents like methyl-methan-sulphonate (MMS), camptothecin (CPT) and phleomycin. Interestingly, deletion of *KU* suppresses the CPT sensitivity of *sae2*Δ cells in an Exo1 dependent manner [233]. This indicates that Sae2 activity is required for the processing of CPT induced DSBs and that the Ku complex inhibits Exo1 activity at DSBs.

The biochemical role of Sae2 in DSB resection is debated [129,130]. Moreover, how short range resection and long range resection are regulated and linked to each other is not completely understood.

For these reasons, we searched for extragenic mutations able to suppress the DNA damage sensitivity of ***sae2***Δ cells in order to identify other possible mechanisms able to bypass Sae2 function in DSB resection. By performing a genetic screen, we identified *SGS1-ss*, *rad53-ss* and *tel1-ss* mutant alleles.

In the first part of this experimental work, I have contributed to the characterization of the Sgs1-ss (Sgs1-G1298R) mutant variant. This allele carries a point mutation that causes the change of the glycine

1298 with an arginine. The mutation falls in the HRDC domain that is implicated in protein-protein interaction and in Sgs1-DNA interaction [147,296,297].

We have shown that Sgs1-ss is able to suppress not only the sensitivity to genotoxic agents of *sae2*Δ cells but also the one of the *mre11* nuclease-dead mutant. This indicates that Sgs1-ss bypasses the functions of both Sae2 and the MRX complex in resection onset. Anyway, this suppression requires the integrity of the MRX complex as Sgs1-ss is not able to suppress the sensitivity of *mre11*Δ mutants. This is consistent with the structural role of MRX complex in recruiting Sgs1 and other resection factors to DSB [298].

As expected [295], the Sgs1-ss variant supports the viability of *sae2*Δ mutants to genotoxic treatment working in concert with Dna2 nuclease. In fact, Sgs1-ss is able to suppress *sae2*Δ cells sensitivity even in the absence of Exo1. By contrast, Sgs1-ss can't rescue the synthetic lethality of the *sae2*Δ *dna2*Δ double mutant.

Cells lacking Sae2 suffer from a resection defect and an unscheduled checkpoint activation. The molecular analysis of the resection process in *sae2*Δ *SGS1-ss* cells has revealed that the presence of Sgs1-ss suppresses the resection defect of *sae2*Δ cells. Furthermore, the double mutant *sae2*Δ *SGS1-ss* showed a checkpoint activation and de-activation kinetics similar to the one of wild type cells. In this context, Sgs1-ss decreases the amount of the MRX complex bound at the DSB.

These findings indicate that Sgs1-ss is able to suppress the sensitivity to genotoxic agents of *sae2*Δ cells by restoring DSB resection which, in turn, decreases the MRX persistence at the DSB.

Interestingly, Sgs1-ss is able to accelerate the resection process even in a wild type context suggesting that this mutant variant might increases the resection efficiency by escaping the effect of negative regulators. In particular, the checkpoint protein Rad9 was implicated in the control of the resection process with an unknown mechanisms [170].

We showed that Rad9 inhibits the action of the Sgs1-Dna2 long-range resection machinery. In fact, extensive resection in Rad9-deficient cells is mainly dependent on Sgs1, whose recruitment at DSBs is inhibited by Rad9. By contrast Sgs1-ss is robustly associated to the DSB ends both in the presence and in the absence of Rad9. These findings indicate that Rad9 inhibits the activity of Sgs1-Dna2 by limiting Sgs1 binding/persistence at DSB ends and that the Sgs1-ss mutant variant escapes this inhibition possibly because it is more tightly bound to DNA. If Rad9 could have an additional effect on the helicase activity of Sgs1 and if Sgs1-ss could escape even this putative control, remains to be determined. Anyway, while Ku increases the requirement for the MRX-Sae2 activities in DSB resection by inhibiting preferentially Exo1 [299], Rad9 mainly restricts the action of Sgs1-Dna2. As MRX and Sae2 are especially important for initial processing of DNA ends that contain protein-DNA adducts, the Rad9- and Ku- mediated inhibitions

of Sgs1/Dna2 and Exo1 activities in initiating DSB resection ensure that all DSBs are processed in a similar manner independently of their nature (**Figure 35**).

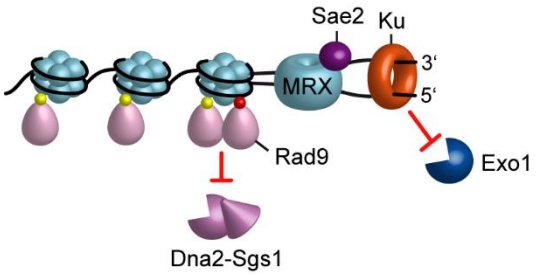

Figure 35 Inhibition of DSB resection by Ku and Rad9.
Ku is bound very close to the DSB end. Rad9 is bound to chromatin even in the absence of DSB via interaction with methylated histone H3 (yellow dots). Rad9 association at DSB is enhanced by γ-H2A generation (red dots). Ku and Rad9 inhibit DSB resection by limiting Exo1 and Sgs1-Dna2 access to DNA ends, respectively.

In the second part of this work, I have contributed to characterized the *rad53-ss* and *tel1-ss* mutant alleles. Rad53-ss (Rad53-H88Y) carries an aminoacidic change from a histidine to a tyrosine in the FHA1 domain, implicated in Rad53 activation [85,249,250]. Tel1-ss (Tel1-N2021D) carries the change of an asparagine into an aspartic acid in the FAT domain, which is implicated in the regulation of Tel1 kinase activity [53].

We show that impairment of Rad53 activity either by affecting its interaction with Rad9 (Rad53-H88Y) or by abolishing its kinase activity (Rad53-kd) suppresses the sensitivity to DNA damaging agents of *sae2*Δ cells. A similar effect can be detected also when Tel1 function

is compromised either by reducing its recruitment to DSBs (Tel1-N2021D) or by abrogating its kinase activity (Tel1-kd). These suppression effects are not due to the escape of the checkpoint-mediated cell cycle arrest, as *CHK1* deletion, which overrides the persistent cell cycle arrest of *sae2*Δ cells, does not suppress the hypersensitivity of the same cells to DNA damaging agents. Rather, we found that impairment of Rad53 or Tel1 signaling suppresses the resection defect of *sae2*Δ by decreasing the amount of Rad9 bound very close to the break site. Since we and others have demonstrated that Rad9 inhibits Sgs1-Dna2 [178,244], this reduced Rad9 association at DSBs relieves inhibition of Sgs1-Dna2 activity that can then compensate for the lack of Sae2 function in DSB resection. In this view, active Rad53 and Tel1 increase the requirement for Sae2 in DSB resection by promoting Rad9 binding to DSBs and therefore by inhibiting Sgs1-Dna2. Consistent with a role of Sgs1 in removing MRX from the DSBs [149], the relieve of Sgs1-Dna2 inhibition by Rad53 or Tel1 dysfunction leads to a reduction of MRX association to DSBs in *sae2*Δ cells.

Our finding that Tel1 or Rad53 inactivation can restore both DNA damage resistance and DSB resection in *sae2*Δ cells is apparently at odds with previous findings that attenuation of the Rad53-dependent checkpoint signaling by decreasing MRX association to DSBs suppresses the DNA damage hypersensitivity of *sae2*Δ cells but not their resection defect [133,134]. Noteworthy, the bypass of Sae2

function by Rad53 or Tel1 dysfunction requires the physical presence of MRX bound at DSBs, which is known to promote stable association of Exo1, Sgs1 and Dna2 to DSBs [299]. Thus, we speculate that a reduced MRX association at DSBs allows *sae2*Δ cells to initiate DSB resection by relieving Rad9-mediated inhibition of Sgs1-Dna2 activity. As DSB repair by HR has been shown to require limited amount of ssDNA at DSB ends [300,301], the ssDNA generated by this initial DSB processing might be sufficient to restore DNA damage resistance in *sae2*Δ cells even when wild type levels of resection are not restored because DSB bound MRX is not enough to ensure stable Sgs1 and Dna2 association.

Surprisingly, *TEL1* deletion, which relieves the persistent Tel1-dependent checkpoint activation caused by the lack of Sae2, did not restore DNA damage resistance and DSB resection in *sae2*Δ cells. We found that the lack of Tel1 protein affects the association of MRX to the DSB ends independently of its kinase activity. As the rescue of *sae2*Δ by Tel1-N2021D requires the physical presence of the MRX complex, this reduced MRX-DNA association can explain the inability of *TEL1* deletion to restore DNA damage resistance and resection in *sae2*Δ cells. Therefore, while an enhanced Tel1 signaling activity in the absence of Sae2 leads to DNA damage hypersensitivity and resection defects, a sufficient amount of Tel1 needs to be present at DSBs to support MRX function at DSBs.

How do Rad53 and Tel1 control Rad9 association to DSB? Rad53-mediated phosphorylation of Rad9 does not appear to promote Rad9 binding to the DSB [302,303]. Because Rad53 and RPA compete for binding to Sgs1 [200], it is tempting to propose that impaired Rad53 signaling activity might shift Sgs1 binding preference from Rad53 to RPA, leading to increased Sgs1 association to RPA-coated DNA that can counteract Rad9 binding and inhibition of resection. In turn, Tel1 and Mec1 can phosphorylate Rad9 [304,305], and abrogation of these phosphorylation events rescues the sensitivity to DNA damaging agents of *sae2*Δ cells [178], suggesting that Tel1 might control Rad9 association to DSBs directly through phosphorylation. On the other hand, Tel1 promotes generation of γH2A [73,81,262,263], which counteracts DSB resection by favoring Rad9 association at the DSB [58]. We show that expression of a non-phosphorylable H2A variant in *sae2*Δ cells suppresses their resection defect and prevents the accumulation of Rad9 at the DSB. Furthermore, γH2A generation close to the break site depends on Tel1 kinase activity. Thus, although we cannot exclude a direct control of Tel1 on Rad9 association to DNA ends, our findings indicate that Tel1 acts in this process mostly through γH2A generation.

Altogether, our results support a model whereby Tel1 and Rad53, once activated, limit DSB resection by promoting Rad9 binding to DSBs and therefore by inhibiting Sgs1-Dna2.

It is already known that Sae2 activates Mre11 endonucleolytic activity that clips the 5'-terminated DNA strand, thus generating 5' and 3' tailed substrates that can be processed by Exo1/Sgs1-Dna2 and Mre11 activity, respectively (**Figure 36, left**). When Sae2 function fails, defective Mre11 nuclease activity causes increased MRX persistence at the DSB that leads to enhanced and prolonged Tel1-dependent Rad53 activation. As a consequence, Tel1- and Rad53-mediated phosphorylation events increase the amount of Rad9 bound at the DSB, which inhibits DSB resection by counteracting Sgs1-Dna2 activity (**Figure 36, middle**). Dysfunction of Rad53 or Tel1 reduces Rad9 recruitment at the DSB ends and therefore relieves inhibition of Sgs1-Dna2, which can compensate for the lack of Sae2 in DNA damage resistance and resection (**Figure 36, right**). In conclusion, we demonstrate that Rad9 increases the requirement for MRX/Sae2 activities in DSB resection by inhibiting the action of Sgs1/Dna2 and that dampening Tel1 or Rad53 signaling bypass Sae2 function in DSB resection. Altogether, these finding indicate that the primary cause of the resection defect of *sae2*Δ cells is an enhanced Rad9 binding to DSBs that is promoted by the persistent MRX-dependent Tel1 and Rad53 signaling activities. This work reveals new details of the molecular mechanisms of DSB resection and the role of Sae2 at DSBs in the model organism *S. cerevisiae*.

ATM inhibition has been proposed as a strategy for cancer treatment. Therefore, the observation that dampening Tel1/ATM signaling activity

restores DNA damage resistance in *sae2*Δ cells might have implications in cancer therapies that use ATM inhibitors for synthetic lethal approaches to threat tumors with deficiencies in the DNA damage response.

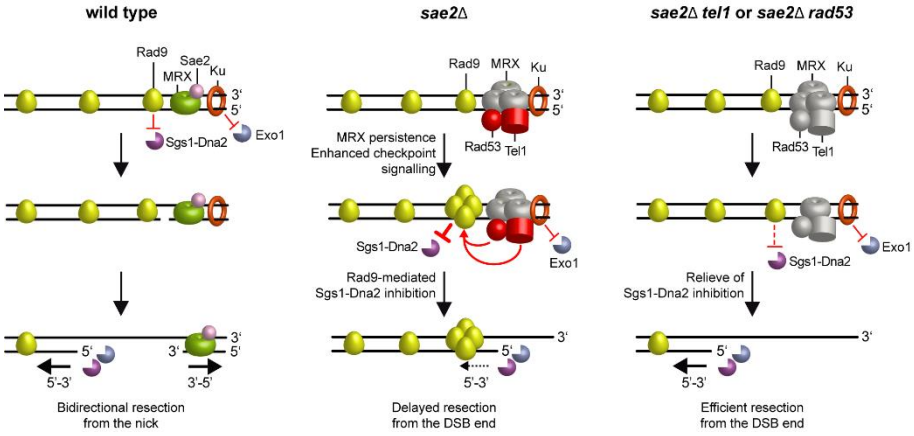

Figure 36 Model for the role of Sae2 at DSBs.
(Wild type, left) Sae2 activates the Mre11 endonuclease activity to incise the 5' strand. Generation of the nick allows bidirectional processing by Exo1/Sgs1-Dna2 in the 5'-3' direction from the nick and MRX in the 3' to 5' direction toward the DSB ends. Ku and Rad9 inhibit DSB resection by limiting Exo1 and Sgs1-Dna2, respectively. (*sae2*Δ, middle) The absence of Sae2 impairs the MRX nuclease activity (nonfunctional MRX nuclease is in grey). As a consequence, the endonucleolytic cleavage of the 5' strand does not occur and resection is carried out by Exo1 and Dna2-Sgs1 that degrade the 5' strands from the DSB ends. Impairment of Mre11 nuclease activity also causes increased MRX association at the DSB, which leads to enhanced Tel1-dependent Rad53 activation. Tel1 and Rad53 activities limit DSB resection from the DSB end (dashed arrow) by increasing the amount of DSB-bound Rad9, which inhibits Sgs1-Dna2 recruitment at DSBs. (*sae2*Δ *tel1* or *sae2*Δ *rad53,* right) Impairments of Tel1 or Rad53 activity (nonfunctional Tel1 and Rad53 are in grey) restore efficient resection in sae2Δ cells by relieving Rad9-mediated inhibition of Sgs1-Dna2. Restored DSB resection by Sgs1-Dna2 also reduces MRX persistence at the DSB.

In the last part of this work, I have evaluated if the control of the resection exerted by Rad9 at DSBs could be also extended to stalled replication fork.

Controlled degradation of replication forks by nucleases can be a relevant mechanism to recover replication fork blockage by promoting HR repair and/or by processing specific stalled replication fork structures. However, unscheduled nuclease action could destroy the fork structure and prevent continued DNA synthesis, leading to genome instability. Structural analysis of DNA replication forks in *S. cerevisiae* has shown that *rad53* mutant cells treated with HU accumulate replication forks with extended ssDNA gaps that appear to be localized on only one of the two newly synthesized strands [193]. On the one hand, formation of these ssDNA gaps is partly dependent on the Exo1 nuclease [215,216], which turns out to be a target of Mec1/ATR [185,270,272], suggesting that the intra-S checkpoint suppresses Exo1-dependent processing of stalled replication forks. On the other hand, Rad53 checkpoint kinase appears to limit ssDNA generation at stalled replication forks by ensuring the coupling of leading- and lagging-strand synthesis possibly through inhibition of excessive template unwinding and upregulation of dNTP levels [213].

In both yeast and mammals, the checkpoint protein Rad9/53BP1 is known to inhibit resection of intra-chromosomal DSBs [170,229,306,307] by counteracting the resection activity of Sgs1-Dna2 [178,244]. Here, we describe a previously undisclosed function

of Rad9 in maintaining viability of Mec1-defective cells upon dNTP depletion by protecting stalled replication forks from detrimental nucleolytic processing. In particular, we show that the sensitivity to HU of cells either lacking Mec1 or expressing *mec1* hypomorphic alleles is exacerbated by loss of Rad9 or expression of an Sgs1 variant (Sgs1-G1298R) that escapes Rad9-mediated inhibition of DSB resection. Furthermore, the HU hypersensitivity of *mec1-100* cells is suppressed in a Rad9-dependent manner by elimination of Slx4 or Fun30, which are known to counteract the inhibition that Rad9 exerts on DSB resection[171–173,177,228]. Finally, both the *rad9*Δ and *sgs1-G1298R* mutations dramatically increase the generation of ssDNA at the replication forks in HU-treated *mec1-100* cells in a Dna2-dependent manner. These findings, together with the observation that Dna2 deficiency is epistatic to *rad9*Δ and *sgs1-G1298R* with respect to HU sensitivity of *mec1-100* cells, indicate a role for Rad9 in supporting viability of Mec1-deficient cells by protecting replication forks from Dna2-mediated degradation. This Rad9 protective function relies mainly on the interaction of Rad9 with Dpb11, which is recruited to stressed replication origins [307] and forms nuclear foci in response to replication stress [308]. Altogether, our data support a model whereby survival to replication stress of Mec1-defective cells is dependent on the Rad9-Dpb11 complex that restrains uncontrolled Dna2-mediated nucleolytic processing of stalled replication forks.

Whether the increased Dna2-dependent ssDNA generation in *rad9*Δ *mec1-100* and *sgs1-G1298R mec1-100* cells arise upon nucleolytic degradation of nascent DNA strands and/or of DSBs that are generated by the action of endonucleases at unprotected stalled replication forks remains to be determined. In any case, the lack of the Mus81 endonuclease, which cleaves branched structures that can be generated at stalled replication forks [309,310], did not suppress the HU hypersensitivity of *rad9*Δ *mec1-100*, suggesting that Mus81 is not responsible for these possible DNA cleavage events. Given the role of Dna2 in Okazaki fragment maturation [155,268,311], we favor the hypothesis that Rad9 prevents Dna2 activity in degrading 5' ends generated at nascent lagging strands.

Altogether, these findings suggest a working model (**Figure 37**), in which the intra-S checkpoint prevents the generation of excessive ssDNA under replication stress both by coordinating DNA unwinding with leading- and lagging-strands synthesis and by limiting exposure of nascent DNA strands to Exo1-mediated degradation [185,215,216,272]. Rad9, in turn, limits nucleolytic degradation of nascent lagging strands by inhibiting Sgs1-Dna2 resection activity. Inactivation of the checkpoint can cause the dislocation of the replisome from sites of DNA synthesis and the exposure of newly synthesized DNA to Exo1-mediated degradation. Under this condition, the lack of Rad9 relieves the inhibition of Sgs1-Dna2 activity and this leads to uncontrolled Dna2-dependent degradation of nascent lagging

strands that, together with Exo1-mediated resection, destroys the fork structure and prevents continued DNA synthesis.

Notably, the Dpb11-Rad9 interaction appears to be conserved in human cells, where TopBP1, the Dbp11 human orthologue, stabilizes 53BP1 to the sites of damage to exert its inhibitory function on DSB resection [187,312].

Our evidences depict a specific role for Rad9 acting on Y-shaped forks. Anyway, it could be of interest to test if this protein could control the processing also in the context of reversed forks, where a controlled nucleolytic activity is required for their resolution.

As replication stress underlies a significant proportion of the genomic instability observed in cancer cells, understanding whether a similar 53BP1-mediated resection block is active also at mammalian damaged replication forks and supports survival to replicative stress of ATR-deficient cells can be important to improve the use of ATR inhibitors in cancer therapy.

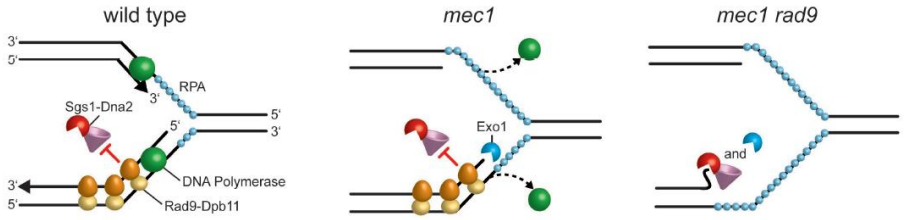

Figure 37 A model for the role of Rad9 in protecting stalled replication forks from degradation.
(Left) In wild type cells, activation of the checkpoint in response to inhibition of DNA replication maintains replisome integrity, couples leading- and lagging-strand synthesis and limits Exo1-mediated degradation. Rad9 limits the resection activity of Sgs1-Dna2 to degrade nascent lagging strands. (Middle) Checkpoint dysfunction leads to the dislocation of the replisome from sites of DNA synthesis and to the exposure of newly synthesized DNA to Exo1- mediated degradation. Rad9 still inhibits the resection activity of Sgs1-Dna2. (Right) When both the checkpoint and Rad9 are dysfunctional, inhibition of both Exo1 and Dna2 activity is relieved, leading to uncontrolled DNA degradation.

Materials and Methods

Yeast and bacterial strains

Yeast strains

The yeast strains used in this study are derivatives of W303, JKM139, YMV45 and SK1 strains. Strains JKM139 and YMV45 were kindly provided by J. Haber (Brandeis University, Waltham, USA). Strains YMV45 are isogenic to YFP17 (*mat*Δ*::hisG hml*Δ*::ADE1 hmr*Δ*::ADE1 ade1 lys5 ura3-52 trp1 ho ade3::GAL-HO leu2::cs*) except for the presence of a *LEU2* fragment inserted 4.6 kb centromere-distal to *leu2::cs*. To induce a persistent G1 arrest with α-factor, some strains carried the deletion of the *BAR1* gene, which encodes for a protease that degrades the α-factor. Deletions were generated by one-step PCR disruption method. PCR one-step tagging methods was used to obtain strains carrying fully functional MYC-tagged or HA-tagged alleles. The accuracy of all gene replacement and integrations was verified by PCR. Strains expressing both the nucleoside transporter hENT1 and the Herpes Simplex virus thymidine kinase (HSV-TK) to allow BrdU incorporation were constructed by transforming cells with p306-BrdU-Inc plasmid kindly provided by O. Aparicio (University of Southern California).

Bacterial strains

E. coli DH5α™ strain (*F-, φ80 dlacZM15, D(lacZTA-argF) U169, deoR, recA1, endA1, hsdR17, (rK-,mK+) phoA supE44, λ−, thi-1, gyrA96, relA1*) is used as bacterial host for plasmid manipulation and amplification. *E. coli* DH5α™ competent cells to transformation are purchased from Invitrogen.

Growth media

S. cerevisiae media

YEP (Yeast-Extract Peptone) is the standard rich media for *S. cerevisiae* and contains 10 g/L yeast extract, 20 g/L peptone and 50 mg/L adenine. YEP must be supplemented with 2% glucose (YEPD), 2% raffinose (YEP+raf) or 2% raffinose and 2% galactose (YEP+raf+gal) as carbon source. YEP-based selective media are obtained including 400 µg/mL G418, 300 µg/mL hygromicin-B or 100 µg/mL nourseotricin. Solid media are obtained including 2% agar. Stock solutions are 50% glucose, 30% raffinose, 30% galactose, 80 mg/mL G418, 50 mg/mL hygromicin-B and 50 mg/mL nourseotricin. YEP and glucose stock solution are autoclave-sterilized and stored at RT. Sugars and antibiotics stock solutions are sterilized by micro-filtration and stored at RT and 4°C respectively.

S.C. (Synthetic Complete) is the minimal growth media for *S. cerevisiae* and contains 1.7 g/L YNB (Yeast Nitrogen Base) without amino acids, 5 g/L ammonium sulphate, 200µM inositol, 25 mg/L uracil, 25 mg/L adenine, 25 mg/L hystidine, 25 mg/L leucine, 25 mg/L tryptophan. S.C. can be supplemented with drop-out solution (20 mg/L arginine, 60 mg/L isoleucine, 40 mg/L lysine, 10 mg/L methionine, 60 mg/L phenylalanine, 50 mg/L tyrosine) based on yeast strains requirements. Different carbon sources can be used in rich media (2% glucose, 2% raffinose or 2% raffinose and 3% galactose). One or more amino acid/base can be omitted to have S.C.-based selective media (e.g. S.C.-ura is S.C. lacking uracil). To obtain G418 or NAT S.C. selective medium the 5 g/L ammonium sulphate are replaced with 1 g/L monosodic glutamic acid. Solid media are obtained by including 2% agar. Stock solutions are 17 g/L YNB + 50 g/L ammonium sulphate (or 10g/L monosodic glutamic acid), 5 g/L uracil, 5 g/L adenine, 5 g/L hystidine, 5 g/L leucine, 5 g/L tryptophan, 100X drop out solution (2 g/L arginine, 6 g/L isoleucine, 4 g/L lysine, 1 g/L methionine, 6 g/L phenylalanine, 5 g/L tyrosine), 20mM inositol. All of these solutions are sterilized by micro-filtration and stored at 4°C.

VB sporulation medium contains 13.6 g/L sodium acetate, 1.9 g/L KCl, 0.35 g/L MgSO4, 1.2 g/L NaCl. pH is adjusted to 7.0. To obtain solid medium include 2% agar. pH is adjusted to 7.0. Sterilization by autoclavation.

E. coli media

LD is the standard growth medium for *E. coli.* LD medium contains 10 g/L tryptone, 5 g/L yeast extract and 5 g/L NaCl. Solid medium is obtained by including 1% agar. LD+Amp selective medium is obtained including 50 µg/mL Ampicillin. LD is autoclave-sterilized and stored at RT. Ampicillin stock solution (2.5 g/L) is sterilized by micro-filtration and stored at 4°C.

Molecular biology techniques

Extraction of yeast genomic DNA (Teeny yeast DNA preps)

Yeast cells are harvested from overnight cultures by centrifugation, washed with 1 mL of 0.9M sorbytol 0.1M EDTA pH 7.5 and resuspended in 0.4 mL of the same solution supplemented with 14mM β-mercaptoethanol. Yeast cell wall is digested by 45 minutes' incubation at 37°C with 0.4 mg/mL 20T zimoliase. Spheroplasts are harvested by 30 seconds centrifugation and resuspended in 400 µL TE. After addition of 90 µL of a solution containing EDTA pH 8.5, Tris base and SDS, spheroplasts are incubated 30 minutes at 65°C. Samples are kept on ice for 1 hour following addition of 80 µL 5M potassium acetate. Cell residues are eliminated by 15 minutes' centrifugation at 4°C. DNA is precipitated with chilled 100% ethanol, resuspended in 500 µL TE and incubated 30 minutes with 25 µL 1 mg/mL RNase to eliminate RNA. DNA is then precipitated with isopropanol and resuspended in the appropriate volume (typically 50 µL) of TE.

Southern blot analysis

Yeast genomic DNA prepared with standard methods is digested with the appropriate restriction enzyme(s). The resulting DNA fragments are

separated by agarose gel electrophoresis in a 0.8% agarose gel. When adequate migration has occurred, gel is washed 40 minutes with a denaturation buffer (0.2N NaOH, 0.6M NaCl), and 40 minutes with a neutralization buffer (1.5M NaCl, 1M Tris HCl, pH 7.4). DNA is blotted onto a positively charged nylon membrane by overnight capillary transfer with 10X SSC buffer (20X SSC: 3M sodium chloride, 0.3M sodium citrate, pH 7.5). Membrane is then washed with 4X SSC and UV-crosslinked. Hybridization is carried out by incubating membrane for 5 hours at 50°C with pre-hybridization buffer (50% formamide, 5X SSC, 0.1% N-lauroylsarcosine, 0.02% SDS, 2% Blocking reagent) following by o/n incubation at 50°C with pre-hybridization buffer + probe. The probe is obtained by random priming method (DECAprime^{TM} kit by Ambion) on a suitable DNA template and with 32P d-ATP. Filter is then washed (45 minutes + 15 minutes) at 55°C with a washing solution (0.2M sodium phosphate buffer pH 7.2, SDS 1%, water), air dried and then exposed to an autoradiography film.

Denaturing gel electrophoresis and southern blot analysis to visualize single-stranded DNA (ssDNA)

A 0.8% agarose gel (in H_2O) is submerged in a gel box containing a 50mM NaOH, 1mM EDTA solution for 30 minutes to equilibrate. Ethidium bromide is omitted because it does not efficiently bind to DNA under these conditions. After digestion with the appropriate restriction enzyme(s), DNA samples are prepared by adjusting the solution to

0.3M sodium acetate and 5mM EDTA (pH 8.0) following by addition of 2 volumes of ethanol to precipitate DNA. After chilling (o/n) and centrifuging the samples (15 minutes, possibly at 4°C), pellet is resuspended in alkaline gel loading buffer (1X buffer: 50mM NaOH, 1mM EDTA pH 8.5, 2.5% Ficoll (Type 400) and 0.025% bromophenol blue). After loading the DNA in the gel, a glass plate can be placed on the gel to prevent the dye from diffusing from the agarose during the course of the run. Because of the large currents that can be generated with denaturing gels, gels are usually run slowly at lower voltages (e.g. 30 V over-night). After the DNA has migrated far enough, the gel can be stained with 0.5 µg/mL ethidium bromide in 1X TAE electrophoresis buffer (1 hour). The DNA will be faint because the DNA is single stranded. Gel is then soaked in 0.25N HCl for 7 minutes with gentle agitation, rinsed with water and soaked in 0.5M NaOH, 1.5M NaCl for 30 minutes with gentle agitation. Gel is then rinsed briefly with water and DNA is blotted by capillary transfer onto neutral nylon membrane using 10X SSC. Hybridization is carried out by incubating membrane for 5 hours at 42°C with pre-hybridization buffer (50% formamide, denhardts solution + 4X BSA, 6% destran sulphate, 100 µg/mL salmon sperm DNA, 200 µg/mL tRNA carrier) following by o/n incubation at 42°C with pre-hybridization buffer + single-stranded RNA (ssRNA) probe. The ssRNA probe is obtained by *in vitro* transcription using Promega Riboprobe System-T7 and a pGEM-7Zf-based plasmid as a template. Following hybridization, membrane is washed twice with 5X

SSPE (20X SSPE = 3M NaCl, 200μM NaH_2PO_4, 20μM EDTA, pH 7.4) at 42°C for 15 minutes, 30 minutes with 1X SSPE 0.1% SDS at 42°C, 30 minutes with 0.1X SSPE 0.1% SDS at 42°C, 15 minutes with 0.2X SSPE 0.1% SDS at 68°C and 5 minutes with 0.2X SSPE at RT. Finally, membrane is exposed to an X-ray film.

Denaturing gel electrophoresis and western blot analysis to analyze BrdU incorporation

Cell were treated as described. After DNA extraction, genomic DNA was loaded on to agarose gel and run under denaturing conditions, as described above. After the run, DNA was transferred onto a nylon membrane. The membrane was then blocked with 4% non- fat milk and incubated overnight with anti-BrdU antibodies (RPN202, GE). Secondary anti-rabbit antibodies conjugated to HRP were then used to visualize BrdU-DNA.

DSB resection and repair by Single-Strand Annealing (SSA)

DSB end resection at the *MAT* locus in JKM139 derivative strains was analyzed on alkaline agarose gels by using a single-stranded probe complementary to the unresected DSB strand. This probe was obtained by *in vitro* transcription using Promega Riboprobe System-T7 and plasmid pML514 as a template. Plasmid pML514 was constructed

by inserting in the pGEM7Zf EcoRI site a 900-bp fragment containing part of the *MATα* locus (coordinates 200870 to 201587 on chromosome III). Quantitative analysis of DSB resection was performed by calculating the ratio of band intensities for ssDNA and total amount of DSB products.

DSB formation and repair in YMV45 strain were detected by Southern blot analysis using an Asp718-SalI fragment containing part of the *LEU2* gene as a probe. Quantitative analysis of the repair product was performed by calculating the ratio of band intensities for SSA product with respect to a loading control.

Quantification of ssDNA by qPCR

Genomic DNA was digested or not with the restriction enzyme SspI, which cuts dsDNA within the PCR amplicon. Digested and mock-digested DNAs were subjected to amplification by qPCR (iQ SYBR green supermix, Biorad, 1708882) using primers annealing on either side of the Ssp1 restriction site. qPCR was performed with a Biorad MiniOpticon. We quantified ssDNA using the formula: ssDNA= $100/[(1+2^{\Delta Ct})/2]$, in which ΔCt is the difference between the threshold cycles of digested and undigested DNA of a given time point. A control locus on chromosome XI with no SspI restriction sites, for which the Ct values for digested and undigested DNA would be expected to be similar, was used to correct the ΔCt values of other primers and to normalize the results relative to the amount of DNA initially loaded onto

the plate. The control locus is located 20 kb and 27 kb from ARS1103 and ARS1102, respectively, on chromosome XI.

Chromatin Immuno-Precipitation (ChIP) analysis

Cell at a concentration of $8x10^6$-$1x10^7$cells/ml, are harvested by adding 1.4 mL of 37% formaldehyde for 5 minutes while shaking, in order to create DNA-protein and protein-protein covalent bounds (cross-link). Then 2.5 mL of 2.5M glycine are added for other 5 minutes while shaking. Treated cells are kept in ice until centrifugation at 1800 rpm for 5 minutes at 4°C. Cell pellet is then washed first with HBS buffer (50mM HEPES pH 7.5, 140mM NaCl) and then with ChIP buffer (50mM HEPES pH 7.5, 140mM NaCl, 1mM EDTA pH 8, 1% IGEPAL CA-630, 0.1% Sodium deoxycholate, 1mM PMSF). Before each wash cells are pelleted by centrifugation at 1800 rpm for 5 minutes at 4°C. After the wash with ChIP buffer and subsequent centrifugation, the supernatant is carefully and completely removed. Then add 0.4 mL of ChIP buffer + complete anti-proteolitic tablets (Roche) is added and samples are stored at -80°C until the following day. Cells are broken for 30 minutes at 4°C with glass beads. After glass beads eliminations, the lysate is subjected to centrifugation at 4°C for 30 minutes. Pellet is resuspended in 0.5 mL ChIP buffer + anti-proteolitics and then sonicated, in order to share DNA in 500-1000 bp fragments. At this point 5 µL as “input DNA” for PCR reactions and 20 µL as “input” for western blot analysis are taken. Then 400 µL of the remaining solution is immunoprecipitated

with specific Dynabeads-coated antibodies. After proper incubation with desired antibodies, Dynabeads can be washed RT as follow: 2X with SDS buffer (50mM HEPES pH 7.5, 1mM EDTA pH 8, 140mM NaCl, 0.025% SDS), 1X with High-salt buffer (50mM HEPES pH 7.5, 1mM EDTA pH 8, 1M NaCl), 1X with T/L buffer (20mM Tris-Cl, pH 7.5, 250mM LiCl, 1mM EDTA pH 8, 0.05% sodium deoxycholate, 0.5%IGEPAL-CA630), and then 2X with T/E buffer (20mM Tris-Cl pH 7.5, 0.1mM EDTA pH 8). All washes are done by pulling down Dynabeads 1 minute and then nutating for 4 minutes with the specific buffer. After the last wash Dynabeads are resuspended in 145 µL TE + 1% SDS buffer, shaked on a vortex, put at 65°C for 2 minutes, shaked on vortex again and then pulled down. then 120 µL of the supernatant are put at 65°C over-night for reverse cross-linking, while 20 µL are stored as sample for western blot analysis of the immunoprecipitated protein amount. Previously taken input DNA samples must be put at 65°C over-night with 115 µL of TE + 1% SDS buffer. Then, DNA is purified for PCR analysis with QIAGEN columns.

Quantification of immunoprecipitated DNA was achieved by quantitative real-time (qPCR) on a Bio-Rad MiniOpticon apparatus using primer pairs located at different distances from the HO-induced DSB and at the *ARO1* fragment of chromosome IV. Data are expressed as fold enrichment at the HO-induced DSB over that at the non-cleaved *ARO1* locus, after normalization of each ChIP signals to the corresponding amount of immunoprecipitated protein and input for

each time point. Fold enrichment was then normalized to the efficiency of DSB induction.

For ChIP assays conducted at ARS305 and ARS607, data are expressed as fold enrichment at these genomic regions over that a region located 14 kb from ARS607, after normalization of each ChIP signals to the corresponding input for each time point.

γH2A was immunoprecipitated by using anti-γH2A antibodies (ab15083) from Abcam; Rad51 with anti-Rad51 (ab104232) from Abcam; MYC-tagged, HA-tagged and FLAG-tagged proteins were immunoprecipitated with anti-MYC (ab32) from Abcam, anti-HA (ab9110) from Abcam and anti-Flag (F1805) from Sigma Aldrich, respectively.

Immunoprecipitation and kinase assay

Protein extracts for the immunoprecipitations were prepared in a lysis buffer containing 50mM HEPES (pH 7.4), 100mM KCl, 0.1mM EDTA (pH 7.5), 0.2% Tween-20, 1mM dithiothreitol (DTT), 25mM NaFl, 100μM sodium orthovanadate, 0.5 mM phenylmethylsulfonyl fluoride, 25mM β-glycerophosphate, and a protease inhibitor cocktail (Roche Diagnostics). After the addition of a 1:1 volume of acid-washed glass beads and breakage, equal amounts of protein of the different clarified extracts were incubated for 2 hours at 4°C with 75 μL of a 50% (vol/vol) protein A-Sepharose resin covalently linked to 12CA5 monoclonal antibody. For the Kinase Assay, resins then were washed three times

in the lysis buffer and were resuspended in 450 µL of a kinase buffer containing 10mM HEPES (pH 7.4), 50mM NaCl, 10mM $MgCl_2$, 10mM $MnCl_2$, 1mM DTT. Resuspended resins (150 µL) were dried, followed by the addition of 11.5 µL of kinase buffer, 1.5 µL of 20µM unlabeled ATP, 10 µCi of 32P-labeled ATP, and 1 µL of Phosphorylated Heat- and Acid-Stable protein I (PHAS-I; 1 µg/µL; Stratagene). Kinase reactions were incubated at 30°C for 30 minutes. Sodium dodecyl sulfate (SDS) gel-loading buffer (15 µL) was added to the resins, and bound proteins were resolved by SDS-18% polyacrylamide gel electrophoresis and visualized after exposure of the gels to autoradiography films. The residual 300 µL of each resuspended resin was dried, resuspended in 10 µL of loading buffer, and subjected to Western blot analysis with anti-HA antibody.

For immunoprecipitation, after incubation with monoclonal antibodies anti-Rad53, A-Sepharose resins were washed twice with lysis buffer. Then, after been dried and boiled, were subjected to Western blot analysis.

SDS-PAGE and western blot analysis

Protein extracts for western blot analysis were prepared by TCA precipitation. Protein extracts are loaded in 10% polyacrylamide gels (composition). Proteins are separated based on their molecular weight by polyacrylamide gel electrophoresis in the presence of sodium dodecyl sulphate (SDS-PAGE). When adequate migration has

occurred proteins are blotted onto nitrocellulose membrane. Membrane is saturated by 1-hour incubation with 4% non-fat milk in TBS containing 0.2% TRITON X-100 and incubated for 2 hours with primary antibodies. Membrane is washed three times with TBS for 10 minutes, incubated for 1 hour with secondary antibodies and again washed with TBS.

Detection is performed with ECL (Enhanced ChemiLuminescence - GE Healthcare) and X-ray films according to the manufacturer.

Primary polyclonal rabbit anti-Rad53 antibodies are purchased at Abcam (ab104232).

Cell cycle analysis

Synchronization of yeast cells with α-factor

α-factor allows to synchronize a population of yeast cells in G1 phase. This pheromone activates a signal transduction cascade which arrests yeast cells in G1 phase. Only *MATa* cells are responsive to α-factor. To synchronize in G1 a population of exponentially growing yeast cells in YEPD, 2 µg/mL α-factor is added to $6x10^6$ cells/mL culture. As the percentage of budded cells will fall below 5% cells are considered to be G1-arrested. Cells are then washed and resuspended in fresh medium with or without 3 µg/mL α-factor to keep cells G1-arrested or release them into the cell cycle respectively. At this time cell cultures can be either treated with genotoxic agents or left untreated. If cells carry the deletion of *BAR1* gene, that encodes a protease that degrades the α-factor, 0.5 µg/mL α-factor is sufficient to induce a G1-arrest that lasts several hours.

Synchronization of yeast cells with nocodazole

Nocodazole allows to synchronize a population of yeast cells in G2 phase. This drug causes the depolimerization of microtubules, thus activating the mitotic checkpoint which arrests cells at the metaphase to anaphase transition (G2 phase). To synchronize in G2 a population of exponentially growing yeast cells in YEPD, 0.5 µg/mL nocodazole is

added to $6x10^6$ cells/mL culture together with DMSO at a final concentration of 1% (use a stock solution of 100X nocodazole in 100% DMSO). As the percentage of dumbbell cells will reach 95% cells are considered to be G2-arrested. Cells are then washed and resuspended in fresh medium with or without 1.5 µg/mL nocodazole to keep cells G2-arrested or release them into the cell cycle respectively. At this time cell cultures can be either treated with genotoxic agents or left untreated.

FACS analysis of DNA contents

FACS (Fluorescence-Activated Cell Sorting) analysis allow to determine the DNA content of every single cell of a given population of yeast cells. $6x10^6$ cells are harvested by centrifugation, resuspended in 70% ethanol and incubated at RT for 1 hour. Cells are then washed with 1 mL 50mM Tris pH 7.5 and incubated overnight at 37°C in the same solution with 1 mg/mL RNase. Samples are centrifuged and cells are incubated at 37°C for 30 minutes with 5 mg/mL pepsin in 55mM HCl, washed with 1 mL FACS Buffer and stained in 0.5 mL FACS buffer with 50 µg/mL propidium iodide. 100 µL of each sample are diluted in 1 mL 50mM Tris pH 7.5 and analyzed with a Becton-Dickinson FACS-Scan. The same samples can also be analyzed by fluorescence microscopy to score nuclear division.

Other techniques

Drug sensitivity assay

Overnight-grown saturated cultures of the indicated strains were serially diluted (10 fold) in water; 10 µl drops of each dilution were deposited on each plate. Images were scanned 2-3 days after plating and growth at 28°C. Each experiment was repeated at least twice.

Search for suppressors of sae2∆ sensitivity to CPT

To search for suppressor mutations of the CPT-sensitivity of *sae2∆* mutant, $5x10^6$ *sae2∆* cells were plated on YEPD in the presence of 30µM CPT. Survivors were crossed to wild type cells to identify by tetrad analysis the suppression events that were due to single-gene mutations. Subsequent genetic analyses allowed grouping the single-gene suppression events in 11 classes. The seven classes that showed the most efficient suppression were chosen and the suppressor genes were identified by genome sequencing and genetic analyses. Genomic DNA from seven single-gene suppressors was analyzed by next-generation Illumina sequencing (IGA technology services) to identify mutations altering open reading frames within the reference *S. cerevisiae* genome. To confirm that, *SGS1-G1298R*, *rad53-H88Y* and *tel1-N2021D* mutations were responsible for the suppression, either *TRP1*, *URA3* or *HIS3* gene was integrated

downstream of the *rad53-H88Y* and *tel1-N2021D* stop codon, respectively, and the resulting strain was crossed to wild type cells to verify by tetrad dissection that the suppression of the *sae2*Δ CPT sensitivity co-segregated with the *TRP1*, *URA3* or *HIS3* allele.

Microscopy analysis

Yeast cells were grown at 23°C. Once harvested, were resuspended in ethanol 100% and kept at -20 C° for 2 hours. After sonication, drops were deposited onto glass microscope slides. Fluorophore was a yellow fluorescent protein (YFP) that was visualized on a Nikon Eclipse 600 equipped with a 100 X 0.5-1.3 Planfluor oil objective (Nikon).

References

1. BW S, CP W *World Cancer Report 2014*.
2. Hanahan D, Weinberg RA (2000) The hallmarks of cancer. *Cell* **100**: 57–70.
3. Hanahan D, Weinberg RA (2011) Hallmarks of cancer: the next generation. *Cell* **144**: 646–674.
4. Negrini S, Gorgoulis VG, Halazonetis TD (2010) Genomic instability--an evolving hallmark of cancer. *Nat Rev Mol Cell Biol* **11**: 220–228.
5. Aguilera A, Gómez-González B (2008) Genome instability: a mechanistic view of its causes and consequences. *Nat Rev Genet* **9**: 204–217.
6. Aguilera A, García-Muse T (2013) Causes of Genome Instability. *Annu Rev Genet* **47**: 1–32.
7. Roos WP, Thomas AD, Kaina B (2016) DNA damage and the balance between survival and death in cancer biology. *Nat Rev Cancer* **16**: 20–33.
8. Finn K, Lowndes NF, Grenon M (2012) Eukaryotic DNA damage checkpoint activation in response to double-strand breaks. *Cell Mol Life Sci* **69**: 1447–1473.
9. Gorgoulis VG, Vassiliou L-VF, Karakaidos P, Zacharatos P, Kotsinas A, Liloglou T, Venere M, Ditullio RA, Kastrinakis NG, Levy B, et al. (2005) Activation of the DNA damage checkpoint and genomic instability in human precancerous lesions. *Nature* **434**: 907–913.
10. Bartkova J, Horejsí Z, Koed K, Krämer A, Tort F, Zieger K, Guldberg P, Sehested M, Nesland JM, Lukas C, et al. (2005) DNA damage response as a candidate anti-cancer barrier in early human tumorigenesis. *Nature* **434**: 864–870.
11. Brosh RM (2013) DNA helicases involved in DNA repair and their roles in cancer. *Nat Rev Cancer* **13**: 542–558.

12. Karlsson A, Deb-Basu D, Cherry A, Turner S, Ford J, Felsher DW (2003) Defective double-strand DNA break repair and chromosomal translocations by MYC overexpression. *Proc Natl Acad Sci* **100**: 9974–9979.
13. Woo RA, Poon RYC (2004) Activated oncogenes promote and cooperate with chromosomal instability for neoplastic transformation. *Genes Dev* **18**: 1317–1330.
14. Halazonetis TD, Gorgoulis VG, Bartek J (2008) An oncogene-induced DNA damage model for cancer development. *Science* **319**: 1352–1355.
15. Macheret M, Halazonetis TD (2015) DNA replication stress as a hallmark of cancer. *Annu Rev Pathol* **10**: 425–448.
16. Andor N, Maley CC, Ji HP (2017) Genomic Instability in Cancer: Teetering on the Limit of Tolerance. *Cancer Res* **77**: 2179–2185.
17. O'Neil NJ, Bailey ML, Hieter P (2017) Synthetic lethality and cancer. *Nat Rev Genet*.
18. Beijersbergen RL, Wessels LFA, Bernards R (2017) Synthetic Lethality in Cancer Therapeutics. *Annu Rev Cancer Biol* **1**: 141–161.
19. Nickoloff JA, Jones D, Lee S-H, Williamson EA, Hromas R (2017) Drugging the Cancers Addicted to DNA Repair. *JNCI J Natl Cancer Inst* **109**:.
20. Aylon Y, Kupiec M (2004) DSB repair: the yeast paradigm. *DNA Repair* **3**: 797–815.
21. Weinert T, Hartwell L (1989) Control of G2 delay by the rad9 gene of Saccharomyces cerevisiae. *J Cell Sci Suppl* **12**: 145–148.
22. Hoeijmakers JHJ (2009) DNA Damage, Aging, and Cancer. *N Engl J Med* **361**: 1475–1485.
23. So A, Le Guen T, Lopez BS, Guirouilh-Barbat J (2017) Genomic rearrangements induced by unscheduled DNA double strand breaks in somatic mammalian cells. *FEBS J* **284**: 2324–2344.

24. Mehta A, Haber JE (2014) Sources of DNA double-strand breaks and models of recombinational DNA repair. *Cold Spring Harb Perspect Biol* **6**: a016428.
25. Lee C-S, Haber JE (2015) Mating-type Gene Switching in Saccharomyces cerevisiae. *Microbiol Spectr* **3**: MDNA3-0013-2014.
26. Gobbini E, Cesena D, Galbiati A, Lockhart A, Longhese MP (2013) Interplays between ATM/Tel1 and ATR/Mec1 in sensing and signaling DNA double-strand breaks. *DNA Repair* **12**: 791–799.
27. Ciccia A, Elledge SJ (2010) The DNA Damage Response: Making It Safe to Play with Knives. *Mol Cell* **40**: 179–204.
28. Pardo B, Crabbé L, Pasero P (2017) Signaling pathways of replication stress in yeast. *FEMS Yeast Res* **17**:.
29. Lisby M, Barlow JH, Burgess RC, Rothstein R (2004) Choreography of the DNA Damage Response: Spatiotemporal Relationships among Checkpoint and Repair Proteins. *Cell* **118**: 699–713.
30. Johzuka K, Ogawa H (1995) Interaction of Mre11 and Rad50: two proteins required for DNA repair and meiosis-specific double-strand break formation in Saccharomyces cerevisiae. *Genetics* **139**: 1521–1532.
31. Trujillo KM, Sung P (2001) DNA Structure-specific Nuclease Activities in theSaccharomyces cerevisiae Rad50·Mre11 Complex. *J Biol Chem* **276**: 35458–35464.
32. Trujillo KM, Yuan S-SF, Lee EY-HP, Sung P (1998) Nuclease Activities in a Complex of Human Recombination and DNA Repair Factors Rad50, Mre11, and p95. *J Biol Chem* **273**: 21447–21450.
33. Stracker TH, Petrini JHJ (2011) The MRE11 complex: starting from the ends. *Nat Rev Mol Cell Biol* **12**: 90–103.
34. Rupnik A, Lowndes NF, Grenon M (2010) MRN and the race to the break. *Chromosoma* **119**: 115–135.

35. Williams RS, Moncalian G, Williams JS, Yamada Y, Limbo O, Shin DS, Groocock LM, Cahill D, Hitomi C, Guenther G, et al. (2008) Mre11 Dimers Coordinate DNA End Bridging and Nuclease Processing in Double-Strand-Break Repair. *Cell* **135**: 97–109.
36. Hopfner K-P, Karcher A, Shin DS, Craig L, Arthur LM, Carney JP, Tainer JA (2000) Structural Biology of Rad50 ATPase. *Cell* **101**: 789–800.
37. Hopfner K-P, Craig L, Moncalian G, Zinkel RA, al et (2002) The Rad50 zinc-hook is a structure joining Mre11 complexes in DNA recombination and repair. *Nat Lond* **418**: 562–566.
38. Wiltzius JJW, Hohl M, Fleming JC, Petrini JHJ (2005) The Rad50 hook domain is a critical determinant of Mre11 complex functions. *Nat Struct Mol Biol N Y* **12**: 403–407.
39. Lammens K, Bemeleit DJ, Möckel C, Clausing E, Schele A, Hartung S, Schiller CB, Lucas M, Angermüller C, Söding J, et al. (2011) The Mre11:Rad50 Structure Shows an ATP-Dependent Molecular Clamp in DNA Double-Strand Break Repair. *Cell* **145**: 54–66.
40. Tsukamoto Y, Mitsuoka C, Terasawa M, Ogawa H, Ogawa T (2005) Xrs2p regulates Mre11p translocation to the nucleus and plays a role in telomere elongation and meiotic recombination. *Mol Biol Cell* **16**: 597–608.
41. Tauchi H, Kobayashi J, Morishima K, Matsuura S, Nakamura A, Shiraishi T, Ito E, Masnada D, Delia D, Komatsu K (2001) The forkhead-associated domain of NBS1 is essential for nuclear foci formation after irradiation but not essential for hRAD50[middle dot]hMRE11[middle dot]NBS1 complex DNA repair activity. *J Biol Chem* **276**: 12–15.
42. Lee J-H, Ghirlando R, Bhaskara V, Hoffmeyer MR, Gu J, Paull TT (2003) Regulation of Mre11/Rad50 by Nbs1 EFFECTS ON NUCLEOTIDE-DEPENDENT DNA BINDING AND ASSOCIATION WITH ATAXIA-TELANGIECTASIA-LIKE

DISORDER MUTANT COMPLEXES. *J Biol Chem* **278**: 45171–45181.

43. Trujillo KM, Roh DH, Chen L, Komen SV, Tomkinson A, Sung P (2003) Yeast Xrs2 Binds DNA and Helps Target Rad50 and Mre11 to DNA Ends. *J Biol Chem* **278**: 48957–48964.
44. Nakada D, Matsumoto K, Sugimoto K (2003) ATM-related Tel1 associates with double-strand breaks through an Xrs2-dependent mechanism. *Genes Dev* **17**: 1957–1962.
45. Greenwell PW, Kronmal SL, Porter SE, Gassenhuber J, Obermaier B, Petes TD (1995) TEL1, a gene involved in controlling telomere length in S. cerevisiae, is homologous to the human ataxia telangiectasia gene. *Cell* **82**: 823–829.
46. Lempiäinen H, Halazonetis TD (2009) Emerging common themes in regulation of PIKKs and PI3Ks. *EMBO J* **28**: 3067–3073.
47. BioMed Research International, Multifunctional Role of ATM/Tel1 Kinase in Genome Stability: From the DNA Damage Response to Telomere Maintenance, Last updated 2014, Accessed on 2014.
48. Clouaire T, Marnef A, Legube G (2017) Taming Tricky DSBs: ATM on duty. *DNA Repair* **56**: 84–91.
49. McKinnon PJ (2004) ATM and ataxia telangiectasia: Second in Molecular Medicine Review Series. *EMBO Rep* **5**: 772–776.
50. Fukunaga K, Kwon Y, Sung P, Sugimoto K (2011) Activation of Protein Kinase Tel1 through Recognition of Protein-Bound DNA Ends. *Mol Cell Biol* **31**: 1959–1971.
51. Guleria A, Chandna S (2016) ATM kinase: Much more than a DNA damage responsive protein. *DNA Repair* **39**: 1–20.
52. Wang X, Chu H, Lv M, Zhang Z, Qiu S, Liu H, Shen X, Wang W, Cai G (2016) Structure of the intact ATM/Tel1 kinase. *Nat Commun* **7**: 11655.
53. Paull TT (2015) Mechanisms of ATM Activation. *Annu Rev Biochem* **84**: 711–738.

54. You Z, Chahwan C, Bailis J, Hunter T, Russell P (2005) ATM Activation and Its Recruitment to Damaged DNA Require Binding to the C Terminus of Nbs1. *Mol Cell Biol* **25**: 5363–5379.
55. Dupré A, Boyer-Chatenet L, Gautier J (2006) Two-step activation of ATM by DNA and the Mre11-Rad50-Nbs1 complex. *Nat Struct Mol Biol* **13**: 451–457.
56. Iwasaki D, Hayashihara K, Shima H, Higashide M, Terasawa M, Gasser SM, Shinohara M (2016) The MRX Complex Ensures NHEJ Fidelity through Multiple Pathways Including Xrs2-FHA–Dependent Tel1 Activation. *PLOS Genet* **12**: e1005942.
57. Sawicka M, Wanrooij PH, Darbari VC, Tannous E, Hailemariam S, Bose D, Makarova AV, Burgers PM, Zhang X (2016) The Dimeric Architecture of Checkpoint Kinases Mec1ATR and Tel1ATM Reveal a Common Structural Organization. *J Biol Chem* **291**: 13436–13447.
58. Clerici M, Trovesi C, Galbiati A, Lucchini G, Longhese MP (2014) Mec1/ATR regulates the generation of single-stranded DNA that attenuates Tel1/ATM signaling at DNA ends. *EMBO J* **33**: 198–216.
59. Jazayeri A, Falck J, Lukas C, Bartek J, Smith GCM, Lukas J, Jackson SP (2006) ATM- and cell cycle-dependent regulation of ATR in response to DNA double-strand breaks. *Nat Cell Biol* **8**: 37–45.
60. Zou L, Elledge SJ (2003) Sensing DNA Damage Through ATRIP Recognition of RPA-ssDNA Complexes. *Science* **300**: 1542–1548.
61. Paciotti V, Clerici M, Lucchini G, Longhese MP (2000) The checkpoint protein Ddc2, functionally related to S. pombe Rad26, interacts with Mec1 and is regulated by Mec1-dependent phosphorylation in budding yeast. *Genes Dev* **14**: 2046–2059.
62. Cortez D, Guntuku S, Qin J, Elledge SJ (2001) ATR and ATRIP: Partners in Checkpoint Signaling. *Science* **294**: 1713–1716.

63. Ball HL, Ehrhardt MR, Mordes DA, Glick GG, Chazin WJ, Cortez D (2007) Function of a Conserved Checkpoint Recruitment Domain in ATRIP Proteins. *Mol Cell Biol* **27**: 3367–3377.
64. MacDougall CA, Byun TS, Van C, Yee M, Cimprich KA (2007) The structural determinants of checkpoint activation. *Genes Dev* **21**: 898–903.
65. Navadgi-Patil VM, Burgers PM (2009) A tale of two tails: Activation of DNA damage checkpoint kinase Mec1/ATR by the 9-1-1 clamp and by Dpb11/TopBP1. *DNA Repair* **8**: 996–1003.
66. Majka J, Niedziela-Majka A, Burgers PMJ (2006) The Checkpoint Clamp Activates Mec1 Kinase during Initiation of the DNA Damage Checkpoint. *Mol Cell* **24**: 891–901.
67. Parrilla-Castellar ER, Arlander SJH, Karnitz L (2004) Dial 9–1–1 for DNA damage: the Rad9–Hus1–Rad1 (9–1–1) clamp complex. *DNA Repair* **3**: 1009–1014.
68. Kumagai A, Lee J, Yoo HY, Dunphy WG (2006) TopBP1 Activates the ATR-ATRIP Complex. *Cell* **124**: 943–955.
69. Lee J, Kumagai A, Dunphy WG (2007) The Rad9-Hus1-Rad1 Checkpoint Clamp Regulates Interaction of TopBP1 with ATR. *J Biol Chem* **282**: 28036–28044.
70. Mordes DA, Nam EA, Cortez D (2008) Dpb11 activates the Mec1-Ddc2 complex. *Proc Natl Acad Sci U S A* **105**: 18730–18734.
71. Puddu F, Granata M, Nola LD, Balestrini A, Piergiovanni G, Lazzaro F, Giannattasio M, Plevani P, Muzi-Falconi M (2008) Phosphorylation of the Budding Yeast 9-1-1 Complex Is Required for Dpb11 Function in the Full Activation of the UV-Induced DNA Damage Checkpoint. *Mol Cell Biol* **28**: 4782–4793.
72. Wang H, Elledge SJ (2002) Genetic and Physical Interactions Between DPB11 and DDC1 in the Yeast DNA Damage Response Pathway. *Genetics* **160**: 1295–1304.

73. Shroff R, Arbel-Eden A, Pilch D, Ira G, Bonner WM, Petrini JH, Haber JE, Lichten M (2004) Distribution and Dynamics of Chromatin Modification Induced by a Defined DNA Double-Strand Break. *Curr Biol* **14**: 1703–1711.
74. Redon C, Pilch DR, Rogakou EP, Orr AH, Lowndes NF, Bonner WM (2003) Yeast histone 2A serine 129 is essential for the efficient repair of checkpoint-blind DNA damage. *EMBO Rep* **4**: 678–684.
75. Georgoulis A, Vorgias CE, Chrousos GP, Rogakou EP (2017) Genome Instability and γH2AX. *Int J Mol Sci* **18**: 1979.
76. Celeste A, Petersen S, Romanienko PJ, Fernandez-Capetillo O, Chen HT, Sedelnikova OA, Reina-San-Martin B, Coppola V, Meffre E, Difilippantonio MJ, et al. (2002) Genomic instability in mice lacking histone H2AX. *Science* **296**: 922–927.
77. Weinert T, Hartwell L (1989) Control of G2 delay by the rad9 gene of Saccharomyces cerevisiae. *J Cell Sci Suppl* **12**: 145–148.
78. Sweeney FD, Yang F, Chi A, Shabanowitz J, Hunt DF, Durocher D (2005) Saccharomyces cerevisiae Rad9 acts as a Mec1 adaptor to allow Rad53 activation. *Curr Biol CB* **15**: 1364–1375.
79. Grenon M, Costelloe T, Jimeno S, O'Shaughnessy A, FitzGerald J, Zgheib O, Degerth L, Lowndes NF (2007) Docking onto chromatin via the Saccharomyces cerevisiae Rad9 Tudor domain. *Yeast* **24**: 105–119.
80. Giannattasio M, Lazzaro F, Plevani P, Muzi-Falconi M (2005) The DNA Damage Checkpoint Response Requires Histone H2B Ubiquitination by Rad6-Bre1 and H3 Methylation by Dot1. *J Biol Chem* **280**: 9879–9886.
81. Hammet A, Magill C, Heierhorst J, Jackson SP (2007) Rad9 BRCT domain interaction with phosphorylated H2AX regulates the G1 checkpoint in budding yeast. *EMBO Rep* **8**: 851–857.
82. Granata M, Lazzaro F, Novarina D, Panigada D, Puddu F, Abreu CM, Kumar R, Grenon M, Lowndes NF, Plevani P, et al. (2010) Dynamics of Rad9 Chromatin Binding and Checkpoint Function

Are Mediated by Its Dimerization and Are Cell Cycle–Regulated by CDK1 Activity. *PLOS Genet* **6**: e1001047.

83. Pfander B, Diffley JFX (2011) Dpb11 coordinates Mec1 kinase activation with cell cycle-regulated Rad9 recruitment. *EMBO J* **30**: 4897–4907.
84. di Cicco G, Bantele SCS, Reusswig K-U, Pfander B (2017) A cell cycle-independent mode of the Rad9-Dpb11 interaction is induced by DNA damage. *Sci Rep* **7**: 11650.
85. Schwartz MF, Duong JK, Sun Z, Morrow JS, Pradhan D, Stern DF (2002) Rad9 Phosphorylation Sites Couple Rad53 to the Saccharomyces cerevisiae DNA Damage Checkpoint. *Mol Cell* **9**: 1055–1065.
86. Goldberg M, Stucki M, Falck J, D'Amours D, Rahman D, Pappin D, Bartek J, Jackson SP (2003) MDC1 is required for the intra-S-phase DNA damage checkpoint. *Nature* **421**: 952–956.
87. Stucki M, Clapperton JA, Mohammad D, Yaffe MB, Smerdon SJ, Jackson SP (2005) MDC1 directly binds phosphorylated histone H2AX to regulate cellular responses to DNA double-strand breaks. *Cell* **123**: 1213–1226.
88. Lou Z, Minter-Dykhouse K, Franco S, Gostissa M, Rivera MA, Celeste A, Manis JP, van Deursen J, Nussenzweig A, Paull TT, et al. (2006) MDC1 maintains genomic stability by participating in the amplification of ATM-dependent DNA damage signals. *Mol Cell* **21**: 187–200.
89. Lou Z, Minter-Dykhouse K, Wu X, Chen J (2003) MDC1 is coupled to activated CHK2 in mammalian DNA damage response pathways. *Nature* **421**: 957–961.
90. Jungmichel S, Stucki M (2010) MDC1: The art of keeping things in focus. *Chromosoma* **119**: 337–349.
91. Wu L, Luo K, Lou Z, Chen J (2008) MDC1 regulates intra-S-phase checkpoint by targeting NBS1 to DNA double-strand breaks. *Proc Natl Acad Sci U S A* **105**: 11200–11205.

92. Stucki M, Jackson SP (2004) MDC1/NFBD1: a key regulator of the DNA damage response in higher eukaryotes. *DNA Repair* **3**: 953–957.
93. Arlt MF, Xu B, Durkin SG, Casper AM, Kastan MB, Glover TW (2004) BRCA1 is required for common-fragile-site stability via its G2/M checkpoint function. *Mol Cell Biol* **24**: 6701–6709.
94. Yarden RI, Pardo-Reoyo S, Sgagias M, Cowan KH, Brody LC (2002) BRCA1 regulates the G2/M checkpoint by activating Chk1 kinase upon DNA damage. *Nat Genet* **30**: 285–289.
95. Pellicioli A, Foiani M (2005) Signal transduction: how rad53 kinase is activated. *Curr Biol CB* **15**: R769-771.
96. Bartek J, Falck J, Lukas J (2001) CHK2 kinase--a busy messenger. *Nat Rev Mol Cell Biol* **2**: 877–886.
97. Gilbert CS, Green CM, Lowndes NF (2001) Budding Yeast Rad9 Is an ATP-Dependent Rad53 Activating Machine. *Mol Cell* **8**: 129–136.
98. Zannini L, Delia D, Buscemi G (2014) CHK2 kinase in the DNA damage response and beyond. *J Mol Cell Biol* **6**: 442–457.
99. Patil M, Pabla N, Dong Z (2013) Checkpoint kinase 1 in DNA damage response and cell cycle regulation. *Cell Mol Life Sci* **70**: 4009–4021.
100. Zhang Y, Hunter T (2014) Roles of Chk1 in cell biology and cancer therapy. *Int J Cancer* **134**: 1013–1023.
101. Ceccaldi R, Rondinelli B, D'Andrea AD (2016) Repair Pathway Choices and Consequences at the Double-Strand Break. *Trends Cell Biol* **26**: 52–64.
102. Li J, Xu X (2016) DNA double-strand break repair: a tale of pathway choices. *Acta Biochim Biophys Sin* **48**: 641–646.
103. Hefferin ML, Tomkinson AE (2005) Mechanism of DNA double-strand break repair by non-homologous end joining. *DNA Repair* **4**: 639–648.

104. Dudášová Z, Dudáš A, Chovanec M (2004) Non-homologous end-joining factors of Saccharomyces cerevisiae. *FEMS Microbiol Rev* **28**: 581–601.
105. Chang HHY, Pannunzio NR, Adachi N, Lieber MR (2017) Non-homologous DNA end joining and alternative pathways to double-strand break repair. *Nat Rev Mol Cell Biol* **18**: 495–506.
106. Williams GJ, Hammel M, Radhakrishnan SK, Ramsden D, Lees-Miller SP, Tainer JA (2014) Structural insights into NHEJ: Building up an integrated picture of the dynamic DSB repair super complex, one component and interaction at a time. *DNA Repair* **17**: 110–120.
107. Cassani C, Gobbini E, Wang W, Niu H, Clerici M, Sung P, Longhese MP (2016) Tel1 and Rif2 Regulate MRX Functions in End-Tethering and Repair of DNA Double-Strand Breaks. *PLoS Biol* **14**: e1002387.
108. Deshpande RA, Williams GJ, Limbo O, Williams RS, Kuhnlein J, Lee J-H, Classen S, Guenther G, Russell P, Tainer JA, et al. (2014) ATP-driven Rad50 conformations regulate DNA tethering, end resection, and ATM checkpoint signaling. *EMBO J* **33**: 482–500.
109. Haber JE (2016) A Life Investigating Pathways That Repair Broken Chromosomes. *Annu Rev Genet* **50**: 1–28.
110. San Filippo J, Sung P, Klein H (2008) Mechanism of Eukaryotic Homologous Recombination. *Annu Rev Biochem* **77**: 229–257.
111. Symington LS, Gautier J (2011) Double-strand break end resection and repair pathway choice. *Annu Rev Genet* **45**: 247–271.
112. Symington LS, Rothstein R, Lisby M (2014) Mechanisms and Regulation of Mitotic Recombination in Saccharomyces cerevisiae. *Genetics* **198**: 795–835.
113. Krejci L, Altmannova V, Spirek M, Zhao X (2012) Homologous recombination and its regulation. *Nucleic Acids Res* **40**: 5795–5818.

114. Holloman WK (2011) Unraveling the mechanism of BRCA2 in homologous recombination. *Nat Struct Mol Biol* **18**: nsmb.2096.
115. Bizard AH, Hickson ID (2014) The Dissolution of Double Holliday Junctions. *Cold Spring Harb Perspect Biol* **6**: a016477.
116. Lilley DMJ (2017) Holliday junction-resolving enzymes—structures and mechanisms. *FEBS Lett* **591**: 1073–1082.
117. Daley JM, Niu H, Miller AS, Sung P (2015) Biochemical mechanism of DSB end resection and its regulation. *DNA Repair* **32**: 66–74.
118. Kass EM, Moynahan ME, Jasin M (2016) When Genome Maintenance Goes Badly Awry. *Mol Cell* **62**: 777–787.
119. Kolinjivadi AM, Sannino V, de Antoni A, Técher H, Baldi G, Costanzo V (2017) Moonlighting at replication forks - a new life for homologous recombination proteins BRCA1, BRCA2 and RAD51. *FEBS Lett* **591**: 1083–1100.
120. Paull TT, Deshpande RA (2014) The Mre11/Rad50/Nbs1 complex: recent insights into catalytic activities and ATP-driven conformational changes. *Exp Cell Res* **329**: 139–147.
121. Cejka P (2015) DNA End Resection: Nucleases Team Up with the Right Partners to Initiate Homologous Recombination. *J Biol Chem* **290**: 22931–22938.
122. Shibata A, Moiani D, Arvai AS, Perry J, Harding SM, Genois M-M, Maity R, van Rossum-Fikkert S, Kertokalio A, Romoli F, et al. (2014) DNA double-strand break repair pathway choice is directed by distinct MRE11 nuclease activities. *Mol Cell* **53**: 7–18.
123. Oh J, Al-Zain A, Cannavo E, Cejka P, Symington LS (2016) Xrs2 Dependent and Independent Functions of the Mre11-Rad50 Complex. *Mol Cell* **64**: 405–415.
124. Nicolette ML, Lee K, Guo Z, Rani M, Chow JM, Lee SE, Paull TT (2010) Mre11–Rad50–Xrs2 and Sae2 promote 5′ strand resection of DNA double-strand breaks. *Nat Struct Mol Biol* **17**: nsmb.1957.

125. Mimitou EP, Symington LS (2008) Sae2, Exo1 and Sgs1 collaborate in DNA double-strand break processing. *Nature* **455**: 770–774.
126. Andres SN, Williams RS (2017) CtIP/Ctp1/Sae2, molecular form fit for function. *DNA Repair* **56**: 109–117.
127. Huertas P, Cortés-Ledesma F, Sartori AA, Aguilera A, Jackson SP (2008) CDK targets Sae2 to control DNA-end resection and homologous recombination. *Nature* **455**: 689–692.
128. Clerici M, Mantiero D, Lucchini G, Longhese MP (2005) The Saccharomyces cerevisiae Sae2 protein promotes resection and bridging of double strand break ends. *J Biol Chem* **280**: 38631–38638.
129. Cannavo E, Cejka P (2014) Sae2 promotes dsDNA endonuclease activity within Mre11-Rad50-Xrs2 to resect DNA breaks. *Nature* **514**: 122–125.
130. Lengsfeld BM, Rattray AJ, Bhaskara V, Ghirlando R, Paull TT (2007) Sae2 is an endonuclease that processes hairpin DNA cooperatively with the Mre11/Rad50/Xrs2 complex. *Mol Cell* **28**: 638–651.
131. Arora S, Deshpande RA, Budd M, Campbell J, Revere A, Zhang X, Schmidt KH, Paull TT (2017) Genetic separation of Sae2 nuclease activity from Mre11 nuclease functions in budding yeast. *Mol Cell Biol*.
132. Clerici M, Mantiero D, Lucchini G, Longhese MP (2006) The Saccharomyces cerevisiae Sae2 protein negatively regulates DNA damage checkpoint signalling. *EMBO Rep* **7**: 212–218.
133. Puddu F, Oelschlaegel T, Guerini I, Geisler NJ, Niu H, Herzog M, Salguero I, Ochoa-Montaño B, Viré E, Sung P, et al. (2015) Synthetic viability genomic screening defines Sae2 function in DNA repair. *EMBO J* **34**: 1509–1522.
134. Chen H, Donnianni RA, Handa N, Deng SK, Oh J, Timashev LA, Kowalczykowski SC, Symington LS (2015) Sae2 promotes DNA damage resistance by removing the Mre11-Rad50-Xrs2

complex from DNA and attenuating Rad53 signaling. *Proc Natl Acad Sci U S A* **112**: E1880-1887.

135. Sartori AA, Lukas C, Coates J, Mistrik M, Fu S, Bartek J, Baer R, Lukas J, Jackson SP (2007) Human CtIP promotes DNA end resection. *Nature* **450**: nature06337.
136. Daley JM, Jimenez-Sainz J, Wang W, Miller AS, Xue X, Nguyen KA, Jensen RB, Sung P (2017) Enhancement of BLM-DNA2-Mediated Long-Range DNA End Resection by CtIP. *Cell Rep* **21**: 324–332.
137. Symington LS (2014) End resection at double-strand breaks: mechanism and regulation. *Cold Spring Harb Perspect Biol* **6**:.
138. Cannavo E, Cejka P, Kowalczykowski SC (2013) Relationship of DNA degradation by Saccharomyces cerevisiae Exonuclease 1 and its stimulation by RPA and Mre11-Rad50-Xrs2 to DNA end resection. *Proc Natl Acad Sci* **110**: E1661–E1668.
139. Myler LR, Gallardo IF, Soniat MM, Deshpande RA, Gonzalez XB, Kim Y, Paull TT, Finkelstein IJ (2017) Single-Molecule Imaging Reveals How Mre11-Rad50-Nbs1 Initiates DNA Break Repair. *Mol Cell* **67**: 891–898.e4.
140. Ngo GHP, Lydall D (2015) The 9-1-1 checkpoint clamp coordinates resection at DNA double strand breaks. *Nucleic Acids Res* **43**: 5017–5032.
141. Ngo GHP, Balakrishnan L, Dubarry M, Campbell JL, Lydall D (2014) The 9-1-1 checkpoint clamp stimulates DNA resection by Dna2-Sgs1 and Exo1. *Nucleic Acids Res* **42**: 10516–10528.
142. Nimonkar AV, Ozsoy AZ, Genschel J, Modrich P, Kowalczykowski SC (2008) Human exonuclease 1 and BLM helicase interact to resect DNA and initiate DNA repair. *Proc Natl Acad Sci U S A* **105**: 16906–16911.
143. Tomimatsu N, Mukherjee B, Hardebeck MC, Ilcheva M, Camacho CV, Harris JL, Porteus M, Llorente B, Khanna KK, Burma S (2014) Phosphorylation of EXO1 by CDKs 1 and 2

regulates DNA end resection and repair pathway choice. *Nat Commun* **5**: ncomms4561.

144. Tomimatsu N, Mukherjee B, Harris JL, Boffo FL, Hardebeck MC, Potts PR, Khanna KK, Burma S (2017) DNA-damage-induced degradation of EXO1 exonuclease limits DNA end resection to ensure accurate DNA repair. *J Biol Chem* **292**: 10779–10790.
145. Colombo CV, Trovesi C, Menin L, Longhese MP, Clerici M (2017) The RNA binding protein Npl3 promotes resection of DNA double-strand breaks by regulating the levels of Exo1. *Nucleic Acids Res* **45**: 6530–6545.
146. Rezazadeh S (2012) RecQ helicases; at the crossroad of genome replication, repair, and recombination. *Mol Biol Rep* **39**: 4527–4543.
147. Bernstein KA, Gangloff S, Rothstein R (2010) The RecQ DNA Helicases in DNA Repair. *Annu Rev Genet* **44**: 393–417.
148. Hardy J, Churikov D, Géli V, Simon M-N (2014) Sgs1 and Sae2 promote telomere replication by limiting accumulation of ssDNA. *Nat Commun* **5**: 5004.
149. Bernstein KA, Mimitou EP, Mihalevic MJ, Chen H, Sunjaveric I, Symington LS, Rothstein R (2013) Resection activity of the Sgs1 helicase alters the affinity of DNA ends for homologous recombination proteins in Saccharomyces cerevisiae. *Genetics* **195**: 1241–1251.
150. Niu H, Chung W-H, Zhu Z, Kwon Y, Zhao W, Chi P, Prakash R, Seong C, Liu D, Lu L, et al. (2010) Mechanism of the ATP-dependent DNA End Resection Machinery from S. cerevisiae. *Nature* **467**: 108–111.
151. Gravel S, Chapman JR, Magill C, Jackson SP (2008) DNA helicases Sgs1 and BLM promote DNA double-strand break resection. *Genes Dev* **22**: 2767–2772.
152. Nimonkar AV, Genschel J, Kinoshita E, Polaczek P, Campbell JL, Wyman C, Modrich P, Kowalczykowski SC (2011) BLM–

DNA2–RPA–MRN and EXO1–BLM–RPA–MRN constitute two DNA end resection machineries for human DNA break repair. *Genes Dev* **25**: 350–362.

153. Daley JM, Chiba T, Xue X, Niu H, Sung P (2014) Multifaceted role of the Topo IIIα-RMI1-RMI2 complex and DNA2 in the BLM-dependent pathway of DNA break end resection. *Nucleic Acids Res* **42**: 11083–11091.
154. Sturzenegger A, Burdova K, Kanagaraj R, Levikova M, Pinto C, Cejka P, Janscak P (2014) DNA2 cooperates with the WRN and BLM RecQ helicases to mediate long-range DNA end resection in human cells. *J Biol Chem* **289**: 27314–27326.
155. Bae SH, Seo YS (2000) Characterization of the enzymatic properties of the yeast dna2 Helicase/endonuclease suggests a new model for Okazaki fragment processing. *J Biol Chem* **275**: 38022–38031.
156. Zhu Z, Chung W-H, Shim EY, Lee SE, Ira G (2008) Sgs1 Helicase and Two Nucleases Dna2 and Exo1 Resect DNA Double-Strand Break Ends. *Cell* **134**: 981–994.
157. Miller AS, Daley JM, Pham NT, Niu H, Xue X, Ira G, Sung P (2017) A novel role of the Dna2 translocase function in DNA break resection. *Genes Dev* **31**: 503–510.
158. Levikova M, Pinto C, Cejka P (2017) The motor activity of DNA2 functions as an ssDNA translocase to promote DNA end resection. *Genes Dev* **31**: 493–502.
159. Cejka P, Cannavo E, Polaczek P, Masuda-Sasa T, Pokharel S, Campbell JL, Kowalczykowski SC (2010) DNA end resection by Dna2–Sgs1–RPA and its stimulation by Top3–Rmi1 and Mre11–Rad50–Xrs2. *Nature* **467**: nature09355.
160. Pinto C, Kasaciunaite K, Seidel R, Cejka P (2016) Human DNA2 possesses a cryptic DNA unwinding activity that functionally integrates with BLM or WRN helicases. *eLife* **5**: e18574.
161. Ira G, Pellicioli A, Balijja A, Wang X, Fiorani S, Carotenuto W, Liberi G, Bressan D, Wan L, Hollingsworth NM, et al. (2004)

DNA end resection, homologous recombination and DNA damage checkpoint activation require CDK1. *Nature* **431**: 1011–1017.
162. Zierhut C, Diffley JFX (2008) Break dosage, cell cycle stage and DNA replication influence DNA double strand break response. *EMBO J* **27**: 1875–1885.
163. Chen X, Niu H, Chung W-H, Zhu Z, Papusha A, Shim EY, Lee SE, Sung P, Ira G (2011) Cell cycle regulation of DNA double-strand break end resection by Cdk1-dependent Dna2 phosphorylation. *Nat Struct Mol Biol* **18**: nsmb.2105.
164. Huertas P, Jackson SP (2009) Human CtIP mediates cell cycle control of DNA end resection and double strand break repair. *J Biol Chem* **284**: 9558–9565.
165. Symington LS (2016) Mechanism and Regulation of DNA End Resection in Eukaryotes. *Crit Rev Biochem Mol Biol* **51**: 195–212.
166. Ferretti LP, Lafranchi L, Sartori AA (2013) Controlling DNA-end resection: a new task for CDKs. *Front Genet* **4**:.
167. Mimitou EP, Symington LS (2010) Ku prevents Exo1 and Sgs1-dependent resection of DNA ends in the absence of a functional MRX complex or Sae2. *EMBO J* **29**: 3358–3369.
168. Balestrini A, Ristic D, Dionne I, Liu XZ, Wyman C, Wellinger RJ, Petrini JHJ (2013) The Ku Heterodimer and the Metabolism of Single-Ended DNA Double-Strand Breaks. *Cell Rep* **3**: 2033–2045.
169. Sun J, Lee K-J, Davis AJ, Chen DJ (2012) Human Ku70/80 Protein Blocks Exonuclease 1-mediated DNA Resection in the Presence of Human Mre11 or Mre11/Rad50 Protein Complex. *J Biol Chem* **287**: 4936–4945.
170. Lazzaro F, Sapountzi V, Granata M, Pellicioli A, Vaze M, Haber JE, Plevani P, Lydall D, Muzi-Falconi M (2008) Histone methyltransferase Dot1 and Rad9 inhibit single-stranded DNA

accumulation at DSBs and uncapped telomeres. *EMBO J* **27**: 1502–1512.

171. Bantele SC, Ferreira P, Gritenaite D, Boos D, Pfander B (2017) Targeting of the Fun30 nucleosome remodeller by the Dpb11 scaffold facilitates cell cycle-regulated DNA end resection. *eLife* **6**:.
172. Chen X, Cui D, Papusha A, Zhang X, Chu C-D, Tang J, Chen K, Pan X, Ira G (2012) The Fun30 nucleosome remodeller promotes resection of DNA double-strand break ends. *Nature* **489**: 576–580.
173. Costelloe T, Louge R, Tomimatsu N, Mukherjee B, Martini E, Khadaroo B, Dubois K, Wiegant WW, Thierry A, Burma S, et al. (2012) The yeast Fun30 and human SMARCAD1 chromatin remodellers promote DNA end resection. *Nature* **489**: 581–584.
174. Chen X, Niu H, Yu Y, Wang J, Zhu S, Zhou J, Papusha A, Cui D, Pan X, Kwon Y, et al. (2016) Enrichment of Cdk1-cyclins at DNA double-strand breaks stimulates Fun30 phosphorylation and DNA end resection. *Nucleic Acids Res* **44**: 2742–2753.
175. Martina M, Bonetti D, Villa M, Lucchini G, Longhese MP (2014) Saccharomyces cerevisiae Rif1 cooperates with MRX-Sae2 in promoting DNA-end resection. *EMBO Rep* **15**: 695–704.
176. Ohouo PY, Bastos de Oliveira FM, Liu Y, Ma CJ, Smolka MB (2013) DNA-repair scaffolds dampen checkpoint signalling by counteracting the adaptor Rad9. *Nature* **493**: 120–124.
177. Dibitetto D, Ferrari M, Rawal CC, Balint A, Kim T, Zhang Z, Smolka MB, Brown GW, Marini F, Pellicioli A (2016) Slx4 and Rtt107 control checkpoint signalling and DNA resection at double-strand breaks. *Nucleic Acids Res* **44**: 669–682.
178. Ferrari M, Dibitetto D, De Gregorio G, Eapen VV, Rawal CC, Lazzaro F, Tsabar M, Marini F, Haber JE, Pellicioli A (2015) Functional interplay between the 53BP1-ortholog Rad9 and the Mre11 complex regulates resection, end-tethering and repair of a double-strand break. *PLoS Genet* **11**: e1004928.

179. Escribano-Díaz C, Orthwein A, Fradet-Turcotte A, Xing M, Young JTF, Tkáč J, Cook MA, Rosebrock AP, Munro M, Canny MD, et al. (2013) A cell cycle-dependent regulatory circuit composed of 53BP1-RIF1 and BRCA1-CtIP controls DNA repair pathway choice. *Mol Cell* **49**: 872–883.
180. Di Virgilio M, Callen E, Yamane A, Zhang W, Jankovic M, Gitlin AD, Feldhahn N, Resch W, Oliveira TY, Chait BT, et al. (2013) Rif1 prevents resection of DNA breaks and promotes immunoglobulin class switching. *Science* **339**: 711–715.
181. Zimmermann M, Lottersberger F, Buonomo SB, Sfeir A, de Lange T (2013) 53BP1 regulates DSB repair using Rif1 to control 5' end resection. *Science* **339**: 700–704.
182. Boersma V, Moatti N, Segura-Bayona S, Peuscher MH, van der Torre J, Wevers BA, Orthwein A, Durocher D, Jacobs JJL (2015) MAD2L2 controls DNA repair at telomeres and DNA breaks by inhibiting 5' end resection. *Nature* **521**: 537–540.
183. Tkáč J, Xu G, Adhikary H, Young JTF, Gallo D, Escribano-Díaz C, Krietsch J, Orthwein A, Munro M, Sol W, et al. (2016) HELB Is a Feedback Inhibitor of DNA End Resection. *Mol Cell* **61**: 405–418.
184. Baroni E, Viscardi V, Cartagena-Lirola H, Lucchini G, Longhese MP (2004) The functions of budding yeast Sae2 in the DNA damage response require Mec1- and Tel1-dependent phosphorylation. *Mol Cell Biol* **24**: 4151–4165.
185. Morin I, Ngo H-P, Greenall A, Zubko MK, Morrice N, Lydall D (2008) Checkpoint-dependent phosphorylation of Exo1 modulates the DNA damage response. *EMBO J* **27**: 2400–2410.
186. Mantiero D, Clerici M, Lucchini G, Longhese MP (2007) Dual role for Saccharomyces cerevisiae Tel1 in the checkpoint response to double-strand breaks. *EMBO Rep* **8**: 380–387.
187. Liu Y, Cussiol JR, Dibitetto D, Sims JR, Twayana S, Weiss RS, Freire R, Marini F, Pellicioli A, Smolka MB (2017) TOPBP1(Dpb11) plays a conserved role in homologous

recombination DNA repair through the coordinated recruitment of 53BP1(Rad9). *J Cell Biol* **216**: 623–639.

188. Kibe T, Zimmermann M, de Lange T (2016) TPP1 Blocks an ATR-Mediated Resection Mechanism at Telomeres. *Mol Cell* **61**: 236–246.
189. Manfrini N, Trovesi C, Wery M, Martina M, Cesena D, Descrimes M, Morillon A, d'Adda di Fagagna F, Longhese MP (2015) RNA-processing proteins regulate Mec1/ATR activation by promoting generation of RPA-coated ssDNA. *EMBO Rep* **16**: 221–231.
190. Berti M, Vindigni A (2016) Replication stress: getting back on track. *Nat Struct Mol Biol* **23**: 103–109.
191. Giannattasio M, Branzei D (2017) S-phase checkpoint regulations that preserve replication and chromosome integrity upon dNTP depletion. *Cell Mol Life Sci CMLS* **74**: 2361–2380.
192. Saldivar JC, Cortez D, Cimprich KA (2017) The essential kinase ATR: ensuring faithful duplication of a challenging genome. *Nat Rev Mol Cell Biol* **18**: 622–636.
193. Sogo JM, Lopes M, Foiani M (2002) Fork Reversal and ssDNA Accumulation at Stalled Replication Forks Owing to Checkpoint Defects. *Science* **297**: 599–602.
194. Byun TS, Pacek M, Yee M, Walter JC, Cimprich KA (2005) Functional uncoupling of MCM helicase and DNA polymerase activities activates the ATR-dependent checkpoint. *Genes Dev* **19**: 1040–1052.
195. Hashimoto Y, Chaudhuri AR, Lopes M, Costanzo V (2010) Rad51 protects nascent DNA from Mre11-dependent degradation and promotes continuous DNA synthesis. *Nat Struct Mol Biol* **17**: nsmb.1927.
196. Van C, Yan S, Michael WM, Waga S, Cimprich KA (2010) Continued primer synthesis at stalled replication forks contributes to checkpoint activation. *J Cell Biol* **189**: 233–246.

197. Thangavel S, Berti M, Levikova M, Pinto C, Gomathinayagam S, Vujanovic M, Zellweger R, Moore H, Lee EH, Hendrickson EA, et al. (2015) DNA2 drives processing and restart of reversed replication forks in human cells. *J Cell Biol* **208**: 545–562.
198. Wanrooij PH, Burgers PM (2015) Yet another job for Dna2: Checkpoint activation. *DNA Repair* **32**: 17–23.
199. Bjergbaek L, Cobb JA, Tsai-Pflugfelder M, Gasser SM (2005) Mechanistically distinct roles for Sgs1p in checkpoint activation and replication fork maintenance. *EMBO J* **24**: 405–417.
200. Hegnauer AM, Hustedt N, Shimada K, Pike BL, Vogel M, Amsler P, Rubin SM, van Leeuwen F, Guénolé A, van Attikum H, et al. (2012) An N-terminal acidic region of Sgs1 interacts with Rpa70 and recruits Rad53 kinase to stalled forks. *EMBO J* **31**: 3768–3783.
201. Kumar S, Burgers PM (2013) Lagging strand maturation factor Dna2 is a component of the replication checkpoint initiation machinery. *Genes Dev* **27**: 313–321.
202. Puddu F, Piergiovanni G, Plevani P, Muzi-Falconi M (2011) Sensing of Replication Stress and Mec1 Activation Act through Two Independent Pathways Involving the 9-1-1 Complex and DNA Polymerase ε. *PLOS Genet* **7**: e1002022.
203. Tsai F-L, Vijayraghavan S, Prinz J, MacAlpine HK, MacAlpine DM, Schwacha A (2015) Mcm2-7 Is an Active Player in the DNA Replication Checkpoint Signaling Cascade via Proposed Modulation of Its DNA Gate. *Mol Cell Biol* **35**: 2131–2143.
204. Lopez-Contreras AJ, Specks J, Barlow JH, Ambrogio C, Desler C, Vikingsson S, Rodrigo-Perez S, Green H, Rasmussen LJ, Murga M, et al. (2015) Increased Rrm2 gene dosage reduces fragile site breakage and prolongs survival of ATR mutant mice. *Genes Dev* **29**: 690–695.
205. Zegerman P, Diffley JFX (2010) Checkpoint-dependent inhibition of DNA replication initiation by Sld3 and Dbf4 phosphorylation. *Nature* **467**: 474–478.

206. Tercero JA, Diffley JFX (2001) Regulation of DNA replication fork progression through damaged DNA by the Mec1/Rad53 checkpoint. *Nature* **412**: 35087607.
207. Lopes M, Cotta-Ramusino C, Pellicioli A, Liberi G, Plevani P, Muzi-Falconi M, Newlon CS, Foiani M (2001) The DNA replication checkpoint response stabilizes stalled replication forks. *Nature* **412**: 557–561.
208. Lucca C, Vanoli F, Cotta-Ramusino C, Pellicioli A, Liberi G, Haber J, Foiani M (2004) Checkpoint-mediated control of replisome-fork association and signalling in response to replication pausing. *Oncogene* **23**: 1206–1213.
209. Dungrawala H, Rose KL, Bhat KP, Mohni KN, Glick GG, Couch FB, Cortez D (2015) The Replication Checkpoint Prevents Two Types of Fork Collapse without Regulating Replisome Stability. *Mol Cell* **59**: 998–1010.
210. De Piccoli G, Katou Y, Itoh T, Nakato R, Shirahige K, Labib K (2012) Replisome Stability at Defective DNA Replication Forks Is Independent of S Phase Checkpoint Kinases. *Mol Cell* **45**: 696–704.
211. Liberi G, Maffioletti G, Lucca C, Chiolo I, Baryshnikova A, Cotta-Ramusino C, Lopes M, Pellicioli A, Haber JE, Foiani M (2005) Rad51-dependent DNA structures accumulate at damaged replication forks in sgs1 mutants defective in the yeast ortholog of BLM RecQ helicase. *Genes Dev* **19**: 339–350.
212. Cobb JA, Bjergbaek L, Shimada K, Frei C, Gasser SM (2003) DNA polymerase stabilization at stalled replication forks requires Mec1 and the RecQ helicase Sgs1. *EMBO J* **22**: 4325–4336.
213. Gan H, Yu C, Devbhandari S, Sharma S, Han J, Chabes A, Remus D, Zhang Z (2017) Checkpoint Kinase Rad53 Couples Leading- and Lagging-Strand DNA Synthesis under Replication Stress. *Mol Cell* **68**: 446–455.e3.

214. Rossi SE, Ajazi A, Carotenuto W, Foiani M, Giannattasio M (2015) Rad53-Mediated Regulation of Rrm3 and Pif1 DNA Helicases Contributes to Prevention of Aberrant Fork Transitions under Replication Stress. *Cell Rep* **13**: 80–92.
215. Cotta-Ramusino C, Fachinetti D, Lucca C, Doksani Y, Lopes M, Sogo J, Foiani M (2005) Exo1 processes stalled replication forks and counteracts fork reversal in checkpoint-defective cells. *Mol Cell* **17**: 153–159.
216. Segurado M, Diffley JFX (2008) Separate roles for the DNA damage checkpoint protein kinases in stabilizing DNA replication forks. *Genes Dev* **22**: 1816–1827.
217. Colosio A, Frattini C, Pellicanò G, Villa-Hernández S, Bermejo R (2016) Nucleolytic processing of aberrant replication intermediates by an Exo1-Dna2-Sae2 axis counteracts fork collapse-driven chromosome instability. *Nucleic Acids Res* **44**: 10676–10690.
218. Schlacher K, Wu H, Jasin M (2012) A distinct replication fork protection pathway connects Fanconi anemia tumor suppressors to RAD51-BRCA1/2. *Cancer Cell* **22**: 106–116.
219. Schlacher K, Christ N, Siaud N, Egashira A, Wu H, Jasin M (2011) Double-strand break repair-independent role for BRCA2 in blocking stalled replication fork degradation by MRE11. *Cell* **145**: 529–542.
220. Lemaçon D, Jackson J, Quinet A, Brickner JR, Li S, Yazinski S, You Z, Ira G, Zou L, Mosammaparast N, et al. (2017) MRE11 and EXO1 nucleases degrade reversed forks and elicit MUS81-dependent fork rescue in BRCA2-deficient cells. *Nat Commun* **8**: 860.
221. Kolinjivadi AM, Sannino V, De Antoni A, Zadorozhny K, Kilkenny M, Técher H, Baldi G, Shen R, Ciccia A, Pellegrini L, et al. (2017) Smarcal1-Mediated Fork Reversal Triggers Mre11-Dependent Degradation of Nascent DNA in the Absence of

Brca2 and Stable Rad51 Nucleofilaments. *Mol Cell* **67**: 867–881.e7.

222. Mijic S, Zellweger R, Chappidi N, Berti M, Jacobs K, Mutreja K, Ursich S, Ray Chaudhuri A, Nussenzweig A, Janscak P, et al. (2017) Replication fork reversal triggers fork degradation in BRCA2-defective cells. *Nat Commun* **8**: 859.
223. Iannascoli C, Palermo V, Murfuni I, Franchitto A, Pichierri P (2015) The WRN exonuclease domain protects nascent strands from pathological MRE11/EXO1-dependent degradation. *Nucleic Acids Res* **43**: 9788–9803.
224. Leuzzi G, Marabitti V, Pichierri P, Franchitto A (2016) WRNIP1 protects stalled forks from degradation and promotes fork restart after replication stress. *EMBO J* **35**: 1437–1451.
225. Su F, Mukherjee S, Yang Y, Mori E, Bhattacharya S, Kobayashi J, Yannone SM, Chen DJ, Asaithamby A (2014) Nonenzymatic role for WRN in preserving nascent DNA strands after replication stress. *Cell Rep* **9**: 1387–1401.
226. Higgs MR, Reynolds JJ, Winczura A, Blackford AN, Borel V, Miller ES, Zlatanou A, Nieminuszczy J, Ryan EL, Davies NJ, et al. (2015) BOD1L Is Required to Suppress Deleterious Resection of Stressed Replication Forks. *Mol Cell* **59**: 462–477.
227. Seeber A, Hauer M, Gasser SM (2013) Nucleosome remodelers in double-strand break repair. *Curr Opin Genet Dev* **23**: 174–184.
228. Eapen VV, Sugawara N, Tsabar M, Wu W-H, Haber JE (2012) The Saccharomyces cerevisiae chromatin remodeler Fun30 regulates DNA end resection and checkpoint deactivation. *Mol Cell Biol* **32**: 4727–4740.
229. Lydall D, Weinert T (1995) Yeast checkpoint genes in DNA damage processing: implications for repair and arrest. *Science* **270**: 1488–1491.
230. Keeney S, Kleckner N (1995) Covalent protein-DNA complexes at the 5’ strand termini of meiosis-specific double-strand breaks in yeast. *Proc Natl Acad Sci U S A* **92**: 11274–11278.

231. Usui T, Ohta T, Oshiumi H, Tomizawa J, Ogawa H, Ogawa T (1998) Complex formation and functional versatility of Mre11 of budding yeast in recombination. *Cell* **95**: 705–716.
232. Deng C, Brown JA, You D, Brown JM (2005) Multiple endonucleases function to repair covalent topoisomerase I complexes in Saccharomyces cerevisiae. *Genetics* **170**: 591–600.
233. Foster SS, Balestrini A, Petrini JHJ (2011) Functional interplay of the Mre11 nuclease and Ku in the response to replication-associated DNA damage. *Mol Cell Biol* **31**: 4379–4389.
234. Shim EY, Chung W-H, Nicolette ML, Zhang Y, Davis M, Zhu Z, Paull TT, Ira G, Lee SE (2010) Saccharomyces cerevisiae Mre11/Rad50/Xrs2 and Ku proteins regulate association of Exo1 and Dna2 with DNA breaks. *EMBO J* **29**: 3370–3380.
235. Mullen JR, Kaliraman V, Brill SJ (2000) Bipartite structure of the SGS1 DNA helicase in Saccharomyces cerevisiae. *Genetics* **154**: 1101–1114.
236. Budd ME, Reis CC, Smith S, Myung K, Campbell JL (2006) Evidence suggesting that Pif1 helicase functions in DNA replication with the Dna2 helicase/nuclease and DNA polymerase delta. *Mol Cell Biol* **26**: 2490–2500.
237. Lee SE, Moore JK, Holmes A, Umezu K, Kolodner RD, Haber JE (1998) Saccharomyces Ku70, mre11/rad50 and RPA proteins regulate adaptation to G2/M arrest after DNA damage. *Cell* **94**: 399–409.
238. Pellicioli A, Lee SE, Lucca C, Foiani M, Haber JE (2001) Regulation of Saccharomyces Rad53 checkpoint kinase during adaptation from DNA damage-induced G2/M arrest. *Mol Cell* **7**: 293–300.
239. Usui T, Ogawa H, Petrini JH (2001) A DNA damage response pathway controlled by Tel1 and the Mre11 complex. *Mol Cell* **7**: 1255–1266.
240. Vaze MB, Pellicioli A, Lee SE, Ira G, Liberi G, Arbel-Eden A, Foiani M, Haber JE (2002) Recovery from checkpoint-mediated

arrest after repair of a double-strand break requires Srs2 helicase. *Mol Cell* **10**: 373–385.

241. Bernstein KA, Mimitou EP, Mihalevic MJ, Chen H, Sunjaveric I, Symington LS, Rothstein R (2013) Resection activity of the Sgs1 helicase alters the affinity of DNA ends for homologous recombination proteins in Saccharomyces cerevisiae. *Genetics* **195**: 1241–1251.
242. Clerici M, Mantiero D, Guerini I, Lucchini G, Longhese MP (2008) The Yku70-Yku80 complex contributes to regulate double-strand break processing and checkpoint activation during the cell cycle. *EMBO Rep* **9**: 810–818.
243. Trovesi C, Falcettoni M, Lucchini G, Clerici M, Longhese MP (2011) Distinct Cdk1 requirements during single-strand annealing, noncrossover, and crossover recombination. *PLoS Genet* **7**: e1002263.
244. Bonetti D, Villa M, Gobbini E, Cassani C, Tedeschi G, Longhese MP (2015) Escape of Sgs1 from Rad9 inhibition reduces the requirement for Sae2 and functional MRX in DNA end resection. *EMBO Rep* **16**: 351–361.
245. Liu C, Pouliot JJ, Nash HA (2002) Repair of topoisomerase I covalent complexes in the absence of the tyrosyl-DNA phosphodiesterase Tdp1. *Proc Natl Acad Sci U S A* **99**: 14970–14975.
246. Chen H, Donnianni RA, Handa N, Deng SK, Oh J, Timashev LA, Kowalczykowski SC, Symington LS (2015) Sae2 promotes DNA damage resistance by removing the Mre11-Rad50-Xrs2 complex from DNA and attenuating Rad53 signaling. *Proc Natl Acad Sci U S A* **112**: E1880-1887.
247. Sandell LL, Zakian VA (1993) Loss of a yeast telomere: arrest, recovery, and chromosome loss. *Cell* **75**: 729–739.
248. Toczyski DP, Galgoczy DJ, Hartwell LH (1997) CDC5 and CKII control adaptation to the yeast DNA damage checkpoint. *Cell* **90**: 1097–1106.

249. Sun Z, Hsiao J, Fay DS, Stern DF (1998) Rad53 FHA domain associated with phosphorylated Rad9 in the DNA damage checkpoint. *Science* **281**: 272–274.
250. Durocher D, Henckel J, Fersht AR, Jackson SP (1999) The FHA domain is a modular phosphopeptide recognition motif. *Mol Cell* **4**: 387–394.
251. Bosotti R, Isacchi A, Sonnhammer EL (2000) FAT: a novel domain in PIK-related kinases. *Trends Biochem Sci* **25**: 225–227.
252. Baretić D, Williams RL (2014) PIKKs--the solenoid nest where partners and kinases meet. *Curr Opin Struct Biol* **29**: 134–142.
253. Mallory JC, Petes TD (2000) Protein kinase activity of Tel1p and Mec1p, two Saccharomyces cerevisiae proteins related to the human ATM protein kinase. *Proc Natl Acad Sci U S A* **97**: 13749–13754.
254. Ogi H, Goto GH, Ghosh A, Zencir S, Henry E, Sugimoto K (2015) Requirement of the FATC domain of protein kinase Tel1 for localization to DNA ends and target protein recognition. *Mol Biol Cell* **26**: 3480–3488.
255. Jia X, Weinert T, Lydall D (2004) Mec1 and Rad53 inhibit formation of single-stranded DNA at telomeres of Saccharomyces cerevisiae cdc13-1 mutants. *Genetics* **166**: 753–764.
256. Sanchez Y, Bachant J, Wang H, Hu F, Liu D, Tetzlaff M, Elledge SJ (1999) Control of the DNA damage checkpoint by chk1 and rad53 protein kinases through distinct mechanisms. *Science* **286**: 1166–1171.
257. Budd ME, Choe W c, Campbell JL (2000) The nuclease activity of the yeast DNA2 protein, which is related to the RecB-like nucleases, is essential in vivo. *J Biol Chem* **275**: 16518–16529.
258. Zhao X, Muller EG, Rothstein R (1998) A suppressor of two essential checkpoint genes identifies a novel protein that negatively affects dNTP pools. *Mol Cell* **2**: 329–340.

259. Fay DS, Sun Z, Stern DF (1997) Mutations in SPK1/RAD53 that specifically abolish checkpoint but not growth-related functions. *Curr Genet* **31**: 97–105.
260. Baldo V, Testoni V, Lucchini G, Longhese MP (2008) Dominant TEL1-hy mutations compensate for Mec1 lack of functions in the DNA damage response. *Mol Cell Biol* **28**: 358–375.
261. Hirano Y, Fukunaga K, Sugimoto K (2009) Rif1 and rif2 inhibit localization of tel1 to DNA ends. *Mol Cell* **33**: 312–322.
262. Javaheri A, Wysocki R, Jobin-Robitaille O, Altaf M, Côté J, Kron SJ (2006) Yeast G1 DNA damage checkpoint regulation by H2A phosphorylation is independent of chromatin remodeling. *Proc Natl Acad Sci U S A* **103**: 13771–13776.
263. Toh GW-L, O'Shaughnessy AM, Jimeno S, Dobbie IM, Grenon M, Maffini S, O'Rorke A, Lowndes NF (2006) Histone H2A phosphorylation and H3 methylation are required for a novel Rad9 DSB repair function following checkpoint activation. *DNA Repair* **5**: 693–703.
264. Desany BA, Alcasabas AA, Bachant JB, Elledge SJ (1998) Recovery from DNA replicational stress is the essential function of the S-phase checkpoint pathway. *Genes Dev* **12**: 2956–2970.
265. Sabatinos SA, Green MD, Forsburg SL (2012) Continued DNA synthesis in replication checkpoint mutants leads to fork collapse. *Mol Cell Biol* **32**: 4986–4997.
266. Cobb JA, Schleker T, Rojas V, Bjergbaek L, Tercero JA, Gasser SM (2005) Replisome instability, fork collapse, and gross chromosomal rearrangements arise synergistically from Mec1 kinase and RecQ helicase mutations. *Genes Dev* **19**: 3055–3069.
267. De Piccoli G, Katou Y, Itoh T, Nakato R, Shirahige K, Labib K (2012) Replisome stability at defective DNA replication forks is independent of S phase checkpoint kinases. *Mol Cell* **45**: 696–704.
268. Kao H-I, Campbell JL, Bambara RA (2004) Dna2p helicase/nuclease is a tracking protein, like FEN1, for flap

cleavage during Okazaki fragment maturation. *J Biol Chem* **279**: 50840–50849.

269. Peng G, Dai H, Zhang W, Hsieh H-J, Pan M-R, Park Y-Y, Tsai RY-L, Bedrosian I, Lee J-S, Ira G, et al. (2012) Human nuclease/helicase DNA2 alleviates replication stress by promoting DNA end resection. *Cancer Res* **72**: 2802–2813.
270. Tsang E, Miyabe I, Iraqui I, Zheng J, Lambert SAE, Carr AM (2014) The extent of error-prone replication restart by homologous recombination is controlled by Exo1 and checkpoint proteins. *J Cell Sci* **127**: 2983–2994.
271. Koundrioukoff S, Carignon S, Técher H, Letessier A, Brison O, Debatisse M (2013) Stepwise activation of the ATR signaling pathway upon increasing replication stress impacts fragile site integrity. *PLoS Genet* **9**: e1003643.
272. Smolka MB, Albuquerque CP, Chen S, Zhou H (2007) Proteome-wide identification of in vivo targets of DNA damage checkpoint kinases. *Proc Natl Acad Sci U S A* **104**: 10364–10369.
273. Hu J, Sun L, Shen F, Chen Y, Hua Y, Liu Y, Zhang M, Hu Y, Wang Q, Xu W, et al. (2012) The intra-S phase checkpoint targets Dna2 to prevent stalled replication forks from reversing. *Cell* **149**: 1221–1232.
274. Duxin JP, Moore HR, Sidorova J, Karanja K, Honaker Y, Dao B, Piwnica-Worms H, Campbell JL, Monnat RJ, Stewart SA (2012) Okazaki fragment processing-independent role for human Dna2 enzyme during DNA replication. *J Biol Chem* **287**: 21980–21991.
275. Howlett NG, Taniguchi T, Durkin SG, D'Andrea AD, Glover TW (2005) The Fanconi anemia pathway is required for the DNA replication stress response and for the regulation of common fragile site stability. *Hum Mol Genet* **14**: 693–701.

276. Schlacher K, Wu H, Jasin M (2012) A distinct replication fork protection pathway connects Fanconi anemia tumor suppressors to RAD51-BRCA1/2. *Cancer Cell* **22**: 106–116.
277. Ying S, Hamdy FC, Helleday T (2012) Mre11-dependent degradation of stalled DNA replication forks is prevented by BRCA2 and PARP1. *Cancer Res* **72**: 2814–2821.
278. Unno J, Itaya A, Taoka M, Sato K, Tomida J, Sakai W, Sugasawa K, Ishiai M, Ikura T, Isobe T, et al. (2014) FANCD2 binds CtIP and regulates DNA-end resection during DNA interstrand crosslink repair. *Cell Rep* **7**: 1039–1047.
279. Karanja KK, Lee EH, Hendrickson EA, Campbell JL (2014) Preventing over-resection by DNA2 helicase/nuclease suppresses repair defects in Fanconi anemia cells. *Cell Cycle Georget Tex* **13**: 1540–1550.
280. Chen X, Bosques L, Sung P, Kupfer GM (2016) A novel role for non-ubiquitinated FANCD2 in response to hydroxyurea-induced DNA damage. *Oncogene* **35**: 22–34.
281. Hickson ID, Mankouri HW (2011) Processing of homologous recombination repair intermediates by the Sgs1-Top3-Rmi1 and Mus81-Mms4 complexes. *Cell Cycle Georget Tex* **10**: 3078–3085.
282. Rodriguez J, Tsukiyama T (2013) ATR-like kinase Mec1 facilitates both chromatin accessibility at DNA replication forks and replication fork progression during replication stress. *Genes Dev* **27**: 74–86.
283. Paciotti V, Clerici M, Scotti M, Lucchini G, Longhese MP (2001) Characterization of mec1 kinase-deficient mutants and of new hypomorphic mec1 alleles impairing subsets of the DNA damage response pathway. *Mol Cell Biol* **21**: 3913–3925.
284. Tercero JA, Longhese MP, Diffley JFX (2003) A central role for DNA replication forks in checkpoint activation and response. *Mol Cell* **11**: 1323–1336.

285. Budd ME, Campbell JL (1997) A yeast replicative helicase, Dna2 helicase, interacts with yeast FEN-1 nuclease in carrying out its essential function. *Mol Cell Biol* **17**: 2136–2142.
286. van Leeuwen F, Gafken PR, Gottschling DE (2002) Dot1p modulates silencing in yeast by methylation of the nucleosome core. *Cell* **109**: 745–756.
287. Huyen Y, Zgheib O, Ditullio RA, Gorgoulis VG, Zacharatos P, Petty TJ, Sheston EA, Mellert HS, Stavridi ES, Halazonetis TD (2004) Methylated lysine 79 of histone H3 targets 53BP1 to DNA double-strand breaks. *Nature* **432**: 406–411.
288. Wysocki R, Javaheri A, Allard S, Sha F, Côté J, Kron SJ (2005) Role of Dot1-dependent histone H3 methylation in G1 and S phase DNA damage checkpoint functions of Rad9. *Mol Cell Biol* **25**: 8430–8443.
289. Ohouo PY, Bastos de Oliveira FM, Almeida BS, Smolka MB (2010) DNA damage signaling recruits the Rtt107-Slx4 scaffolds via Dpb11 to mediate replication stress response. *Mol Cell* **39**: 300–306.
290. Flott S, Rouse J (2005) Slx4 becomes phosphorylated after DNA damage in a Mec1/Tel1-dependent manner and is required for repair of DNA alkylation damage. *Biochem J* **391**: 325–333.
291. Neves-Costa A, Will WR, Vetter AT, Miller JR, Varga-Weisz P (2009) The SNF2-family member Fun30 promotes gene silencing in heterochromatic loci. *PloS One* **4**: e8111.
292. Ait Saada A, Teixeira-Silva A, Iraqui I, Costes A, Hardy J, Paoletti G, Fréon K, Lambert SAE (2017) Unprotected Replication Forks Are Converted into Mitotic Sister Chromatid Bridges. *Mol Cell* **66**: 398–410.e4.
293. Flott S, Kwon Y, Pigli YZ, Rice PA, Sung P, Jackson SP (2011) Regulation of Rad51 function by phosphorylation. *EMBO Rep* **12**: 833–839.
294. Niu H, Chung W-H, Zhu Z, Kwon Y, Zhao W, Chi P, Prakash R, Seong C, Liu D, Lu L, et al. (2010) Mechanism of the ATP-

dependent DNA end-resection machinery from Saccharomyces cerevisiae. *Nature* **467**: 108–111.

295. Zhu Z, Chung W-H, Shim EY, Lee SE, Ira G (2008) Sgs1 helicase and two nucleases Dna2 and Exo1 resect DNA double-strand break ends. *Cell* **134**: 981–994.
296. Kitano K, Yoshihara N, Hakoshima T (2007) Crystal Structure of the HRDC Domain of Human Werner Syndrome Protein, WRN. *J Biol Chem* **282**: 2717–2728.
297. Liu Z, Macias M, Bottomley M, Stier G, Linge J, Nilges M, Bork P, Sattler M (1999) The three-dimensional structure of the HRDC domain and implications for the Werner and Bloom syndrome proteins. *Structure* **7**: 1557–1566.
298. Cejka P, Cannavo E, Polaczek P, Masuda-Sasa T, Pokharel S, Campbell JL, Kowalczykowski SC (2010) DNA end resection by Dna2-Sgs1-RPA and its stimulation by Top3-Rmi1 and Mre11-Rad50-Xrs2. *Nature* **467**: 112–116.
299. Shim EY, Chung W-H, Nicolette ML, Zhang Y, Davis M, Zhu Z, Paull TT, Ira G, Lee SE (2010) Saccharomyces cerevisiae Mre11/Rad50/Xrs2 and Ku proteins regulate association of Exo1 and Dna2 with DNA breaks. *EMBO J* **29**: 3370–3380.
300. Jinks-Robertson S, Michelitch M, Ramcharan S (1993) Substrate length requirements for efficient mitotic recombination in Saccharomyces cerevisiae. *Mol Cell Biol* **13**: 3937–3950.
301. Ira G, Haber JE (2002) Characterization of RAD51-independent break-induced replication that acts preferentially with short homologous sequences. *Mol Cell Biol* **22**: 6384–6392.
302. Naiki T, Wakayama T, Nakada D, Matsumoto K, Sugimoto K (2004) Association of Rad9 with double-strand breaks through a Mec1-dependent mechanism. *Mol Cell Biol* **24**: 3277–3285.
303. Usui T, Foster SS, Petrini JHJ (2009) Maintenance of the DNA-damage checkpoint requires DNA-damage-induced mediator protein oligomerization. *Mol Cell* **33**: 147–159.

304. Emili A (1998) MEC1-dependent phosphorylation of Rad9p in response to DNA damage. *Mol Cell* **2**: 183–189.
305. Vialard JE, Gilbert CS, Green CM, Lowndes NF (1998) The budding yeast Rad9 checkpoint protein is subjected to Mec1/Tel1-dependent hyperphosphorylation and interacts with Rad53 after DNA damage. *EMBO J* **17**: 5679–5688.
306. Bunting SF, Callén E, Wong N, Chen H-T, Polato F, Gunn A, Bothmer A, Feldhahn N, Fernandez-Capetillo O, Cao L, et al. (2010) 53BP1 inhibits homologous recombination in Brca1-deficient cells by blocking resection of DNA breaks. *Cell* **141**: 243–254.
307. Bothmer A, Robbiani DF, Di Virgilio M, Bunting SF, Klein IA, Feldhahn N, Barlow J, Chen H-T, Bosque D, Callen E, et al. (2011) Regulation of DNA end joining, resection, and immunoglobulin class switch recombination by 53BP1. *Mol Cell* **42**: 319–329.
308. Balint A, Kim T, Gallo D, Cussiol JR, Bastos de Oliveira FM, Yimit A, Ou J, Nakato R, Gurevich A, Shirahige K, et al. (2015) Assembly of Slx4 signaling complexes behind DNA replication forks. *EMBO J* **34**: 2182–2197.
309. Fricke WM, Bastin-Shanower SA, Brill SJ (2005) Substrate specificity of the Saccharomyces cerevisiae Mus81-Mms4 endonuclease. *DNA Repair* **4**: 243–251.
310. Hanada K, Budzowska M, Davies SL, van Drunen E, Onizawa H, Beverloo HB, Maas A, Essers J, Hickson ID, Kanaar R (2007) The structure-specific endonuclease Mus81 contributes to replication restart by generating double-strand DNA breaks. *Nat Struct Mol Biol* **14**: 1096–1104.
311. Levikova M, Cejka P (2015) The Saccharomyces cerevisiae Dna2 can function as a sole nuclease in the processing of Okazaki fragments in DNA replication. *Nucleic Acids Res* **43**: 7888–7897.

312. Cescutti R, Negrini S, Kohzaki M, Halazonetis TD (2010) TopBP1 functions with 53BP1 in the G1 DNA damage checkpoint. *EMBO J* **29**: 3723–3732.